# Insights into host-virus interactions: Using a metabolomics approach to study *Aedes aegypti*-Dengue virus compatibility

**by**

**Keenan Elliott**

BSc, Simon Fraser University, 2018

Thesis Submitted in Partial Fulfillment of the
Requirements for the Degree of
Master of Science

in the
Department of Biological Sciences
Faculty of Science


SIMON FRASER UNIVERSITY
Fall 2022

## Declaration of Committee

| | |
|---|---|
| **Name:** | **Keenan Elliott** |
| **Degree:** | **Master of Science (Biological Sciences)** |
| **Title:** | **Insights into host-virus interactions: Using a metabolomics approach to study *Aedes aegypti*-Dengue virus compatibility** |
| **Committee:** | **Chair: David Green**<br>Professor, Biological Sciences |
| | **Carl Lowenberger**<br>Supervisor<br>Professor, Biological Sciences |
| | **Norbert Haunerland**<br>Committee Member<br>Professor, Biological Sciences |
| | **Christopher Beh**<br>Examiner<br>Professor, Molecular Biology and Biochemistry |

## Abstract

Approximately half of the world population lives in areas with circulating dengue virus (DENV) and are at risk of contracting an infection. DENV infection can cause severe complications, including hemorrhagic fever and death. Currently, no effective vaccines or drugs are available for treating DENV infection in humans, making vector control the most efficacious strategy for preventing infection. DENV is principally transmitted by *Aedes aegypti*; however, not all female *Ae. aegypti* will transmit the virus. Our group has identified two populations of *Ae. aegypti* in Cali, Colombia, that are refractory (do not transmit, Cali-MIB) or susceptible (Cali-S) to the virus. Here, we utilized metabolic and lipidomic profiling to identify changes in host metabolism that correlate with DENV resistance or susceptibility. This research has identified multiple compounds and metabolic pathways altered in Cali-MIB populations after DENV infection. These compounds should be further investigated to understand their role in DENV infection.



**Keywords**: Metabolomics; Lipidomics; Aedes aegypti; Dengue virus; Host-pathogen interactions

## Acknowledgements

I began graduate school in May of 2020; the pandemic was just beginning, and it was unclear how research would be impacted. I spent the first semester of my master's at home trying to read papers between naps, YouTube videos, and coffee. It was an atypical start to a unique graduate experience, and I have many to thank for their help throughout.

First, my senior supervisor, Dr. Carl Lowenberger. In one of my early interactions with Carl, he jokingly remarked that I had picked a terrible time to start graduate school. This comment punctuates his demeanour throughout the last two years; although research was made significantly more difficult because of the pandemic, he always had an easygoing sense of humour. Thank you, Carl, for your patience, teaching, guidance, and trust in me. I believe my degree would not have been as successful or instructive anywhere else on campus. To my other committee member, Dr. Norbert Haunerland, thank you for your positive comments, pragmatism, and eagerness to discuss all matters of subjects, science or other (and for constantly reminding me how much more cycling I should be doing!).

I am tremendously grateful to my colleagues in the Lowenberger lab, Nicolás Salcedo, Claudia Umana Diaz, and Diana Giron Ceron. Nicolas, your passion for science is inspiring, and how you consider complex problems has changed my approach to scientific questions. Claudia, thank you for persisting with me through the countless failed culture experiments and for your companionship as the Lowenberger lab shrunk to two. Diana, you were the first person I worked with in the lab. Your attention to detail will remain with me for the remainder of my career. Although we have embarked on new journeys, I hope we can work together again one day!

A thank you to all my family and friends for their support, wisdom, and much-needed distractions from academic life. My friends have been crucial to maintaining my mental health during difficult periods by reminding me there is more to life than school. My parents and siblings have supported me more than I could ever deserve; thank you for your continual interest in my research. Finally, a special thank you to my partner, Grace (and Nitro), who has patiently endured numerous practice presentations and provided much-needed moral support over the years.

# Table of Contents

# List of Tables

# List of Figures

# List of Acronyms

| | |
|---|---|
| ADE | Antibody-dependant enhancement |
| Aub | Aubergine |
| CHK | Chikungunya virus |
| CIL | Chemical Isotope labelling |
| DENV | Dengue virus |
| DHF | Dengue hemorrhagic fever |
| FDR | False discovery rate |
| hpbm | Hours post bloodmeal |
| IAP | Inhibitor of apoptosis |
| IMD | Immune deficiency pathway |
| JAK-STAT | Janus kinase-signal transducer and activator of transcription |
| KD | Knock-down |
| LC-MS | Liquid chromatography mass spectrometry |
| MEB | Midgut escape barrier |
| MIB | Midgut infection barrier |
| miRNA | Micro RNA |
| NOS | Nitric oxide synthase |
| NTD | Neglected tropical disease |
| PAMP | Pathogen associated molecular pattern |
| PCA | Principal component analysis |
| PGRP | Peptidoglycan recognition proteins |
| piRNA | Piwi-interacting RNA |
| PLS-DA | Partial least squares discriminant analysis |
| PM | Peritrophic membrane |
| PRR | Pattern recognition receptor |
| RNAi | RNA interference |
| SAM | Significance analysis of microarray |
| siRNA | Small interfering RNA |
| SIT | Sterile insect technique |

| | |
|---|---|
| Spz | Spaetzle |
| Upd | Unpaired |
| VC | Vector Control |
| WHO | World Health Organization |
| YF | Yellow fever virus |
| ZIK | Zika virus |

# Chapter 1.

# Introduction

## 1.1. Abstract

*Aedes aegypti* are the principal vectors of dengue virus (DENV) transmission to humans. It has been established that not all female *Ae. aegypti* transmit the virus as some insects possess the innate immune mechanisms necessary for viral elimination. Here we review the current literature on innate immune pathways in mosquitoes, Toll, JAK-STAT, IMD, RNAi, and autophagy, and their purported function in DENV infection. Additionally, we discuss host-virus interactions and barriers that have been described to prevent DENV infection in *Ae. aegypti.* Finally, we propose using metabolomics as a novel method to uncover mechanisms that may contribute to DENV resistance.

## 1.2. Dengue virus

### 1.2.1. Prevalence, Morbidity and Mortality

Over the past two decades, dengue virus (DENV) has emerged as one of the most significant vector-borne diseases, second only to malaria (World Health Organization, 2020). Nearly half of the world's population resides in areas with circulating DENV and are at risk of contraction (World Health Organization, 2022). An estimated 400 million people are infected yearly in more than 100 countries, with approximately 15 000 deaths annually (Aliaga-Samanez et al., 2021; World Health Organization, 2022). Further, the number of cases has seen a drastic uptick; there has been an 800% increase in the last two decades, stressing the urgent need to mitigate viral spread (World Health Organization, 2022).

DENV infection presents with a range of clinical symptoms, and morbidity with infection is considerable. Colloquially, the disease is referred to as *Break-bone fever* (Clarke, 2002). Although some patients are asymptomatic, others will develop severe dengue or dengue hemorrhagic fever (DHF), characterized by excessive vascular leakage (World Health Organization, 2022). DHF is the leading cause of mortality from infection. Even in less severe cases, symptoms can last from days to weeks and prevent those infected from working, causing substantial financial loss. The estimated global cost of illness related to DENV infection in 2013 was 8.9 billion USD (Shepard et al., 2016). Thereby, viral transmission creates an economic feedback loop, where areas endemic to DENV are often developing nations that cannot afford to combat the spread.

There are four circulating DENV serotypes that are antigenically distinct (World Health Organization, 2022). Recently, a putative fifth serotype has emerged, underscoring the need to limit infections as virus evolution progresses (Mustafa et al., 2015). The most significant risk factor for an individual developing severe dengue is a secondary infection with a serotype distinct from the primary infection. This phenomenon, known as antibody-dependent enhancement (ADE), is thought to be facilitated through the host's adaptive immune system (Katzelnick et al., 2017). In ADE, the antibodies developed during primary infection are ineffective at neutralizing the virus and mediate viral transport across the membrane through interactions with FC receptors (Katzelnick et al., 2017).

Managing ADE presents a significant hurdle to developing effective vaccines as they must generate immunity towards all serotypes. The first commercially available vaccine developed for DENV, Dengavaxia, was shown to worsen outcomes for some patients that had not been infected with DENV previously (World Health Organization, 2022). Determining an individual's infection status prior to administering the vaccine is costly and infeasible for most at risk. With these considerations, the Dengavaxia vaccine is no longer recommended by the World health organization without serological testing (World Health Organization, 2022). At present, there are no approved therapeutics for the treatment of dengue and control of mosquito vectors remains the greatest public health tool to combat dengue transmission. While insecticides have been used globally to reduce mosquito vector populations, these have also affected beneficial insects, and their long-term use has resulted in insecticide resistance. Modern insect controls have emerged, including genetic modification of vectors to eliminate or severely reduce populations or replacement strategies in which susceptible mosquitoes (those that transmit DENV) are replaced by mosquitoes that are refractory to DENV (do not transmit DENV). These approaches have been applied in the field in different areas of the world with varying success.

### 1.2.2. Viral Structure

DENV is a member of the genus *Flaviviridae*, which includes other medically relevant viruses such as West Nile, Zika, and yellow fever (de Borba et al., 2019). The virus has a positive-sense single-stranded RNA genome of ~10kb, containing ten proteins, including three structural and seven non-structural (de Borba et al., 2019). The structural proteins make up the viral particle that will bud from the host membrane and include the capsid protein, the precursor membrane protein, and the envelope protein (de Borba et al., 2019). The non-structural proteins are essential for the virus's replication and are denoted NS1, NS2A, NS2B, NS3, NS4A, NS4B, NS5 (Fig. 1.1).

## 1.3. Transmission: Vectors

### 1.3.1. *Aedes aegypti* and *Aedes albopictus*

The primary vector of DENV, Yellow Fever (YF), Zika (ZIK) and Chikungunya (CHK) viruses is *Aedes aegypti* (Moncayo et al., 2004). Other mosquitoes of the genus

*Aedes,* such as *Ae. albopictus,* have been shown to transmit DENV; however, their competence is limited. *Aedes aegypti* originated in Africa and has since spread to most tropical and subtropical regions (Kraemer et al., 2015). At present, *Ae. aegypti* is found throughout central and south America, the southern United States, Mexico, and southeast Asia (Kraemer et al., 2015).

In contrast, *Ae. albopictus* originated in Asia and, during the 1980s, expanded rapidly to the United States, Europe, and Brazil (Kraemer et al., 2015). The geographic distribution of *Ae. albopictus* resembles *Ae. aegypti* with a higher density in the southern United States and a sparser presence elsewhere (Kraemer et al., 2015). Both vectors appear to have emigrated to new territories following human movement patterns. Areas with confirmed *Aedes* sp. mosquito habitation are expanding, and with-it cases of DENV (Kraemer et al., 2019). It has been speculated that rising global temperatures drive geographic expansion due to increases in suitable climates for survival (Kraemer et al., 2019). Additionally, urbanization may have an equally significant role in habitat expansion (Kraemer et al., 2019).

The life cycle of *Ae. aegypti* consists of four stages: Egg, Larvae, Pupae, and adult (Fig. 1.2) (*Aedes* | *Description, Life Cycle, & Disease Transmission* | *Britannica*). Eggs are laid near a water source such as ponds and marshes or human structures such as tires or pots. The eggs are robust and can survive prolonged periods of drought or cold, making them suitable for cooler temperatures. Under controlled laboratory conditions, an adult can survive up to 38 days, but lifespan in the wild is presumably less (Brady et al., 2013). Only female insects feed on blood to obtain the nutrient resources required to produce eggs (oviposition). During a single oviposition, a female *Ae. aegypti* mosquito will often consume a blood meal from multiple hosts—a unique behaviour for mosquitoes (Scott et al., 2000). This multiple-host feeding behaviour exhibited by *Ae. aegypti* provides ideal conditions for viral spread.

A vector obtains DENV when they ingest the blood of an infected vertebrate; for *Ae. aegypti*, humans represent the primary vertebrate host. Once the virus enters the midgut cavity, there are multiple barriers it must overcome to disseminate throughout the insect. At each stage of infection, the virus interacts with numerous host factors, including host immune responses. First, DENV must cross the peritrophic membrane (PM), which may be partially formed when the virus enters (Black IV et al., 2002). The

PM is produced upon ingestion of a bloodmeal and acts as a semipermeable extracellular structure made of immune molecules, proteins, proteoglycans, and chitin that protects the midgut cells from pathogens and digestive enzymes (Davenport et al., 2006). Once across the PM, viral particles bind to receptors on the surface of the midgut epithelium and cross the cell membrane. The specific receptors used by DENV for entry in invertebrates are not fully resolved; however, glycosaminoglycans such as heparin-sulphate have been implicated in aiding viral entry (Hidari & Suzuki, 2011). Viral particles are endocytosed via a clathrin-dependant mechanism and escape the endosome upon acidification (Guzman & Harris, 2015). Endosomal escape allows the virus to enter the cytoplasm, replicate, and disseminate to the hemocoel. Entry to the hemocoel represents a crucial step to viral spread. The hemocoel contains circulatory fluid and facilitates systemic infection in numerous tissues, the most important being the salivary glands. Once the virus replicates within the salivary glands, it can transfer to a new host with a subsequent blood meal. Infection of the salivary glands occurs approximately 10-14 days after the ingestion of an infectious blood meal (Sánchez-Vargas et al., 2009).

Numerous infection barriers have been characterized in *Aedes* sp. mosquitoes, preventing systemic DENV infection and eliminating viral transfer. Insects unable to transmit the virus are herein referred to as *refractory*, and those that transmit the virus are referred to as *susceptible*. A first barrier, termed the midgut infection barrier (MIB), is characterized by limitations early in midgut infection, such as the inability to pass into or replicate within the midgut epithelium (Black IV et al., 2002). A second barrier, denoted the midgut escape barrier (MEB), prevents the virus from disseminating into the hemocoel, likely due to inefficient particle assembly (Black IV et al., 2002). The insect will avoid systemic infection if either of these barriers is present. A final barrier, known as the salivary gland escape barrier, has been confirmed to prevent the deposition of infectious saliva in a new host (Black IV et al., 2002). The mechanisms for the establishment and maintenance of these barriers are not known. If the virus can overcome these bottlenecks, it may replicate in the salivary glands and be transmitted to a new host.

### 1.3.2. Vector Control

The expansion of *Aedes* sp. mosquitoes globally raises concerns about vector-borne diseases, and novel strategies are needed to minimize the impact of these

viruses. Preventative methods have primarily relied upon vector control which aims to limit population size of competent vectors or limit the capacity of the vector to carry the pathogen. The former has traditionally used mass administration of insecticides to lessen the number of insects. However, these programs are often transiently effective as insect populations rebound (Maciel-de-Freitas & Valle, 2014) or develop insecticide resistance. Moreover, eliminating breeding habitats has shown promise for reducing insect numbers. But these methods require large-scale organization due to unique oviposition behaviour in *Aedes*; female *Aedes* mosquitoes prefer to lay eggs in small bodies of clean water such as pots or puddles, making the elimination of all breeding sites technically challenging.

Given the shortcomings of traditional population suppression techniques, there is strong interest in using genetics to manipulate genomes to reduce vector populations. Indeed, genetic manipulation has been tested in *Ae. aegypti* to reduce populations through the release of modified insects. The first of such methods involved the release of irradiated sterile insects, aptly termed the sterile insect technique (SIT) (Carvalho et al., 2015). Sterile insects directly compete with native insect populations reducing the pool of viable mates and causing suppression. Irradiated insects have shown promise in some species but have little efficacy for mosquito populations, presumably due to male insects having reduced fitness. Recently, more sophisticated genetic tools have emerged. Oxitec, a UK-based biotechnology company, has developed a genetic control system to suppress the local population of mosquitoes through the release of transgenic insects possessing a lethal gene (Carvalho et al., 2015) (Fig. 1.3). The offspring of wildtype and transgenic insects are inviable, leading to a population decrease. Oxitec insects have been field-tested in the Cayman Islands and Brazil and showed strong efficacy, diminishing local populations by 80-95% (Carvalho et al., 2015). However, this method requires the continual release of modified insects, making Oxitec's strategy very costly.

Population replacement (Fig. 1.3) has been proposed to manage viral spread as an alternative to population suppression. Replacement aims to restore the wildtype insects with mosquitoes that have decreased competence for transmitting the virus. Perhaps the most promising replacement technique utilizes the intracellular bacteria *Wolbachia*. Mosquitoes that have established infections with the intracellular bacterium *Wolbachia sp*. show diminished or ablated DENV transmission (Walker et al., 2011). Moreover, if a *Wolbachia*-uninfected female mates with a *Wolbachia*-infected male, the

offspring do not survive (Turelli & Hoffmann, 1991). This phenomenon, known as cytoplasmic incompatibility, provides strong penetrance of *Wolbachia sp.* into the population (Turelli & Hoffmann, 1991; Walker et al., 2011). The mechanism by which *Wolbachia*-induced DENV-resistance occurs is unresolved (King et al., 2018; Manokaran et al., 2020; Rancès et al., 2012), and there has been concern regarding the efficacy of *Wolbachia sp*. at blocking DENV replication. Some studies show *Wolbachia* may not reduce viral replication under all conditions, and more research is needed (King et al., 2018). Moreover, modified populations need comparable fitness to the wild population to ensure adequate replacement (Walker et al., 2011), but evaluating an organism's fitness is challenging.

Finally, using the CRISPR-Cas9 system to engineer organisms has gained popularity in recent years. Indeed, CRISPR-Cas9 systems have been developed in numerous mosquito species, including *Ae. aegypti* and the malaria mosquito *Anopheles gambiae* (Kistler et al., 2015; Kyrou et al., 2018; Li et al., 2018; Liu et al., 2019). These systems have demonstrated promising future efficacy, but no CRISPR insects have been deployed successfully in the field.

Although the impact of DENV on humans is extremely significant, the use of GMO Insects is controversial and must be tested thoroughly to ensure there are no negative repercussions to the environment. Yet, even with rigorous, controlled experiments, there remains great uncertainty about whether an ecosystem will be disrupted. Moreover, many of these technologies are patentable and have a large propensity for monetary gains. As such, researchers and companies should be forthright about the limitations of these technologies while consulting local governments and citizens to ensure the financial incentives are not prioritized over the interests of communities.

All the above-described genetic and biological control measures rely on our understanding of host-virus interactions at the molecular level. As our knowledge of molecular interactions expands, our ability to mitigate viral spread will follow.

## 1.4. Vector immunology: immune pathways

For DENV to replicate within the insect vector, it must avoid or evade components of the innate immune system. To ensure passage to a new host, DENV must successfully replicate within cells and move throughout the body cavity of the insects towards the salivary glands. Invertebrates lack an adaptive immune system and rely exclusively on the innate immune response to eliminate pathogens. The first critical step in initiating an immune response is distinguishing pathogen molecules from self. Pathogens are recognized through conserved molecules known as pathogen-associated molecular patterns (PAMPs) (Ankit Kumar et al., 2018). PAMPs bind to pattern recognition receptors (PRRs), initiating signalling cascades connected to innate immune responses. Signalling pathways implicated in DENV immunity are Toll, JAK-STAT, IMD, RNAi, apoptosis, and autophagy (Fig. 1.4). Products of these pathways, such as antimicrobial peptides (AMPs), may interfere with pathogen replication to control or eliminate infections.

The above-listed immune pathways were initially described as responses to bacterial, fungal, and protozoan infections. Their functions in viral immune responses are less well understood. Additionally, viruses are intracellular parasites, and spatial differences between viral and other parasitic infections make soluble effector molecules such as AMPs less functional. Nonetheless, these same pathways appear to manage viral infections (Fig. 1.4), albeit with different relative importance. Traditionally, these pathways have been thought to act linearly and respond to a limited set of pathogens. However, new research shows extensive crosstalk between these pathways and demonstrates they are likely active in response to a diverse range of pathogens (Sim et al., 2014, Kageyama et al., 2019).

### 1.4.1. Toll pathway

The Toll pathway is a member of the NF-κB family and is conserved across vertebrates and invertebrates. NF-κB signalling is central to developmental, metabolic, and immune function (Gilmore & Wolenski, 2012; Tikhe & Dimopoulos, 2021). Toll pathway activation begins with a ligand, Spatzle (spz), binding to the Toll receptor. For spz to become active, it requires proteolytic processing following PRRs binding to PAMPs. After cleavage, the c-terminal domain is free to bind the receptor. Once spz is

bound, the signalling cascade initiates through the binding of MyD88 to the intracellular domain of the Toll receptor. MyD88 acts as a scaffold for a kinase protein Pelle, which phosphorylates cactus, a negative regulator of the pathway. Cactus phosphorylation targets it for degradation liberating the transcription factor, Rel1. Free Rel1 then translocates to the nucleus promoting the expression of effector AMP genes.

The Toll pathway was originally implicated in the immune response to fungal pathogens, and Gram-positive bacteria, but has since shown to be activated during infections with DENV (Xi et al., 2008). Transcriptomics analysis of insects inoculated with DENV showed increased expression of Toll-related genes such as spz and Rel1 (Xi et al., 2008). Moreover, alterations in pathway function produced significantly different viral titres after blood feeding challenge (Xi et al., 2008).

### 1.4.2. Janus kinase signal transducer and activator of transcription (JAK-STAT)

The JAK-STAT signalling cascade is a well-conserved pathway from arthropods to humans and has many functions in cell maintenance, homeostasis, development, and immunity (Seif et al., 2017). JAK-STAT was first identified in *Drosophila melanogaster* while studying developmental dysfunction and is now recognized for its antiviral function (Ankit Kumar et al., 2018). The receptor is a transmembrane protein, Dome, which has Janus kinases bound to the intracellular portion of the receptor (Ankit Kumar et al., 2018; Tikhe & Dimopoulos, 2021). Upon ligand binding, receptors dimerize and initiate multiple phosphorylation events recruiting binding of STAT proteins. STATs are transcription factors activated through phosphorylation and dimerization by Janus kinases. Active STAT transcription factors translocate into the nucleus to regulate the expression of target genes.

Many proteins in this pathway have not been resolved in *Ae. aegypti* (Ankit Kumar et al., 2018; Tikhe & Dimopoulos, 2021). In *D. melanogaster*, the ligand has been identified as unpaired (Upd) and has three isoforms. In *Ae. aegypti,* the ligand has not been identified (Tikhe & Dimopoulos, 2021). Nonetheless, studies suggest the JAK-STAT pathway has crucial antiviral action. Overexpression of the receptor Dome or the Janus Kinase protein Hop in the mosquito fat body showed decreased susceptibility to DENV (Jupatanakul et al., 2017). Further, transcriptomics of insect midguts after

infection with Zika virus demonstrated increased expression of JAK-STAT immune pathway genes (Angleró-Rodríguez et al., 2017).

### 1.4.3. Immune Deficiency (IMD) Pathway

Akin to many other pathways, seminal work uncovering IMD pathway function was primarily performed in *D. melanogaster* in response to infection with Gram-negative bacteria. The mosquito IMD pathway was initially characterized in *Anopheles gambiae* in response to the malaria parasite plasmodium. Since, activation has shown antifungal and antibacterial properties (Garver et al., 2012; Meister et al., 2005; Ramirez et al., 2019).

The receptors for the IMD pathway are known as peptidoglycan recognition proteins (PGRPs), which bind the peptidoglycan component of bacterial cell walls. PGRPs can be categorized based on location, size, and activity. At present, there are seven identified PGRPs encoded in the *Ae. aegypti* genome, although each may have multiple isoforms (Wang & Beerntsen, 2015). The IMD pathway is stimulated through peptidoglycan binding to a transmembrane PGRP, causing the recruitment of numerous scaffold proteins, including Fadd, Imd, and Dredd. The negative regulator, Caspar, is inactivated through a series of ubiquitination and phosphorylation events, liberating an NF-κB transcription factor, Rel2. Activated Rel2 translocates to the nucleus to induce the expression of genes, including AMPs (Tikhe & Dimopoulos, 2021).

The Imd pathway's involvement in viral infections appears limited (Angleró-Rodríguez et al., 2017; Barletta et al., 2017; McFarlane et al., 2014). In managing Sindbis virus, Imd aids in controlling the infection indirectly through modulation of the microbiota. Imd may function in a supportive role, where activation modulates other pathways through crosstalk.

### 1.4.4. RNA interference

Viruses are primarily intracellular pathogens, rendering secreted immune factors less effective in managing the infection. RNA interference (RNAi) is thought to have evolved to combat this through sensing and degrading viral RNA within cells. Initially discovered in *Caenorhabditis elegans,* RNAi is the most effective innate antiviral

pathway and contributes greatly to clearing infections (Fire et al., 1998). There are three known RNAi pathways, small interacting RNA (siRNA), p-element induced wimpy testis interacting RNA (piRNA), and micro-RNA (miRNA).

siRNA is the primary antiviral division of the RNAi pathway and is triggered by the presence of dsRNA in the cytoplasm (Olson & Blair, 2015). Double-stranded RNA (dsRNA) is not present in eukaryotic biology but is an intermediate during viral genome replication and thus can be a reliable signal of viral presence. Sensing of viral dsRNA occurs via a protein complex, Dicer, which binds and cleaves dsRNA into 19-22 bp siRNA segments (Olson & Blair, 2015). siRNAs are loaded onto the RNA-induced silencing complex (RISC), where Argonaute2 uses siRNAs as a guide for degrading complementary RNA present in the cell (Olson & Blair, 2015). siRNAs effectively target viral genome RNA before it can be packaged into viral particles and exit the cell.

piRNA is a less well-resolved RNAi pathway. In animals, piRNA functions to prevent transposons, or 'jumping genes', which can be detrimental to genome stability (Joosten et al., 2021). In Drosophila, piRNA prevents transposon mobilization, but in addition, piRNAs undergo 'ping-pong' amplification that expands the piRNA library. For both animals and Drosophila, piRNAs are only observed in germline tissues to preserve the genome (Joosten et al., 2021).

The mechanism of piRNA function in *D. melanogaster* is as follows. Pre-piRNAs are generated by cleavage of piRNA precursors derived from the genome. The Zucchini enzyme processes the pre-piRNA with endonuclease activity and loads them onto the PIWI protein Aubergine (Aub). Aub locates and cleaves transposon mRNA with complementary sequences to the piRNA loaded. Cleaved fragments are attached to Argonaute3 (Ago3), which creates a positive feedback 'ping-pong' loop to generate multiple copies of active piRNAs.

In *Ae. aegypti,* piRNA functions similarly to *D. melanogaster,* with some crucial distinctions (Joosten et al., 2021). First, piRNA expression is observed in somatic and germline tissues. Second, piRNAs interact with viral RNA, and mosquito piRNA clusters within the genome, due to the high number of inserted non-retroviral sequences in the mosquito genome (Suzuki et al., 2017). Finally, *Ae. aegypti* contains an expanded repertoire of PIWI-proteins, possibly indicating enhanced importance. Taken together,

these results suggest an expanded role of piRNA in mosquitoes for managing viral infections. The piRNA pathway has been speculated to function as a form of immune memory whereby inserted viral sequences may guide degradation upon reinfection (Castillo-Méndez & Valverde-Garduño, 2020; Varjak et al., 2018). Nevertheless, the antiviral activity of the pathway has not been demonstrated conclusively. piRNA knockdown has been shown to influence Semliki Forest virus replication in cells, primarily associated with the PIWI4 protein (Schnettler et al., 2013).

Lastly, miRNAs regulate post-transcriptional gene expression and significantly affect development, metabolism, and host-parasite interactions (Feng et al., 2018). miRNAs are approx. 22nt long and arise from stem-loop pre-miRNA structures cleaved by Drosha and Dicer. The nucleotide sequences are loaded onto RISC complexes and guide mRNA cleavage by Ago1. The reduction in mRNA concentration is what elicits the effects on cellular processes.

The effects of miRNAs on parasitic infections are primarily related to their impact on development (X. Feng et al., 2018). However, certain miRNAs expression changes during a response to viral infection (Campbell et al., 2014; Saldaña et al., 2017), suggesting a viral defence mechanism related to miRNA, but this has not been extensively shown.

### 1.4.5. Autophagy and Apoptosis

Apoptosis is a controlled mechanism of cellular death that responds to a physiological signal. This process differs from other cell death mechanisms, such as necrosis, as apoptosis is a programmed state acting to produce a positive result.

Many physiological states induce apoptosis, one of which responds to a pathogenic infection, whereby infected tissue is sacrificed to minimize pathogen replication. Apoptosis occurs through the action of two families of caspases, initiator and effector caspases (Cooper et al., 2007; Cooper et al., 2007, 2009; Ocampo et al., 2013). Initiator caspases mediate the signal to undergo apoptosis, and effector caspases execute degradation of downstream products leading to cell death (Cooper et al., 2007; Cooper et al., 2007, 2009; Ocampo et al., 2013). In *Ae. aegypti*, one initiator caspase is Aedronc which activates the effector Caspases Casps 7 and Casps 8 (Cooper et al.,

2007; Eng et al., 2016). These caspases are inhibited by the inhibitor of apoptosis protein (IAP) which is tightly controlled to prevent unwanted commitment to apoptosis and cell death.

Autophagy is a cellular process that recycles cellular components to maintain homeostasis and has functions in immunity, development, and disease (Brackney et al., 2020). During autophagy, damaged cellular organelles, misfolded proteins, and foreign materials are targeted for degradation by sequestration into specialized double-membrane vesicles called phagosomes (Brackney, 2017; Brackney et al., 2020). The phagosome fuses with a lysosome to degrade the contents via acidification (Brackney, 2017; Brackney et al., 2020). Contents are targeted for degradation through a selective process using polyubiquitination, or bulk autophagy, where large quantities of cytoplasmic material are encased by the phagosome membrane (Brackney et al., 2020).

Apoptosis and autophagy may be intertwined, as apoptosis-related genes show regulation of autophagy in viral infections (Brackney et al., 2020; Eng et al., 2016; Ocampo et al., 2013). Mammalian experiments have demonstrated that autophagy is a significant driver of infection through alterations in lipid metabolism (Heaton & Randall, 2010; Lee et al., 2008). In mosquito experiments, this relationship is less clear (Brackney et al., 2020). Our group has demonstrated that populations with differing susceptibility to DENV have differential expression of apoptosis-related genes and that pro-apoptotic genes partially contribute to a refractory phenotype (Ocampo et al., 2013). More work is needed to fully elucidate the role of apoptosis during DENV infection and unwind the contribution of autophagy, given the redundancy in the two pathways.

## 1.5. *Aedes aegypti*-DENV compatibility

### 1.5.1. Viral Tropism

Viruses are simple machines with genomes often in the thousands of bases encoding relatively few proteins. For instance, the DENV genome encodes only ten proteins to execute all functions necessary for replication (de Borba et al., 2019). Given the size of the DENV genome, it is remarkable that the virus can infect both invertebrates and vertebrates.

Tropism is the capacity of a pathogen to infect a specific organism, tissue, or cell type; tropism influences host-pathogen specificity. Without the relevant factors present, a pathogen cannot replicate and spread. Viral tropism is primarily contingent on entry into the cell (Nomaguchi et al., 2012). However, numerous positive and negative factors need to be met for successful infection, including evasion of the host's immune system.

During DENV infection in mosquitoes, the virus can be found replicating in numerous tissues, including midgut, salivary, fat body, haemocytes, and nervous tissue, highlighting its nearly ubiquitous infection strategy (Reyes-del Valle et al., 2014; Salazar et al., 2007). Interestingly, DENV is highly specialized for *Aedes* sp. as other mosquito genera cannot be infected or are infected at a low rate. For the virus to infect a diverse range of tissues, the tissues likely share common receptors for the virus to enter the cell. In fact, numerous molecules have demonstrated involvement. Three molecules identified in mosquito cell culture experiments are heparin sulfate, the laminin receptor, and Prohibitin (Reyes-del Valle et al., 2014). The relative contribution of each of these to viral uptake is unknown. In human cells, a receptor on dendritic cells, DC-SIGN, has been shown to mediate uptake (Guzman & Harris, 2015). The virus enters through clathrin-dependent receptor-mediated endocytosis once bound to the cell's surface (Guzman & Harris, 2015). Upon acidification of the endosome, viral envelopes fuse with the endosomal membrane and viral RNA is liberated into the cytoplasm. With each stage of viral passage (binding to the receptor, endosomal transport, and viral RNA liberation), the virus must interact the innate immune system.

The pathways described above likely influence host-pathogen specificity and alter barriers to infection (MIB, MEB, Salivary barriers). Each barrier represents a possible bottleneck the virus must overcome to ensure passage to the vertebrate organism. These barriers likely represent areas where the virus is most susceptible to the organism's immune responses. Additionally, there are stochastic aspects of infection. For example, if a population possesses a MIB, all insects will not be resistant to infection (Barón et al., 2010; Ocampo & Wesson, 2004; Tabachnick, 1982). The incomplete penetrance of refractory phenotypes may partly be due to the strong temporal and spatial requirements for immune responses and infections.

### 1.5.2. Our Previous Studies—Naturally Refractory and Susceptible populations in the field

Areas of high viral prevalence are likely to develop vector populations with a spectrum of competence due to increased selection pressures; one such area is Cali, Colombia. In this area, ~70 % of female *Ae.* aegypti are susceptible to DENV and transmit all four DENV serotypes, while ~30% are refractory and do not transmit the virus.

We are uniquely situated to study the differential immune responses of *Ae. aegypti* in populations that are susceptible or refractory to DENV due to our collaborations with researchers in CIDEIM in Colombia. We have characterized these strains through our collaborations and identified both MIB and MEB barriers. The relative percentage of mosquitoes with each phenotype varies based on region, and pupae or adults with different phenotypes can be collected from the same oviposition site. These strains have been laboratory-reared and selected for maximal resistance and susceptibility.

Using a method of isofemale selection, three populations were obtained (Caicedo et al., 2013), a hyper-susceptible population (Cali-S, 96.4% susceptible at generation 19), a refractory midgut infection barrier population (Cali- MIB, 40% refractory at generation 16), and a refractory midgut escape barrier (Cali-MEB, 44.1% refractory at generation 15). Interestingly, refractory populations initially showed a stark increase in viral resistance, which rapidly levelled off. An asymptotic resistance curve may be due to negative costs associated with immune responses toward the virus. Reportedly, refractoriness in the Cali-MIB strain has increased to 47% (Ocampo et al., 2013) since the initial publication of lab-reared insects. Understanding the mechanisms of VC variation between these strains may hold the key to developing resistant populations or antiviral therapeutics.

These populations have been studied extensively through various methods. First, we hypothesized that Cali-MIB might eliminate DENV through apoptosis (Cooper et al., 2007). Using suppressive subtraction hybridization assays, we demonstrated significantly higher expression of apoptosis-related genes in Cali-MIB than in Cali-S, although not enough to eliminate transmission (Ocampo et al., 2013). Additionally, RNAi targeting components of the apoptotic pathway revealed that apoptosis is a significant

contributor to a refractory phenotype (Ocampo et al., 2013). The apoptotic antiviral response is independent of the DENV serotype, albeit in differing amounts (Serrato et al., 2017). Next, RNA-seq approaches were used to identify differentially expressed genes between the strains (Coatsworth et al., 2021). Genes that were identified by microarrays (Caicedo et al., 2019) and RNA-seq (Coatsworth et al., 2021) were transiently knocked down (KD) to identify functionality (Caicedo et al., 2019). While multiple genes altered the phenotype during infection, none were able to replicate the entire phenotype. Finally, we theorized that the microbiota of the strains might contribute to viral susceptibility, as demonstrated previously (Dennison et al., 2014). We performed 16s rRNA profiling on Cali-S and Cali-MIB (Coatsworth et al., 2018). Unexpectedly, no differences in the abundance of bacterial communities were observed. In the microbiota study, it is worth noting that many of the bacteria were identifiable to the family or genus level, and many were not identified by the BLAST analyses, which may have missed essential differences in the microbial population within these strains.

Although a significant understanding of viral susceptibility has been gained, a complete understanding of viral resistance remains elusive, likely due to the combinatorial nature of host-pathogen interactions. Future studies should elucidate the interplay between genes, expression profiles, and proteins to discern how viral resistance is derived. To that end, we have studied the metabolic differences between Cali-MIB and Cali-S to understand the mechanism of viral replication better.

## 1.6. Metabolomics

### 1.6.1. Background

Bioinformatics has generated massive interest in recent decades and catalyzed the development of the omics sciences. The expansion of omics into standard research techniques is mediated by decreasing data storage costs, computer processing speed, and computational methods to accommodate 'Big Data'. The size of data produced with omics experiments exacerbates these issues, and we increasingly rely on modern statistical methods to interpret our findings. Notwithstanding, the omics sciences have revolutionized how we do research.

Genomics, transcriptomics, proteomics, and metabolomics are the most common omics methods. Genomics involves reading and assembling the genetic material of an organism. The genome is relatively static and, therefore, can provide little contextual data during an environmental challenge. In contrast, the transcriptome, proteome, and metabolome readily change in response to environmental conditions, the most dynamic being the metabolome. Metabolomics quantifies the metabolome by measuring small molecules (<1500 daltons) present under differing treatments (Lamichhane et al., 2018).

Metabolomics is an extremely powerful omics science due to the high sensitivity of metabolites to environmental perturbations. Additionally, metabolomics can be considered a bottom-up approach, whereby the genome, transcriptome, and proteome mediate the metabolic reactions. Therefore, the metabolome can indicate the cell's physiological state at a given time. Until recently, metabolomics was highly laborious and had low analysis depth and quality, providing little information. However, with new analysis methods, better statistical pipelines, and extensive databases, metabolomics has emerged as a viable and powerful research technique.

Metabolomic experiments can broadly be categorized into targeted and untargeted methods (Roberts et al., 2012). Targeted approaches measure a few previously annotated metabolites that have demonstrated prior significance, whereas untargeted approaches attempt to measure the entire metabolome and provide an overview of the metabolic environment (Gertsman & Barshop, 2018; Roberts et al., 2012). A subset of untargeted metabolomics uses comparative metabolomics or metabolic fingerprinting to identify changed metabolites in response to treatment. Metabolites are extracted, identified, and quantified from tissues or organisms upon treatment. Significantly changed metabolites are flagged as potential markers of phenotypes. Untargeted metabolomics is termed hypothesis generating, as the inferences must be experimentally validated.

A typical experimental workflow can be broadly divided into two parts, data acquisition and analysis. During data acquisition, metabolites are extracted and quantified. First, samples must be separated into groups and treated according to the experimental design. For example, two populations may be separated based on differing responses to an environmental stressor. Next, the metabolome is extracted and quenched. Quenching halts metabolic reactions so that there is little change or

degradation to the metabolites, aiming to provide the most accurate snapshot of metabolism at a timepoint. Finally, separation methods divide metabolites based on physical properties and quantify them using sensitive analytical instruments.

There are numerous options for analytical instruments to use when performing metabolomics. Some of the most commonly used are liquid chromatography-mass spectrometry (LC-MS), gas chromatography-mass spectrometry (GC-MS), and nuclear magnetic resonance (NMR). Typically, NMR is used for compound identification but not for high-throughput experiments due to the inability to detect compounds in low concentrations (Emwas et al., 2019). CG-MS and LC-MS are more sensitive and are thus used more frequently for untargeted projects (Emwas et al., 2019). However, when performing GC-MS, compounds must be readily volatile for detection (Fiehn, 2016), a significant drawback for its use. Alternatively, LC-MS detects compounds present in low concentrations while maintaining high metabolome coverage. LC-MS studies are not without limitations. Metabolites with differing chemical properties exist in one solution and react differently with the chosen instrument (Zhao & Li, 2020), leading to difficulties in quantifying the concentrations of a given metabolite. However, chemical derivatization can be utilized to overcome quantification issues.

Chemical derivatization involves reacting a subsample with a reagent that targets a specific chemical group (Zhao & Li, 2020). Some common chemical groups targeted are amines, phenols, carboxyls, and hydroxyls. Once the subsamples react with the various reagents, they are analyzed by traditional LC-MS. Derivatization has many benefits, including enhanced metabolite detection, increased separation by chromatography, improved metabolite stability, and better quantification (Zhao & Li, 2020), making it ideal for metabolite quantification with small tissue volumes such as mosquito midguts.

### 1.6.2. Metabolomics in Vector Biology

Metabolomics has been used successfully in mosquito studies to uncover and identify small molecules influencing growth and disease transmission, with many studies investigating arbovirus replication (Chotiwan et al., 2018; Hoxmeier et al., 2015; Koh et al., 2020; Mamai et al., 2014; Vial et al., 2019, 2020). Moreover, numerous reviews have

been written on this topic in the last decade, demonstrating the expansion of this field (Horvath et al., 2021; Nunes & Canuto, 2020; Romagnolo & Carvalho, 2021).

DENV has been a significant focus of metabolomics research in vector biology, likely due to the increased transmission of the virus coinciding with the advancement of metabolomics methods. There are increased lipid concentrations and diversity post-DENV infection (Chotiwan et al., 2018). Changes to fatty acyls, glycerophospholipids, and sphingolipids were observed along with markers of mitochondrial dysfunction (Chotiwan et al., 2018). These findings agree with other studies indicating significant phospholipid remodelling during infection (Vial et al., 2019, 2020). Metabolomics has been used to elucidate Wolbachia-mediated viral resistance. Again, lipid modulation appears altered but does not directly mediate viral resistance (Koh et al., 2020). These studies point to energetics and membrane composition as being influential in DENV infection. However, to our knowledge, no research has investigated metabolomic differences in populations with divergent susceptibility to DENV.

## 1.7. Objectives of this work

### 1.7.1. Molecular interactions of virus and host

Until effective vaccines or therapeutics are developed, millions will suffer from DENV infection every year. Vector control remains our greatest defence to curb viral spread but requires an intricate understanding of host-pathogen interactions at the molecular and population level. At present, we do not understand the mechanisms of viral resistance or susceptibility underlying vector competence and transmission. As stated previously, our research on susceptible and resistant populations has yielded an incomplete picture of what drives viral replication. Understanding the intimate interactions between *Ae. aegypti* and DENV, especially mechanisms that the virus uses to evade, avoid, or turn off the innate immune systems of the vector, are crucial to understanding and exploiting these interactions to reduce mosquito-DENV compatibility.

The proposed metabolomic investigation of DENV-infected *Ae. aegypti* that are susceptible or resistant to infection will provide a unique biochemical understanding of viral infection dynamics in these strains and will elucidate important compounds and molecules enhancing or resisting viral infection.

### 1.7.2. Thesis objectives

Previous investigations have demonstrated metabolic constituents changed during viral infection; however, none have been performed in populations with differing susceptibilities. We hypothesize that lipid metabolism will be a significant driver of viral resistance due to the involvement in viral uptake. Additionally, molecules implicated in mitochondrial function, such as acylcarnitines, may be significant due to the energetics of viral replication. Lipid metabolism and mitochondrial function are hypothesized to contribute to the development of a MIB, preventing the virus from entering or replicating within midgut cells. The main objectives of this thesis are as follows:

1. Use bioinformatics and statistical methods to identify small molecule changes in response to DENV infection in two populations with differing susceptibility to the virus.

2. Investigate the biological context of changed molecules to propose a mechanism of viral replication and immunity.

The hope is that the results of metabolomic and bioinformatic investigations will be experimentally validated for causation and may provide new information that might be used in subsequent genetic modification designs to generate lines of DENV-refractory *Ae. aegypti*.

## 1.8. Figures

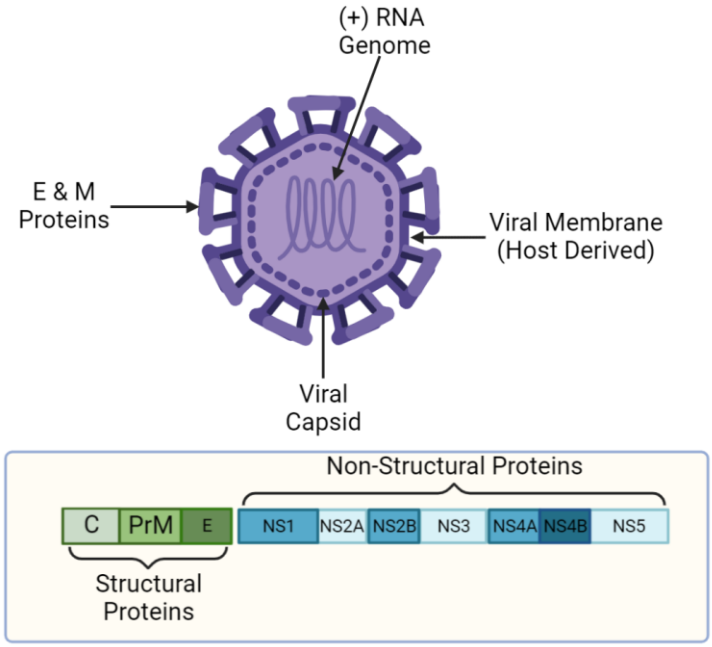


**Figure 1.1. Dengue virus structure and genes, adaped from (Hottz et al., 2011).**

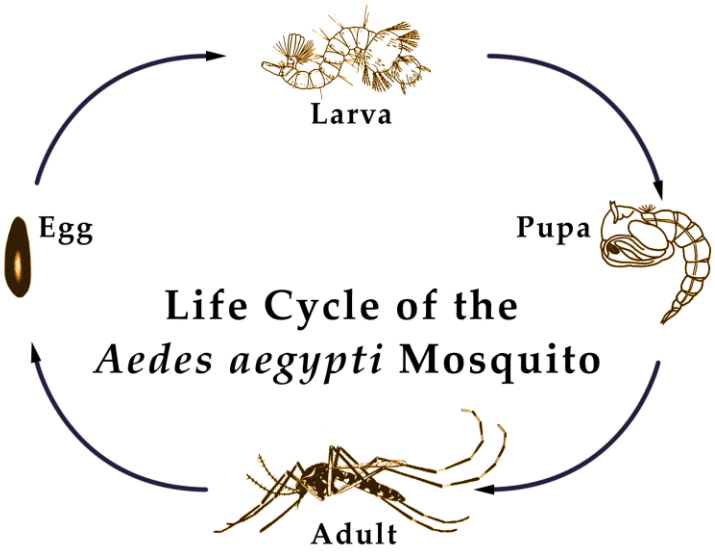


**Figure 1.2. The Life cycle of Aedes aegypti, Center for Disease Control Public health Image Library (https://phil.cdc.gov/default.aspx)**

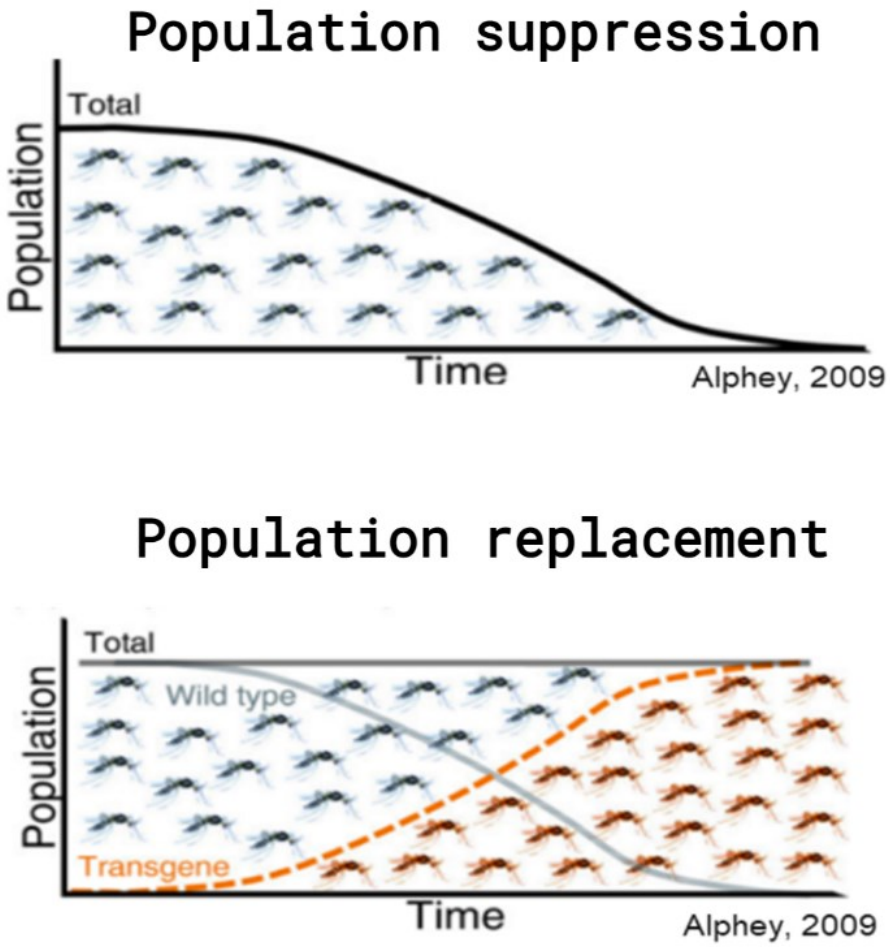


**Figure 1.3.** **Concepts in modifying population structures of mosquitoes to reduce the transmission of arboviruses to humans. In Population Suppression (A) the concept is to essentially eliminate all mosquitoes while Population Replacement (B) would replace the wild-type mosquitoes with strains that cannot support and transmit the pathogen.**

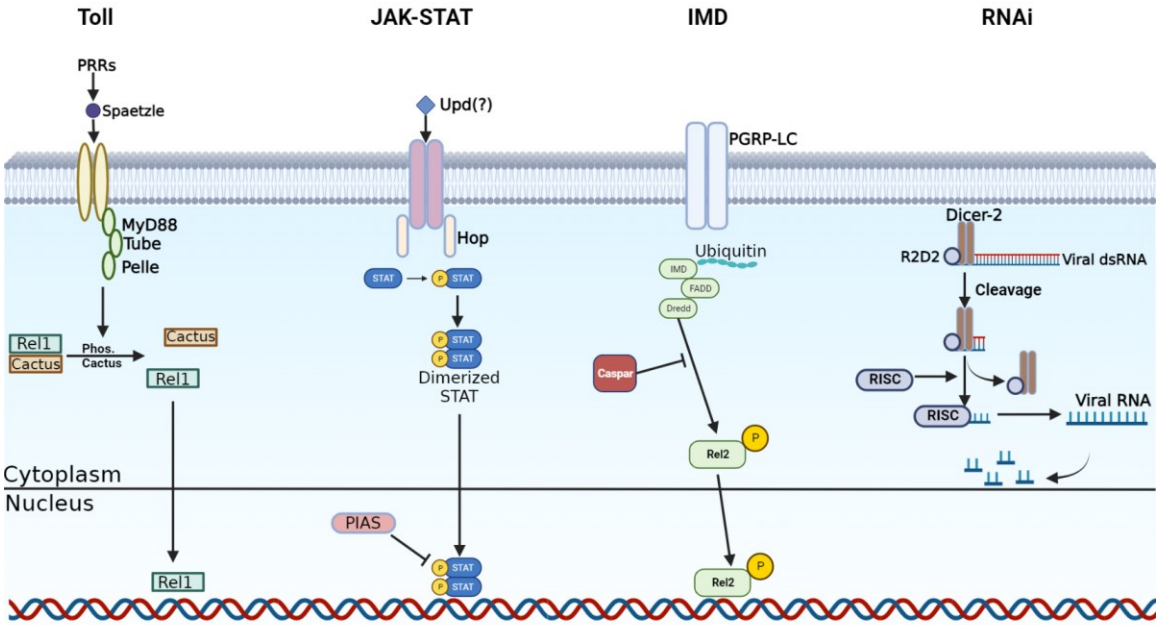


**Figure 1.4.** **Mosquito immune pathways. The major immune pathways involved in response to dengue virus; Toll, JAK-STAT, IMD, RNAi. Figure modified after (Sim et al., 2014).**

## Connecting Statement 1

In chapter one, we discussed the prevalence of DENV, the vectors that transmit DENV, and the molecular events that can contribute to or hinder viral infection in *Ae. aegypti*. Additionally, we introduced two strains of *Ae. aegypti* identified in Cali, Colombia, that are refractory (Cali-MIB) or susceptible (Cali-S) to DENV infection. Despite considerable effort from us and others to elucidate the molecular events governing DENV immunity, the mechanisms present in refractory insects are poorly understood. To supplement the currently available data on the differences between Cali-MIB and Cali-S populations, we chose to investigate the global metabolic differences between the two strains when challenged with DENV, using highly sensitive chemical isotope labelling liquid chromatography-mass spectrometry. The next chapter describes this procedure and the differently regulated metabolites between the Cali-MIB and Cali-S strains.

# Chapter 2.

# Metabolomics analysis of two strains of *Aedes aegypti* that differ in their ability to transmit Dengue viruses.

## 2.1. Abstract

*Aedes aegypti* is the principal vector for numerous disease-causing human flaviviruses, including dengue, Zika, yellow fever, and West Nile. Millions each year are infected with these viruses causing significant morbidity and mortality; there is an urgent need to limit infections. However, not all female *Aedes aegypti* will transmit these viruses. Some insects possess intrinsic immunity capable of managing and eliminating flaviviruses upon ingestion with an infected blood meal. We have identified a population of *Ae. aegypti* in Cali, Colombia, that do not transmit dengue virus by preventing viral replication in the midgut tissue (Cali-MIB). Here, we utilized chemical isotope labelling liquid chromatography-mass spectrometry to survey the midgut metabolome of Cali-MIB and susceptible insects (Cali-S) to observe differences in metabolism in response to dengue virus. Moreover, we surveyed the metabolome at three time points post-infectious blood meal, 18, 24, and 36 hours to observe temporal patterns associated with viral resistance and correlate various metabolic pathways and compounds to the resistant phenotype. This research expands our understanding of viral infection mechanisms and highlights novel hypotheses to be tested.

## 2.2. Introduction

Vector-borne diseases account for nearly one-fifth of all infectious diseases worldwide, disproportionately affecting people in the developing world (World Health Organization, 2020). The mosquito is assuredly the most important vector of parasites causing human disease, transmitting the parasites causing malaria, in addition to multiple flaviviruses, including dengue, Zika, Yellow Fever, and West Nile. Collectively, these pathogens are responsible for over 700 000 deaths annually (The Lancet Global Health, 2017).

Historically, malaria has been the most significant vector-borne threat to human health; more than 2000 people died each day from malaria in 2002 (Sachs & Malaney, 2002). However, cost-effective preventative measures such as bed nets and antimalarials have significantly reduced the disease burden (Lindsay et al., 2021). In contrast, dengue virus (DENV) infections have been increasing rapidly; globally, there has been an 800% increase in the last two decades, with over half of the world's population living in areas with circulating dengue virus (World Health Organization, 2022). Currently, no pharmaceutical interventions are available for DENV infection, and no broadly neutralizing vaccines are commercially available. Thus, the elimination of the mosquito vector has typically been the focus of disease control programs.

The increase in DENV cases is in part facilitated by the rising global temperatures and the widespread distribution of mosquito vectors (Kraemer et al., 2019). DENV is primarily transmitted by female *Aedes aegypti* and, to a lesser extent, by *Aedes albopictus* (Moncayo et al., 2004). Two approaches are commonly deployed to control the spread of DENV: population suppression or population manipulation. Population suppression attempts to reduce the number of insects to lessen the chance of transmission. Historically, this has been accomplished through insecticides, but these programs may affect off-target organisms and often have limited long-term efficacy as insecticide resistance can develop in mosquito populations (Maciel-de-Freitas & Valle, 2014). More modern approaches to population suppression include genetically modified mosquitoes, including those from Oxitec that carry a lethal gene. Modified males are released to mate with wild-type females, and their offspring die (Carvalho et al., 2015). The Oxitec mosquito approach requires the repeated release of lab-reared insects and is

an expensive enterprise that works best in an island setting where there are few immigrant mosquitoes to replenish the population.

Alternatively, population manipulation approaches aim to reduce the population's vector competence and limit the capacity for an insect to transmit the pathogen (McGraw & O'Neill, 2013). One such approach uses the intracellular bacterium *Wolbachia sp.*, to reduce vector competence. Mosquitoes that have been transinfected with *Wolbachia sp.* have a diminished capacity to transmit DENV (Walker et al., 2011). The *Wolbachia* sp. used in mosquito studies is maternally transmitted. When a non-*Wolbachia*-carrying female mates with a *Wolbachia*-infected male, the offspring are inviable; however, when the opposite occurs, the offspring will all possess *Wolbachia* sp. and subsequently have reduced DENV competence (Turelli & Hoffmann, 1991; Walker et al., 2011). This phenomenon, known as cytoplasmic incompatibility, allows *Wolbachia* to spread throughout a population (Turelli & Hoffmann, 1991; Walker et al., 2011). There has been concern over whether *Wolbachia* is the panacea it appears to be. For instance, some studies show that *Wolbachia* may not block DENV infection under all conditions (King et al., 2018). More research is needed to ascertain the mechanism of viral resistance related to *Wolbachia* infection in mosquitoes, and a fundamental molecular understanding of viral-host interactions will supplement this.

Despite their role as the principal vectors for DENV, not all female *Ae. aegypti* will transmit DENV. In some areas, proportions of natural field-collected female *Ae. aegypti* are refractory to DENV and can eliminate the virus before it can be transmitted. In Cali, Colombia, ~30% of field-collected insects are refractory to all four DENV serotypes (Barón et al., 2010; Caicedo et al., 2013; Ocampo et al., 2013; Ocampo & Wesson, 2004). These mosquito strains are sympatric, and eggs from the susceptible and refractory phenotypes can be collected from the same oviposition trap. Field-derived laboratory-reared colonies have been selected from these field populations for increased resistance, with ~50% refractory to DENV (Barón et al., 2010; Caicedo et al., 2013; Ocampo et al., 2013). Naturally resistant insects are a valuable research tool as they possess the necessary molecular factors to eliminate the virus. These resistant populations are the focus of the present study.

The mosquitoes identified in Colombia have three described natural barriers to DENV; A midgut infection barrier (MIB), a midgut escape barrier (MEB), and a salivary

gland infection barrier (Ocampo et al., 2013). Midgut barriers halt viral replication earlier in viral development by preventing replication within the midgut tissues (MIB) or preventing viral release from the midgut (MEB) (Ocampo et al., 2013). Although these barriers were initially described within laboratory-reared and selected populations, we have identified MIB and MEB within our field-derived insects providing a more natural context to investigate their molecular characteristics (Ocampo et al., 2013). We have denoted these populations as Cali-S (a naturally susceptible strain), Cali-MIB, and Cali-MEB.

The mechanisms governing viral resistance have been investigated previously by us and others. We have studied resistance in the Cali, Colombia populations in detail through suppressive subtractive hybridization assays (Barón et al., 2010), microarray analysis (Caicedo et al., 2019), comparative transcriptomics (Ocampo et al., 2013), RNA-seq (Coatsworth et al., 2021), RNAi applications (Caicedo et al., 2019) and microbiota studies (Coatsworth et al., 2018). These experiments have highlighted immune differences between the Cali-S and Cali-MIB strains, including differences in the expression of genes related to apoptosis (Ocampo et al., 2013). However, we have been unable to resolve all the molecular events contributing to the refractory strains. Thus, more research is needed to identify pathways and immune factors related to resistance. Consequently, in the present study, we have utilized midgut metabolic profiling to identify small molecule changes (<1500 Daltons) in the midguts of Cali-MIB and Cali-S females in response to DENV challenge at three timepoints, 18, 24, and 36 hours post blood meal (hpbm). These times were chosen to represent critical viral stages when the virus enters, replicates within, and disseminates from the midgut cells, respectively (Caicedo et al., 2013; Coatsworth et al., 2018, 2021; Ocampo et al., 2013; Serrato et al., 2017).

Until recently, metabolomics was a laborious technique with little utility. However, with modern advances in instruments and databases, metabolomics has become a sensitive omics method that can profile metabolic changes in response to environmental changes to indicate the cell's physiological state at an instance. Therefore, since the time to DENV entry into mosquito midgut cells and replication are extremely short, metabolomics is an ideal method to study DENV infection mechanisms and is the most appropriate omics approach to capture the changes occurring at a molecular level.

Metabolomics experiments follow one of two methodologies. Targeted metabolomics detects and quantifies a limited number of pre-determined important metabolites in response to treatment (Roberts et al., 2012). Untargeted metabolomics does not limit the measured metabolites *a priori* and instead attempts to measure all metabolites present within a sample (Alonso et al., 2015). The latter is typically used for exploratory studies and requires validating metabolites found to be responsive to treatment.

This study uses untargeted metabolomics to identify molecules and pathways altered in the midgut tissues of Cali-MIB compared with Cali-S strains in response to DENV challenge. Ultimately, these altered metabolites and pathways may contribute to the refractory phenotype observed in the field. Metabolomics has been utilized for other disease vectors (Bing et al., 2017) and mosquitoes challenged with DENV (Chotiwan et al., 2018; Koh et al., 2020; Vial et al., 2019, 2020). However, no studies to date have compared the metabolic changes in response to DENV in a naturally refractory or susceptible strain, making this comparative approach uniquely situated to determine novel factors related to DENV immunity in mosquitoes.

Viruses are molecular machines that rely entirely on the host's metabolism for their propagation. This parasitic relationship leads to unusual metabolic demands on host cells during viral replication and assembly. Therefore, we would expect the metabolic profiles among the two strains of mosquitoes exposed to DENV to have compounds present in different concentrations. Previous research has shown that metabolic constituents participating in energy production and mitochondrial function are regularly altered during DENV infection (Chotiwan et al., 2018; Shrinet et al., 2019). Thus, in our screen comparing metabolism between the Cali-MIB and Cali-S strains, we hypothesize that energy-producing metabolic pathways, such as glycolysis and the TCA cycle, will be differently regulated between the two strains.

## 2.3. Materials and Methods

### 2.3.1. Mosquito rearing

Mosquitoes were maintained under standard laboratory conditions (26 +/- 2°C, 12:12 light-dark cycle with 70% relative humidity). Cali-S vs Cali-MIB were reared and selected as described in (Caicedo et al., 2013). Adults were fed a 10% sugar solution.

### 2.3.2. Virus Isolation

*Ae. albopictus* C6/36 HT cells were used to propagate DENV-2 New Guinea C strain. Cells were incubated for 14 days after infection at 32°C in L15 media supplemented with 2% heat-inactivated fetal bovine serum, 1% L-glutamine, and 1% penicillin/streptomycin. Cells and virus were collected in a 15mL centrifuge tube. The infected cell suspension was mixed 1:1 with defibrinated rabbit blood to create an infectious blood meal. Viral titers were quantified in the infectious blood meal and the cell suspension using the method described previously by (Bennett et al., 2002). Viral titers in the suspension ranged from $10^8$ to $10^{8.5}$ TCID50/mL in all oral challenges. These procedures have been described previously (Caicedo et al., 2013, Caicedo et al., 2019, Ocampo et al., 2013)

### 2.3.3. Mosquito Infections

Five-to-eight-day-old female adult *Ae. aegypti,* Cali-S and Cali-MIB, were provided with an infectious blood meal for 2 hours via an artificial pig intestine membrane feeder as described previously (Caicedo et al., 2013; Ocampo et al., 2013). After exposure to blood meals with or without DENV, fully-fed females were transferred to containers (~20 mosquitoes/container) and given a 10% sucrose solution. Containers were maintained under standard laboratory conditions described above.

### 2.3.4. Mosquito Dissections

Midguts from adult female mosquitoes fed on either infectious DENV blood meal or blood alone were dissected on a cold table and immediately transferred to a microcentrifuge tube containing 100% ice-cold methanol. The midguts were dissected

from either Cali-S or Cali-MIB strains, with or without DENV, at 18, 24, and 36 hpbm (Fig. 2.1). Ten midguts were pooled for each treatment and timepoint to obtain adequate tissue mass for metabolite quantification. Each treatment and timepoint was performed in triplicate for a total of 36 samples. Samples were immediately frozen at -80°C after dissection. All samples were transported from CIDEIM in Cali, Colombia, to Simon Fraser University in Burnaby, British Columbia. During transport, samples were kept frozen on dry ice and, upon arrival, were stored at -80°C.

### 2.3.5. LC-MS Analysis

Samples were analyzed at The Metabolomics Innovation Centre (TMIC) in Calgary, Alberta, using Chemical Isotope Labelling Liquid Chromatography Mass Spectrometry (CIL LC-MS). Samples were dried, re-suspended, and chemically labelled as described (Zhao et al., 2022), using 2-channel amine/phenol and carboxyl labelling. LC-MS was done using an Agilent 1290 ultra-high-performance LC (Agilent, Santa Clara, CA) linked to a Bruker Impact II QTOF Mass Spectrometer (Bruker, Billerica, MA). Quality control samples were injected every 15 samples to monitor performance.

### 2.3.6. Data Processing, Cleansing, and Metabolite Identification

LC-MS runs were uploaded to IsoMS Pro 1.2.15 for quality checking and raw data processing (Zhao et al., 2022; Zhou et al., 2014). Peak pairs not present in at least 50% of all samples were filtered and removed. Data were normalized based on the ratio of total useful signals, and missing peak pair values were replaced by a ratio determined by a zero-imputation program.

Metabolite identification was performed using a three-tier approach. The first tier used accurate mass and retention time to search the labelled metabolite library (CIL Library). In the second tier, the remaining unidentified metabolites were searched against a linked identity library (LI Library) and identified on accurate mass and predicted retention time. In the third tier, the remaining unidentified metabolites were putatively identified based on accurate mass only within the MyCompoundID library. Confidence in the correct identification of metabolites is greatest in Tier one, followed by tiers two and three.

### 2.3.7. Data Analysis and Visualization

Metabolite concentration tables were uploaded to Metaboanalyst 5.0 for statistical testing. Samples were auto-scaled prior to statistical testing (mean-centred and divided by the standard deviation of each variable). Significance analysis of microarrays (SAM) was used to identify significantly changed features. The delta value for each statistical test was adjusted to control for the estimated false discovery rate (FDR) at 10% (Tusher et al., 2001). Features that showed greater than expected differences in concentration after controlling the FDR were considered to be statistically significant. Principle Component analysis (PCA) was performed to assess data quality and between-group differences. A concentration table was uploaded to perform pathway analysis using Metaboanalyst 5.0. Compounds were identified and mapped onto metabolic pathways based on name, and data were auto-scaled before analysis. A global enrichment test and relative-betweenness centrality were used to determine a pathways significance. The KEGG *Drosophila melanogaster* was used as a reference pathway library. Data visualizations were constructed using a combination of Metaboanalyst 5.0 and R (v. 4.1.1).

## 2.4. Results

### 2.4.1. Metabolite Detection and Identification

To study the metabolic changes after viral challenge in refractory and susceptible *Ae. aegypti*, we utilized untargeted metabolomics to survey the midgut metabolites at different stages of DENV infection. Midguts of refractory or susceptible insects were extracted at three timepoints post-viral challenge, 18, 24, or 36 hpbm. As controls, refractory and susceptible insects were fed on blood only, and midguts were dissected at the same time points. After dissection, the samples were subject to untargeted metabolic profiling, using chemical isotope labelling LC-MS to identify metabolites and their relative concentrations.

Across all samples, 2192 peak pairs were detected, representing distinct metabolites or features (Table 2.1); herein, metabolite and feature will be used interchangeably. A three-tier approach was used to ID the metabolites (see materials and methods). Metabolites identified in the first two tiers were considered high-

confidence identifications and high-confidence putative identifications, respectively, based on matches with two analytical values (accurate mass and retention time). In tier three, the remaining unidentified peak pairs were searched based on accurate mass alone. Compounds reported in this tier provided putative identifications, and the structures cannot be resolved due to many compounds possessing the same mass. Based on the three-tier approach, 212 (9.7%), 238 (10.9%), and 1485 (67.7%) compounds were identified in tiers 1, 2, and 3, respectively (Fig. 2.1). 1935 of the 2192 detected compounds were identified (tier 1 and 2) or putatively matched (tier 3). Summaries of identification results are presented in Table 2.1 and Fig. 2.2.

Metabolites identified in tiers 1 and 2 were suitable for more detailed analysis, such as pathway analysis, because of the decreased error associated with identification. Alternatively, compounds identified in tier three are used for statistical analysis only because we cannot confidently identify molecules within this tier. Given this limitation, we performed statistical analyses on the full feature set but only considered those metabolites identified in tiers 1 and 2 for more thorough investigations.

### 2.4.2. Tier 1, 2, & 3 Principal Component Analysis

Principal component analysis (PCA) was performed first to assess overall metabolic differences between the Cali-S and Cali-MIB phenotypes and the data quality. PCA is an unsupervised machine learning algorithm which models high-dimensional data in a reduced number of dimensions to capture most of the variance (Vidal et al., 2016). Three comparisons were made for each timepoint; each phenotype was compared to itself with or without DENV challenge (Cali-S vs Cali-S and Cali-MIB vs Cali-MIB), and the DENV-challenged Cali-MIB was compared to DENV-challenged Cali-S strains. The PCA plots can be seen in Fig. 2.3.

The PCA plots of the Cali-S phenotype with or without virus display moderate separation, with 18 hpbm and 36 hpbm having the greatest resolution (Fig. 2.3). Interestingly, far greater separation is observed in PCA of the Cali-MIB strain challenged with DENV compared to Cali-MIB control (Fig. 2.3). In all three timepoints, Cali-MIB insects challenged with DENV cluster closely together, with the narrowest clustering observed at 18hpbm. The PCA plots comparing DENV-challenged Cali-MIB and Cali-S strains display modest separation at 18 and 24 hpbm. However, at 36 hpbm, the

algorithm cannot resolve the two phenotype categories (Fig. 2.3). Insufficient PCA resolution at 36 hpbm aligns with prior knowledge of viral infection dynamics; by 36h, DENV has disseminated from midgut tissues and spread systemically (Caicedo et al., 2013; Coatsworth et al., 2018, 2021; Ocampo et al., 2013; Serrato et al., 2017).

### 2.4.3. Differential Analysis of Metabolites- Tiers 1, 2, & 3

Multiple statistical methods were evaluated to determine significant features, including Benjamini-Hochberg adjusted Students two-sided t-test, significance analysis of microarray (SAM), and partial least squares discriminant analysis (PLS-DA). Features identified by the three methods had considerable commonalities. Ultimately, SAM was chosen because it provides an estimate of the false discovery rate (FDR) through permutations of metabolite sampling (Tusher et al., 2001). The FDR can be set to a specific value using a threshold variable known as delta, which can be specified by the user (Tusher et al., 2001). Although initially developed for microarrays, SAM can be used for multiple testing on high-dimensional data, such as metabolomics (Xia et al., 2009). For our experiments, the delta value for each statistical comparison was set to control the FDR at 10%. Features discussed here as significant have been selected by the model to have greater than expected variance under the null hypothesis after adjustment of the FDR.

Venn diagrams showing a summary of the number of significant features identified with each treatment can be seen in Fig. 2.4. In the Cali-S strain challenged with DENV, 3, 200, and 17 features were identified as significant (SAM FDR<0.1) at 18, 24, and 36 hpbm, respectively. In the Cali-MIB strain challenged with DENV, 154, 125, and 5 features were identified (SAM FDR<0.1) at 18, 24, and 36 hpbm, respectively. Finally, between Cali-MIB and Cali-S strains challenged with DENV, 9, 5, and 0 metabolites were identified as significant (SAM FDR<0.1) at 18, 24, and 36 hpbm, respectively.

The Cali-MIB strain had 162 over-represented metabolites at 18 hpbm, whereas the Cali-S strain had only 4 (Fig. 2.4). Additionally, at 24 hpbm, the Cali-S strain had 204 differently regulated metabolites, whereas Cali-MIB had 131. Interestingly, at 24 hpbm, ~88% of the differently regulated metabolites in the Cali-S phenotype were upregulated

versus ~31% in the Cali-MIB group. This trend continues at 36 hpbm, where ~59% of significant metabolites were upregulated in the Cali-S strain and 0% in Cali-MIB insects.

The number of features identified in the Cali-MIB vs Cali-S strains challenged with DENV is considerably less; this is an expected trend, given that both strains are under the same DENV infection metabolic stress. At 18 hpbm, 16 metabolites were significantly different (SAM FDR<0.1), with a high proportion being upregulated (~88%) (Fig. 2.4). By 24 hpbm, there were fewer metabolites reaching statistical significance (SAM FDR<0.1); seven were identified as different, with ~86% being downregulated in the Cali-MIB (Fig. 2.4).

### 2.4.4. Tiers 1 & 2 Principal Component Analysis

Many features in the full feature set cannot be identified with high confidence; 67.7% of the features were identified in the third tier through accurate mass alone. As such, the remainder of our analysis will focus on those features which can be identified within tiers 1 & 2.

We performed PCA on the reduced feature set to determine if metabolic differences can resolve phenotypic classes. The same three comparisons for each timepoint were performed as above and can be seen in Fig. 2.5. Overall, within-group comparisons (Cali-S vs Cali-S, Cali-MIB vs Cali-MIB) display profile differences shown by separation between the DENV-challenged samples and the controls at all time points (Fig. 2.5). Interestingly, the separation between Cali-MIB DENV-challenged samples from the Cali-MIB controls is more prominent than the same comparison within the Cali-S samples. Additionally, DENV-challenged Cali-MIB samples cluster closer together, showing lower within-group variance than other samples. For the across-phenotype comparison (Cali-MIB B+V vs Cali-S B+V), there is a moderate separation between the two strains challenged with DENV at 18hpbm, which is more prominent at 24 hpbm (Fig. 2.5). However, by 36 hpbm the two strains are indistinguishable by PCA. These results align well with the PCA performed on the full feature set.

### 2.4.5. Differential Analysis of Metabolites- Tiers 1 & 2

SAM was used to identify significantly different metabolites. Venn diagrams depicting the number of changed features and their relative expression levels can be seen in Fig. 2.6. In the Cali-S strain, 2, 43, and 61 features were significantly changed (SAM FDR<0.1) in response to DENV at 18, 24, and 36hpbm, respectively. Across the three timepoints, the proportion of upregulated significant features changed. At 18 hpbm, 50% were upregulated, at 24nhpbm, ~70% of features were upregulated, and at 36 hpbm, 0% were upregulated. Likewise, in Cali-MIB midguts, 49, 7, and 32 features were significantly different at 18, 24, and 36 hpbm, respectively. At 18 hpbm, ~39% of the features were upregulated, by 24 hpbm, 100% were upregulated, and by 36 hpbm, ~16%. Comparing the metabolism of Cali-MIB to Cali-S midguts, 3, 9, and 1 feature were significantly changed (SAM FDR<0.1) at 18, 24, and 36hpbm. At the earliest timepoint, 100% of features were upregulated. All features had reduced concentrations by 24 hpbm and 36 hpbm (Fig. 2.6).

The identities of the top ten significantly identified features can be seen in Table 2.2. Some statistical comparisons had less than ten significant features. In these cases, only the significant features are listed. Moreover, each feature is listed with either a '-DR' depicting down-regulation of that metabolite or '-UR' for metabolites with increased concentration. Heatmaps displaying concentrations of the top 20 features for the refractory compared to the susceptible strain are shown in Fig. 2.7 with hierarchical clustering results above. The remainder of the heatmaps can be viewed in appendix A.

### 2.4.6. Pathways Altered by DENV in the Bloodmeal

Pathway analysis combines multiple metabolites defined into directional metabolic pathways (Ma et al., 2019; Xia et al., 2010). This method uses relative-betweenness centrality and a global enrichment test to determine metabolite changes that have high influence on pathway function. Pathways with large numbers of metabolites affected, or with concentration changes corresponding to high-influence nodes (metabolites), will have a higher significance. This analysis can provide a system-wide understanding of the metabolic changes associated with treatment. The most significantly altered pathways and the number of metabolites changed for the Cali-MIB

vs. Cali-S at 24 hpbm are shown in Fig. 2.8. Raw and adjusted p-values for the pathway analysis can be viewed in Table 2.3.

In Cali-S mosquitoes challenged with DENV, no pathways achieved significance at 18 hpbm, only two at 24 hpbm, and one at 36 hpbm (FDR adjusted *p-value*< 0.1). The Cali-MIB strain showed considerably more reactivity to DENV at the pathway level; at 18, 24, and 36hphm, 17, 7, and 13, pathways showed significance at the 10% level. When comparing across phenotypes, only the 24h timepoint reached statistical significance, with 18 pathways having p-values<0.1 (Table 2.3).

Pyruvate metabolism was the pathway with the lowest adjusted *p-value* (p=0.038331) with four metabolites from our dataset identified within the 22-metabolite pathway (acetate, lactate, pyruvate, fumarate). Interestingly, pyruvate and lactate were the most differentially regulated molecules in the two strains and are counter-regulated; pyruvate has an increase in concentration in the Cali-MIB strain, whereas lactate has a decreased concentration. Arginine metabolism had the second lowest FDR adjusted *p-value* (p=0.038523) and had a high molecule match rate; 9 of the 12 molecules described in arginine metabolism were identified within our dataset (Fig. 2.8). The most significantly altered compounds were L-Ornithine, 2-Oxoglutarate, and L-Citrulline. The Cali-MIB strain had reduced concentrations of L-Ornithine and increased concentrations of 2-Oxoglutarate and L-Citrulline.

### 2.4.7. Metabolic Profiles of blood-fed Cali-MIB and Cali-S

We wanted to determine whether the metabolic changes observed after DENV challenge were specific to DENV or whether Cali-MIB and Cali-S strains differ in metabolic responses to other stressors, such as blood meal alone. To test this, we performed PCA on the profiles of Cali-MIB vs Cali-S samples fed on blood only. The PCA plots for Cali-MIB+blood vs Cali-S+blood at each timepoint can be observed in Appendix B. The PCA plots display a similar trend to those shown for the blood+DENV samples discussed above. At 18 and 24 hpbm, the algorithm can resolve group differences based on variations in the profiles, but at 36 hpbm, the profiles are less differentiated.

We then used SAM analysis to determine features with significantly different concentrations (SAM FDR<0.1) at each timepoint and compared those to features determined to be significant at the same timepoint in the blood+DENV samples. Venn diagrams showing the number of overlapped features can be seen in Appendix B. No common features were observed at any timepoints between Cali-MIB+blood vs Cali-S+blood and Cali-MIB+blood+DENV vs Cali-S+blood+DENV comparisons.

### 2.4.8. Choosing Probable Anti-DENV Metabolites and Pathways

This study's focus was to understand better the metabolic events that may contribute to a refractory phenotype and elucidate how the Cali-MIB strain responds differently to DENV. As such, candidate metabolites and pathways chosen are differently regulated in refractory Cali-MIB midguts compared with Cali-S when both populations were challenged with DENV. Upregulated metabolites have higher concentrations in Cali-MIB samples, and down-regulated metabolites have reduced concentrations. Metabolites with increased concentrations may directly inhibit DENV replication by interacting with viral components or indirectly through alterations in immune responses that prevent DENV replication. Conversely, down-regulated metabolites may aid viral entry, assembly, or exit from the cell.

## 2.5. Discussion

### 2.5.1. Differential Expression Analysis of Metabolites

The ultimate goal of untargeted metabolomics is to identify and quantify all metabolites in a sample. The identification of all metabolites, or complete metabolite profiling, is not possible at this time. Nonetheless, four hundred fifty features were identified with high confidence (Tiers 1 & 2), and an additional 1485 features were putatively identified (Tier 3).

Performing PCA with the full and reduced feature sets allowed us to examine metabolic trends among treatment groups. We were able to distinguish among treatment groups at each time point, except 36 hpbm, when comparing the Cali-MIB and Cali-S strains, both challenged with DENV. Lack of resolution at 36 hpbm aligns well with our biological understanding of DENV infection dynamics. Earlier timepoints during infection

are critical for determining the phenotype (Caicedo et al., 2013; Coatsworth et al., 2018, 2021; Ocampo et al., 2013; Serrato et al., 2017) and by 36 hpbm, the virus has disseminated from midgut tissues into the hemocoel. PCA resolution provided confidence that each strain's metabolic profiles differ and provided the impetus for investigating pathway and metabolite differences. Here we will use the reduced feature set to discuss significantly altered pathways and metabolites.

## 2.5.2. Pathways Altered by DENV Bloodmeal

Pathway analysis was performed using MetPA through the Metaboanalyst web platform based on the *Drosophila melanogaster* KEGG library (Pang et al., 2021; Xia et al., 2010). Here, we will discuss two pathways displaying high significance and a high molecule match rate, pyruvate metabolism and arginine biosynthesis.

### *Pyruvate Metabolism*

Pyruvate metabolism had the lowest adjusted p-value with four metabolites from our dataset identified within the 22-metabolite pathway (acetate, lactate, pyruvate, fumarate). Pyruvate is generated during the last step of glycolysis, which occurs in the cytoplasm (Melkonian & Schury, 2021). Depending on the oxidative state of the cell, pyruvate has various reaction options, partly governed by cellular oxygen concentration. If the cell contains sufficient oxygen, pyruvate can cross the mitochondrial membrane and enter the citric acid cycle for oxidative phosphorylation. Alternatively, under scarce oxygen conditions, pyruvate can be converted to lactate which acts as an energy storage molecule and provides cofactors necessary for continual glycolysis (Melkonian & Schury, 2021). Changes in pyruvate metabolism could indicate alterations in energetics that differ between the two strains responding to DENV infection.

Pyruvate metabolism is coupled to glycolysis, another significantly regulated pathway (Table 2.3). In human cells, DENV induces glycolysis during infection and inhibition of the glycolytic pathway reduces DENV titres (Fontaine et al., 2015). The inhibition of lactate dehydrogenase, the enzyme that converts pyruvate to lactate, has a dose-dependent decrease in DENV infectious particles (Fontaine et al., 2015). In *Ae. aegypti* infected with DENV, glycolysis was reported to significantly influence infection dynamics using a multi-omics approach (Shrinet et al., 2018). Taken together, previous work demonstrates that carbon and energy metabolism are significant drivers of viral

kinetics. Our results agree and demonstrate that the refractory Cali-MIB strain may respond less energetically favourably to viral replication. The mechanisms governing differing energetic responses cannot be elucidated here.

### *Arginine Biosynthesis*

Arginine is an essential nutritional metabolite for many organisms, including mosquitoes (Raghupathi Reddy & Campbell, 1969; Singh & Brown, 1957). Pathway analysis identified 9 of the 12 molecules described in arginine metabolism within our dataset (Fig. 2.8). The most significantly altered compounds were L-Ornithine, 2-Oxoglutarate, and L-Citrulline. The Cali-MIB strain had reduced concentrations of L-Ornithine and increased concentrations of 2-Oxoglutarate and L-Citrulline.

In invertebrates, arginine metabolism has two crucial but counter roles (Bayliak et al., 2018; Kraaijeveld et al., 2011). First, arginine can be utilized to produce nitric oxide (NO) through nitric oxide synthase, which can activate and induce immune responses to pathogens (Kraaijeveld et al., 2011). Alternatively, arginine can be used for the synthesis of polyamines through the conversion of arginine to ornithine (Pegg, 2009; Pegg & McCann, 1982). Polyamines, such as spermidine and spermine, are small, positively charged molecules well conserved across eukaryotes and involved in cellular growth (Kogan & Hagedorn, 2000; Pegg, 2009; Pegg & McCann, 1982). Interestingly, polyamine synthesis has been proposed as a drug target for human viral infection and has shown significant efficacy in reducing DENV titers (Huang et al., 2020; Mounce et al., 2016). Given reduced concentrations of ornithine in the refractory Cali-MIB strain, the polyamine synthesis pathway may be less active in refractory insects. Alterations in arginine metabolism may direct metabolites towards immune functions rather than growth and synthesis, negatively impacting the optimal milieu for viral success.

## 2.5.3. Molecules Altered by DENV in the Bloodmeal

It is assumed that genes, proteins, or molecules that exhibit biological significance will show large fold-change differences. However, as observed previously in our research, immune genes may not display significant absolute changes in expression despite having crucial biological relevance (Caicedo et al., 2013; Coatsworth et al., 2018, 2021; Ocampo et al., 2013; Serrato et al., 2017). Altered fold-change differences in immune responses highlight the issue of parsing biological significance using

statistical methods. Our differential analysis used SAM to identify significantly changed features in our metabolite set. SAM was chosen over a fold-change analysis with an FDR-adjusted *p*-value because it provides an empirical FDR based on resampling and may provide a more robust analysis with metabolites with lower fold-change concentration differences (Tusher et al., 2001). Traditionally an adjusted $p<0.05$ threshold is chosen to indicate significance. However, an empirical FDR of 10% was used for our analysis. First, because our analysis uses untargeted metabolomics, the results require further validation; any features identified are not yet confirmed to be important for viral resistance. Second, our dataset contains a modest number of features, meaning fewer metabolites will be identified compared with other omics analyses, such as transcriptomics. For these reasons, we have accepted a higher empirical FDR, as determined by SAM, in an attempt to capture more biologically relevant metabolites.

We focused our discussion on the features differentially regulated between the Cali-MIB and Cali-S strains challenged with DENV. However, statistically, significant features identified with the different comparisons at all time points can be seen in Table 2.2. Moreover, for this discussion, we will not discuss dipeptides identified as significant as their link to DENV resistance will be highly tenuous. For 24 hpbm, only the top three most significantly changed features will be discussed.

### *Molecules Altered by DENV at 18hpbm*

Three compounds were significantly upregulated in the Cali-MIB strain at 18 hpbm, 4-Carboxypyrazole, Alanyl-Valine, 2'-Deamino-2'-hydroxy-6'-dehydroparomamine. Boxplots of the concentrations of 4-carboxypyrozole and 2'-Deamino-2'-hydroxy-6'-dehydroparomamine can be seen in Fig. 2.9; alanyl-valine was not included.

4-carboxypyrazole is a heterocyclic pyrazole ring with a carboxylic acid group replacing a hydrogen group (*Human Metabolome Database: (HMDB0060760)*, n.d.). Medically, pyrazole derivatives have been used to treat methanol poisoning (Blomstrand et al., 1979). Pyrazole and pyrazole derivatives have been investigated as anti-tumour and anti-viral agents for decades (Kumar et al., 2013; Pancic et al., 1981; Petrie III et al., 1986; Shih et al., 2010; Wassel et al., 2020). The earliest report from 1981 investigated their effects on herpes virus infection in mice and guinea pigs (Pancic et al., 1981). However, the compounds used in these studies were highly conjugated forms of

pyrazole and are significantly larger than 4-carboxypyrozole. In 2005, a patent was filed for the use of 4-carboxypyrozole derivatives as anti-viral agents (*WO2007039146A1 - 4-Carboxy Pyrazole Derivatives as Anti-Viral Agents - Google Patents*, n.d.).

Interestingly, pyrazoles are uncommon in nature, likely due to the nitrogen-nitrogen bond formation, which is energetically intensive (Kumar et al., 2013). However, pyrazoles have been isolated from a few organisms, including *Streptomyces candidus* and *Cucumis sativus* (cucumber) (Comber et al., 1992; Kumar et al., 2013). Given the rarity of pyrazole compounds in nature, it is unlikely that 4-carboxypyrazole was synthesized by the insect. Moreover, since both mosquito strains were fed on the same bloodmeal, it is unlikely that the compound was provided in the diet in excess only to the Cali-MIB strain. Thus, we speculate that 4-carboxypyrazole is synthesized in the gut by the resident microbiome, although this cannot be validated using currently available data. Previously, we compared the composition of microbiome bacteria in the midguts of refractory and susceptible insects and found no significant differences (Coatsworth et al., 2018). However, these analyses were done using 16s rRNA sequencing, which may not have adequate resolution to uncover differences between the microbiome populations.

2'-Deamino-2'-hydroxy-6'-dehydroparomamine (2-DHD) is a derivative of 2-deoxystreptamine and an amino cyclitol glycoside (*2’-Deamino-2’-Hydroxy-6’-Dehydroparomamine | C12H22N2O8 - PubChem*, n.d.). 2-DHD is an intermediate product in Kanamycin synthesis, an aminoglycoside antibiotic produced by *Streptomyces kanamyceticus* (*KEGG PATHWAY: Neomycin, Kanamycin and Gentamicin Biosynthesis - Reference Pathway*, n.d.; Won Park et al., 2011).

Since kanamycin is an antibiotic, it is unlikely to possess antiviral activity. Indeed, in vertebrate hamster kidney cells, kanamycin did not affect DENV replication (Zhang et al., 2009). Therefore, 2-DHD is likely not functioning to manage DENV infection. An alternative possibility is that 2-DHD is an artifact of infection and indicates microbiome changes in response to DENV infection. Gut microbiome alterations have been noted in DENV infection in *Ae. albopictus* (Zhao et al., 2022). Perhaps increased 2-DHD, and possibly kanamycin, is produced by the microbiome in response to DENV-induced dysbiosis. However, why only the Cali-MIB strain would have altered 2-DHD concentrations remains unclear.

### *Molecules Altered by DENV Bloodmeal at 24hpbm*

Nine compounds were identified as significantly different between Cali-MIB and Cali-S strains at 24 hpbm, the highest number of any timepoint tested. Interestingly, all nine compounds were significantly downregulated in the Cali-MIB strain, suggesting that removing pro-viral molecules may be more efficacious than producing antiviral ones.

The four most significant compounds, as determined by SAM, are N-Methyl-a-aminoisobutyric acid, 3-Amino-2-piperidone, Ornithine, and 4-Aminobutyraldehyde. The last three compounds will be discussed together as they are closely related. Boxplots showing the relative concentration of each of these metabolites in the two strains can be seen in Fig. 2.9.

N-Methyl-a-aminoisobutyric acid (N-MAA), alternatively referred to as 2-(methylamino)isobutyrate, is an alpha amino acid where the amino group is attached to the alpha carbon (*2-(Methylamino)Isobutyric Acid | C5H11NO2 - PubChem*, n.d.; *Human Metabolome Database: N-Methyl-a-Aminoisobutyric Acid (HMDB0002141)*, n.d.). N-MAA is a derivative of isobutyric acid downstream of alanine metabolism and a non-proteinogenic alpha amino acid. Little research has been done into N-MAA in invertebrates; therefore, a mechanism explaining its contribution to viral resistance is unclear. However, Isobutyric acid, a precursor of N-MAA and a branched fatty acid, has been observed to influence the sensitivity of $CO_2$ detectors in *Ae. aegypti* (Kumar et al., 2020).

Ornithine, as discussed previously, is an arginine metabolite that is an intermediate in polyamine synthesis (Pegg, 2009; Pegg & McCann, 1982; Raghupathi Reddy & Campbell, 1969). An intermediate step in the conversion of ornithine to the polyamine spermidine is putrescine, which can be converted to 4-Aminobutyraldehyde (Rashmi et al., 2018), a compound identified as significant by our analysis. 4-aminobutyraldehyde is converted through a non-canonical pathway to γ-aminobutyric acid (GABA). Additionally, 3-Amino-2-piperidone is referred to as cyclo-ornithine and is the lactam form of ornithine (Gadowet al., 1983; Oberholzer & Briddon, 1978). Although the biology of 3-Amino-2-piperidone is not well resolved, it has been identified in the urine of humans (Oberholzer & Briddon, 1978). There is potential for 3-Amino-2-piperidone to be involved in the same metabolic pathways as ornithine and 4-Aminobutyraldehyde to influence GABA production.

GABA is a conserved neurotransmitter in vertebrates and invertebrates that functions to inhibit neuronal excitability (Cole et al., 1995; Rashmi et al., 2018; Tremblay et al., 2016; Zhu et al., 2017) and recently was demonstrated to function in mosquito innate immunity (Zhu et al., 2017). Increased GABAergic activation enhanced DENV replication in *Ae. aegypti*. Reduced concentrations of ornithine and 4-Aminobutyraldehyde may be indicative of a less active GABA synthesis pathway, which negatively influences viral replication. Moreover, these results are consistent with our pathway analysis results and provide a mechanism of arginine metabolism where products are shunted away from pro-viral GABA and polyamine synthesis, possibly towards nitric oxide production and immune activation.

### *Molecules Altered by DENV Bloodmeal at 36 hpbm*

Only one compound was found to be significant at 36 hpbm. Agmatine was shown to have reduced concentration; however, given the minimal separation between the groups in the PCA, the biological link is tenuous. Nonetheless, agmatine showed an approx. 1.8-fold difference between the two groups (Fig. 2.8).

Agmatine is the decarboxylation product of arginine and has been categorized as a polyamine with spermidine, spermine, and putrescine (Guan et al., 2018; *Human Metabolome Database: (HMDB0001432)*, n.d.). In rat pup models, agmatine has decreased nitric oxide production and, in turn, inflammation (Feng et al., 2002). If this were to hold in our Cali-MIB strain, decreased agmatine concentrations could indicate an increased pro-inflammatory milieu in response to DENV. Moreover, agmatine, as a derivative of arginine, reinforces the importance of arginine metabolism in refractory midgut tissues seen throughout our analysis.

## 2.5.4. Metabolism of Blood-fed Cali-MIB and Cali-S Strains

After observing the differences between Cali-MIB and Cali-S strains in response to DENV, we noted that many metabolic pathway differences occurred in pathways related to energetics or energy production. We then postulated that the refractory strain might have an altered metabolic profile after a metabolic stressor other than DENV.

To test our hypothesis, we compared the profiles of Cali-MIB and Cali-S insects in response to blood meal alone and found that the midguts of refractory Cali-MIB

samples had differing profiles in response to blood meal without DENV. Moreover, the molecules identified as significant in the blood-only analysis did not overlap with those identified in the blood+DENV comparison. We glean two main points from these results. First, the midgut metabolism of Cali-MIB refractory midguts is generally different in response to metabolic demands placed on the cells. Demonstrating this first point, in our blood-only analysis, more features were significantly different in response to blood alone than in the blood+DENV comparison. Second, the differences in metabolism are influenced by the type of metabolic stressor; the metabolic features identified as significant in the blood-only analysis did not overlap with those identified in the blood+DENV samples. These results provide impetus to investigate both the individual metabolites identified in the Cali-MIB strain in response to DENV and the mechanisms that underly differing general metabolism in this strain, for example, by investigating mitochondrial function, which is central to metabolic regulation.

## 2.6. Conclusion

Here we present a metabolomic analysis of two sympatric strains of *Ae. aegypti* that demonstrate altered susceptibility to DENV. We performed numerous analyses using two metabolite datasets, one with high-quality identified metabolites and another with putative identifications. PCA was used to assess data quality and broad metabolic differences in strain profiles. Next, using SAM, we determined the differentially regulated metabolites between the two strains at different time points after ingesting DENV. Finally, using pathway analysis, we uncovered systematic metabolic changes in response to DENV.

Through this work, we discovered two potentially important metabolic pathways were significantly altered in the refractory Cali-MIB strain during DENV challenge: pyruvate metabolism and arginine biochemistry. Pyruvate metabolism is central to the energy state of the cell and agrees with our hypothesis, as mentioned earlier, regarding the energetic demands of viral infection. However, metabolic differences in arginine metabolism were an unexpected finding of our screen. Through literature review, we have proposed mechanisms by which these pathways may influence DENV replication. Although these propositions are tenuous, we believe these pathways warrant further investigation to determine if modifying the balance of metabolites can influence DENV infection dynamics in *Ae. aegypti*.

Additionally, we discussed molecules determined to be significant within our experiment. One molecule is unlikely to exhibit strong anti-viral properties capable of recapitulating a refractory phenotype. Nevertheless, the previous interest in developing 4-carboxypyrazole derivatives as anti-viral agents leads us to believe this may be a worthwhile compound to investigate further.

The design of our untargeted metabolomics study makes it impossible to determine if any of the pathways or metabolites described here are causally related to viral resistance. More molecular research is needed to prove causation, but we propose that the pathways and molecules discussed above may be the most likely to provide meaningful results. Nonetheless, this work provides the first metabolomic analysis of a naturally occurring population of *Ae. aegypti* that are refractory to DENV and introduces novel hypotheses to be tested regarding DENV immunity.

## 2.7. Figures and Tables

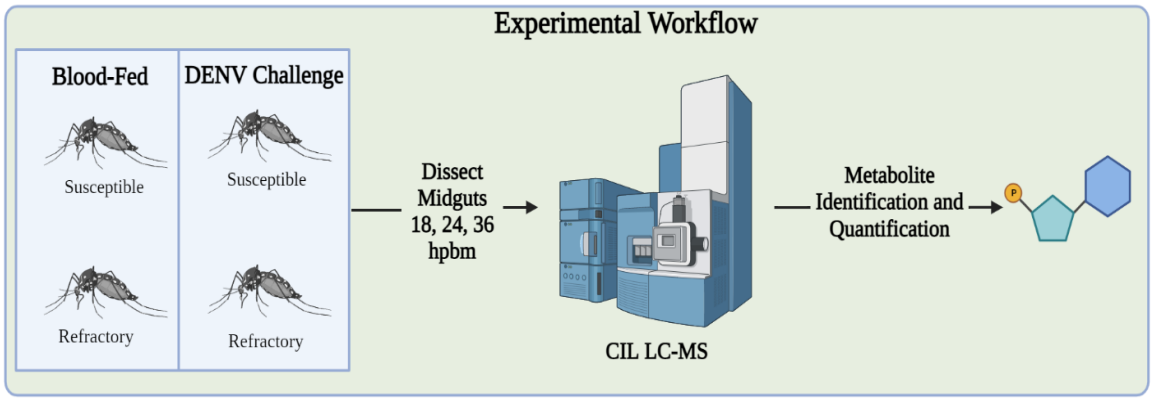


**Figure 2.1.** **Experimental workflow. Schematic showing the four treatment groups dissected in triplicate at three time points, 18, 24, and 36 hours post blood meal. Ten midguts were pooled for each treatment at each timepoint and were subjected to chemical isotope labelling liquid chromatography-mass spectrometry (CIL LC-MS) to identify metabolites and their concentrations.**

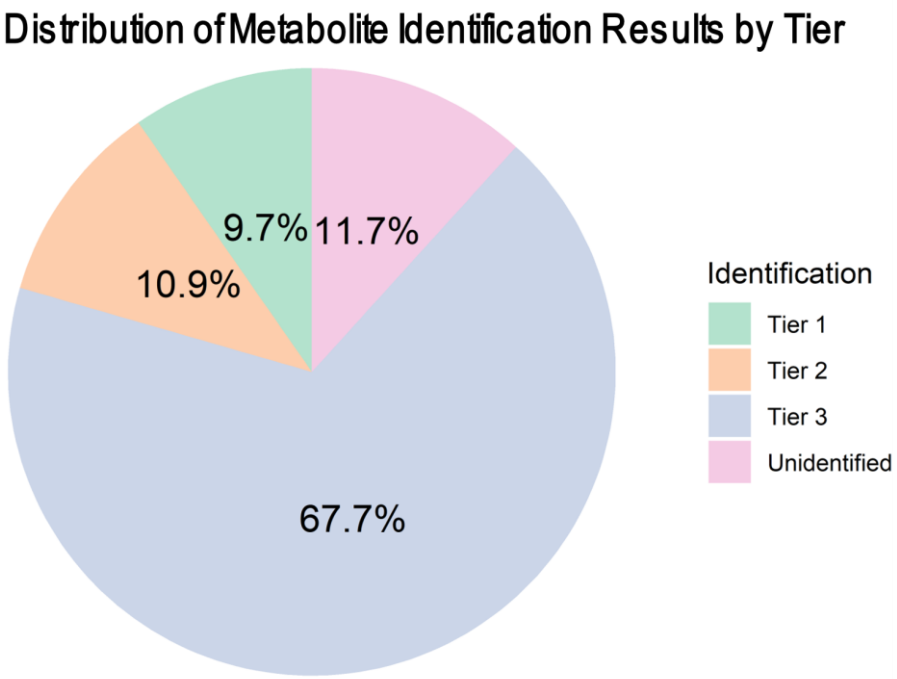


**Figure 2.2.** **Distribution of metabolite identification results by confidence tier. The pie chart shows the percentage of metabolites identified in each accuracy tier. Tiers one and two are considered high-confidence identifications, and tier 3 are putative identifications based on mass alone.**

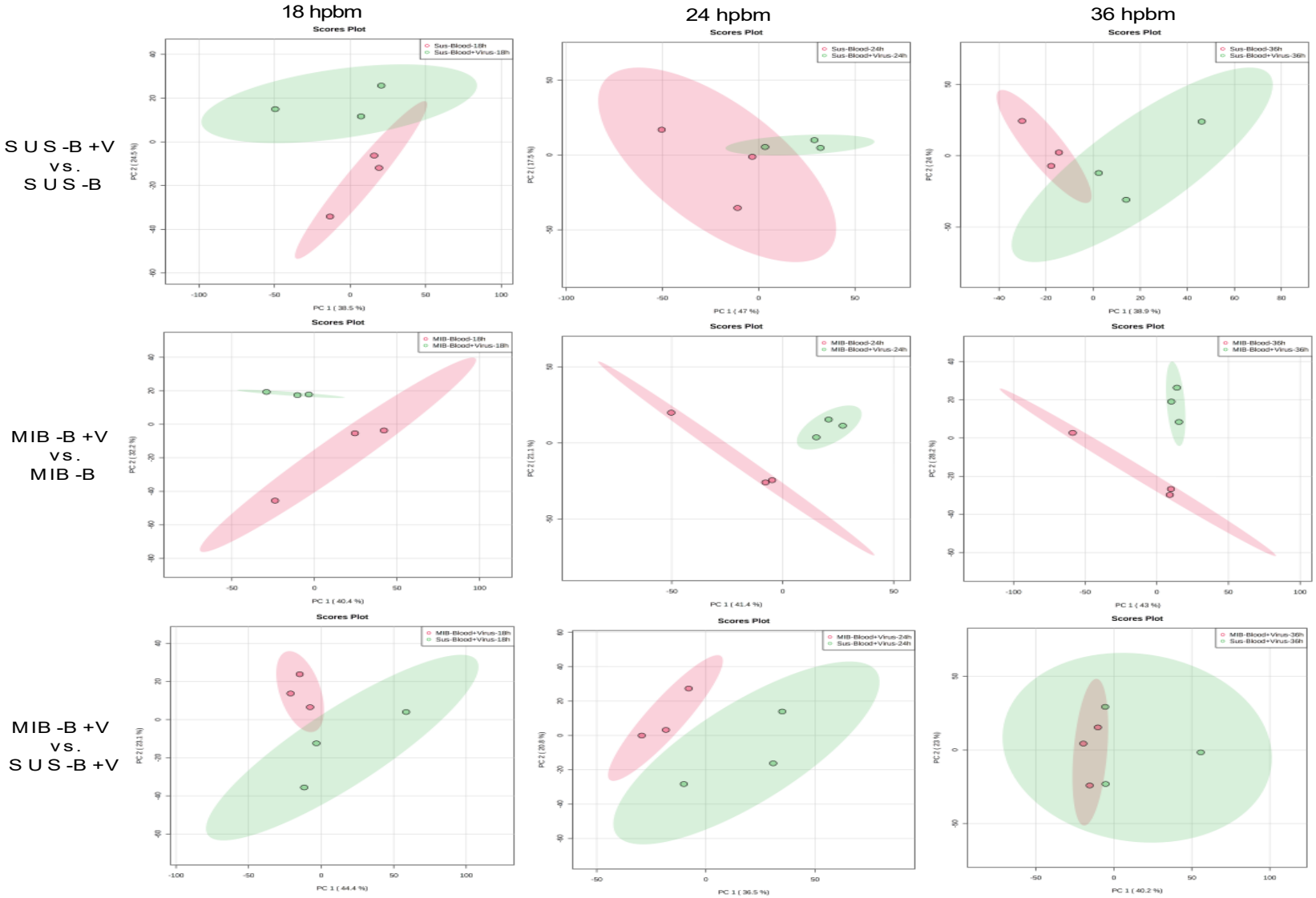
18 hpbm
24 hpbm
36 hpbm
S U S -B +V
vs.
S U S -B
MIB -B +V
vs.
MIB -B
MIB -B +V
vs.
S U S -B +V
Scores Plot
Sus-Blood-18h
Sus-Blood+Virus-18h
Sus-Blood-24h
Sus-Blood+Virus-24h
Sus-Blood-36h
Sus-Blood+Virus-36h
MIB-Blood-18h
MIB-Blood+Virus-18h
MIB-Blood-24h
MIB-Blood+Virus-24h
MIB-Blood-36h
MIB-Blood+Virus-36h
MIB-Blood+Virus-18h
Sus-Blood+Virus-18h
MIB-Blood+Virus-24h
Sus-Blood+Virus-24h
MIB-Blood+Virus-36h
Sus-Blood+Virus-36h

**Figure 2.3. PCA plots of data from Tier 1, 2, & 3. Principal component analysis (PCA) of a) Cali-S blood+virus fed (SUS-B+V) vs. Cali-S blood-fed (SUS-B), b) Cali-MIB blood+virus fed (MIB-B+V) vs. Cali-MIB blood-fed (MIB-B), and c) Cali-MIB blood+virus vs. Cali-S blood+virus fed, at 18, 24, and 36 hpbm. The X-axis has the first principal component, and the Y-axis the second. Each data point represents one sample of 10 pooled insect midguts with the 95% confidence interval displayed as the ellipsis. A) and b) virus-challenged samples are shown in green, and blood-fed samples are shown in red. In c) Samples from Cali-MIB samples are in red, and those from Cali-S are in green.**

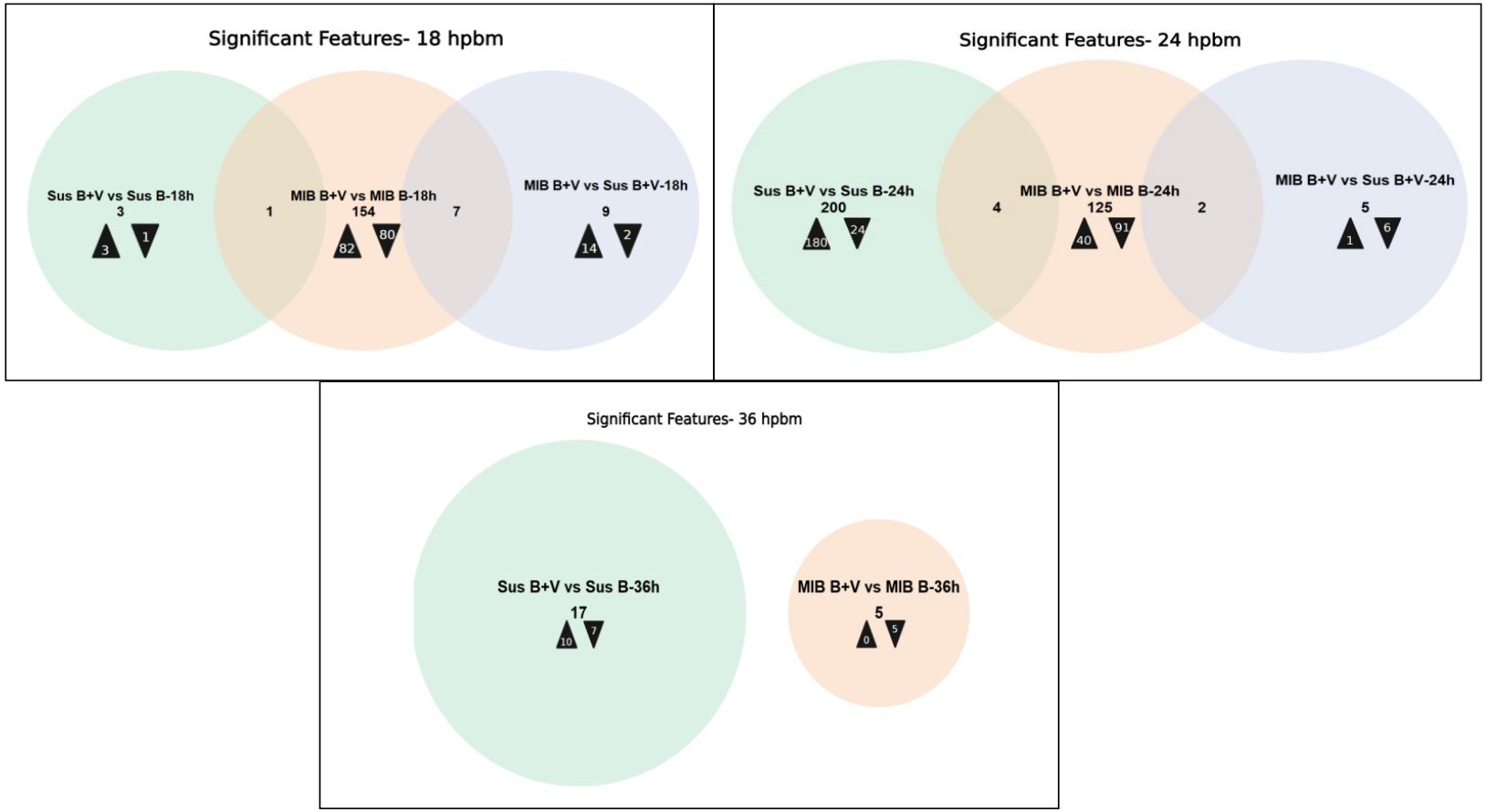


**Figure 2.4.** **Differentially regulated metabolites—Full feature set. Venn Diagrams showing the number of significantly differently regulated metabolites selected using the SAM model at each time point for each sample comparison (Cali-S-B+V vs. Cali-S-B, Cali-MIB-B+V vs. Cali-MIB-B, Cali-MIB-B+V vs. Cali-S-B+V). Black arrowheads pointing up depict the number of metabolites that were increased in concentration compared with the control group, and arrowheads pointing down show the number of metabolites that were decreased in concentration compared with the control. The control groups are listed second in each comparison.**

| | 18 hpbm | 24 hpbm | 36 hpbm |
|---|---|---|---|
| S U S -B +V vs. S U S -B | 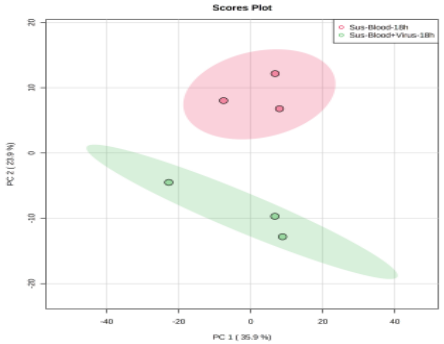 | 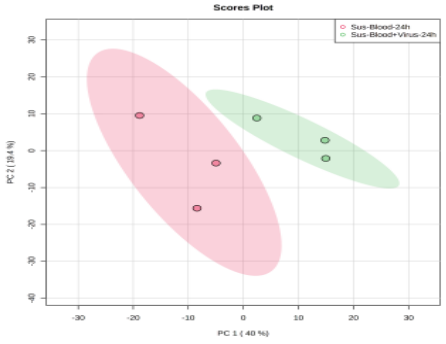 | 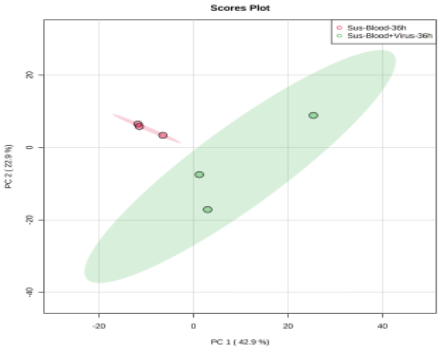 |
| MIB -B +V vs. MIB -B | 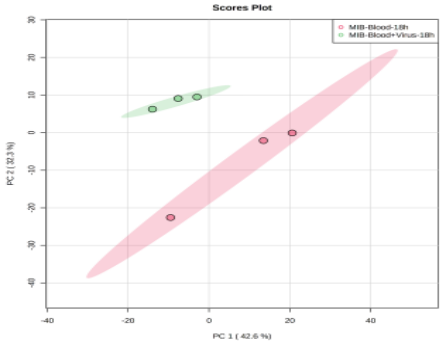 | 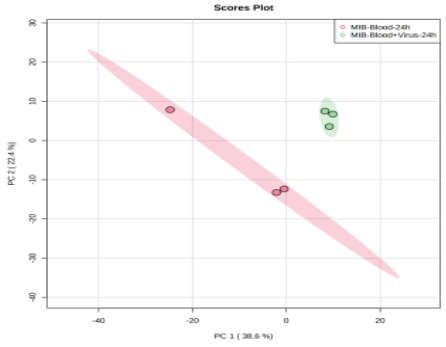 | 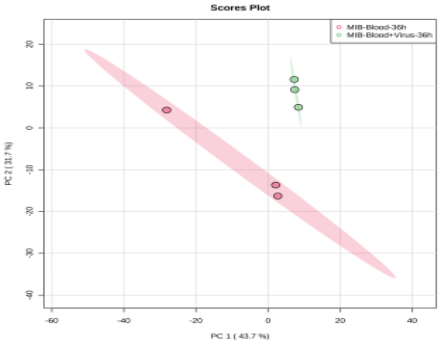 |
| MIB -B +V vs. S U S -B +V | 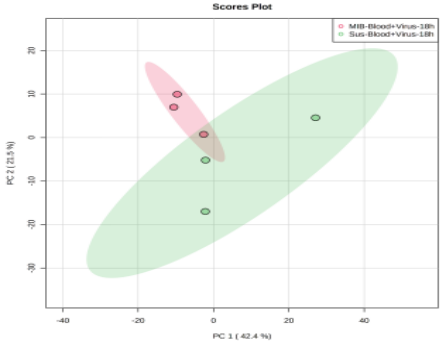 | 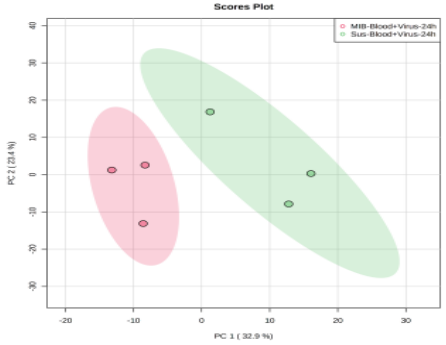 | 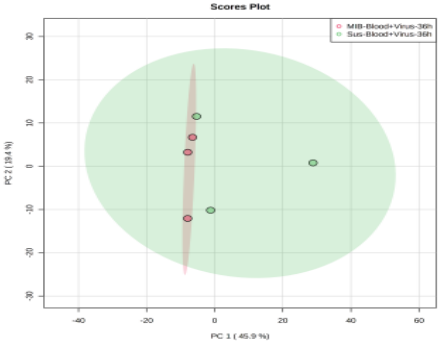 |

**Figure 2.5.** **PCA plots—reduced feature set (Tiers 1 & 2). Principal component analysis (PCA) of a) Cali-S blood+virus fed (SUS-B+V) vs. Cali-S blood-fed (SUS-B), b) Cali-MIB blood+virus fed (MIB-B+V) vs. Cali-MIB blood-fed (MIB-B), and c) Cali-MIB blood+virus fed vs. Cali-S blood+virus fed, at 18, 24, and 36 hpbm. The X-axis has the first principal component, and the Y-axis the second. Each data point represents one sample of 10 pooled insect midguts with the 95% confidence interval displayed as the ellipsis. A) and b) virus-challenged samples are shown in green, and blood-fed samples are shown in red. In c), Cali-MIB samples are in red, and Cali-S samples are in green.**

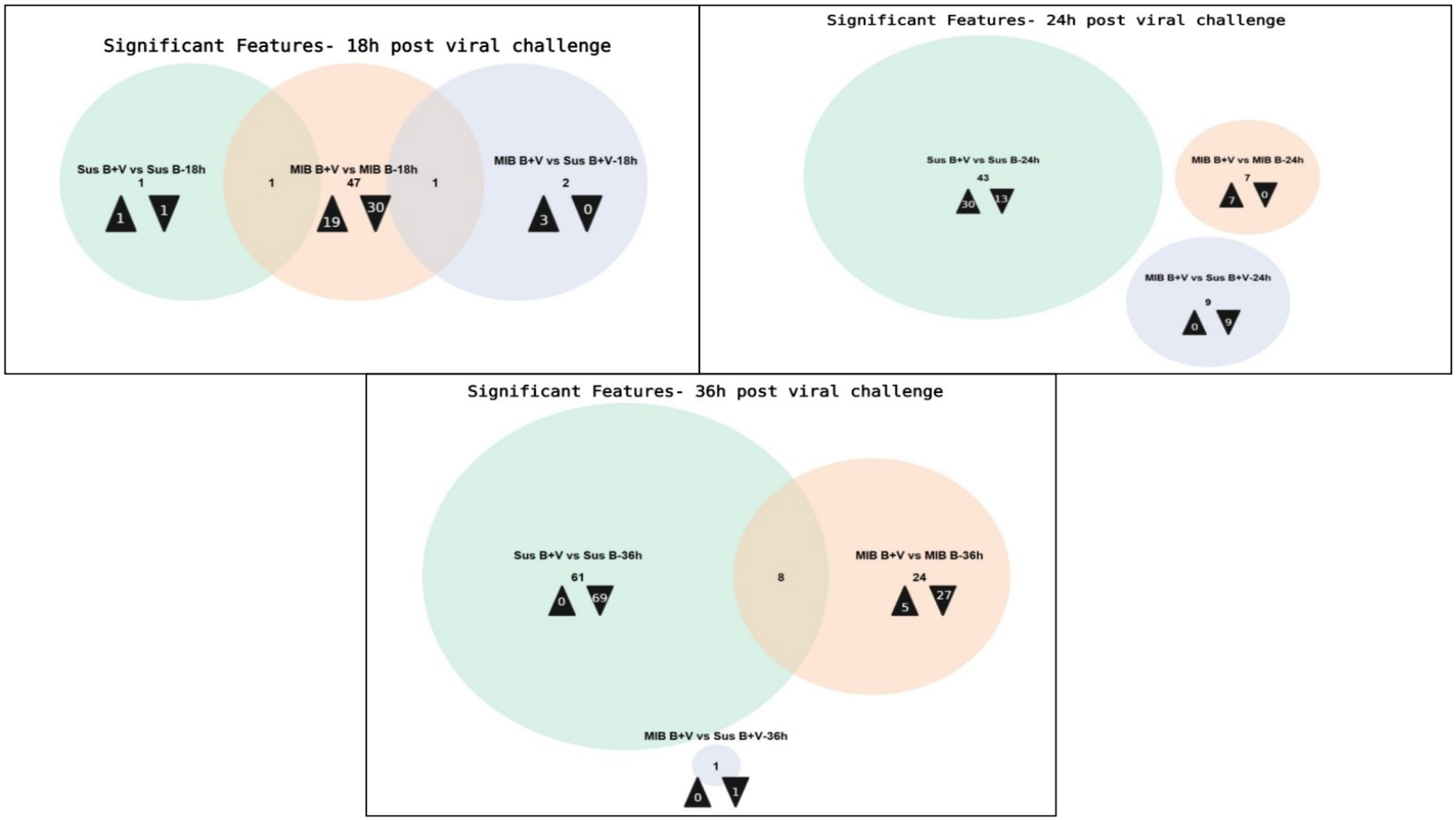


**Figure 2.6. Differentially regulated metabolites—Reduced feature set (Tiers 1 & 2). Venn Diagrams showing the number of significantly differently regulated metabolites selected using the SAM model at each time point for each sample comparison (Cali-S-B+V vs. Cali-S-B, Cali-MIB-B+V vs. Cali-MIB-B, Cali-MIB-B+V vs. Cali-S-B+V). Black arrowheads pointing up show the number of metabolites that were increased in concentration compared to the control group, and arrowheads pointing down show the number of metabolites that were decreased in concentration compared to the control. The control groups are listed second in each comparison.**

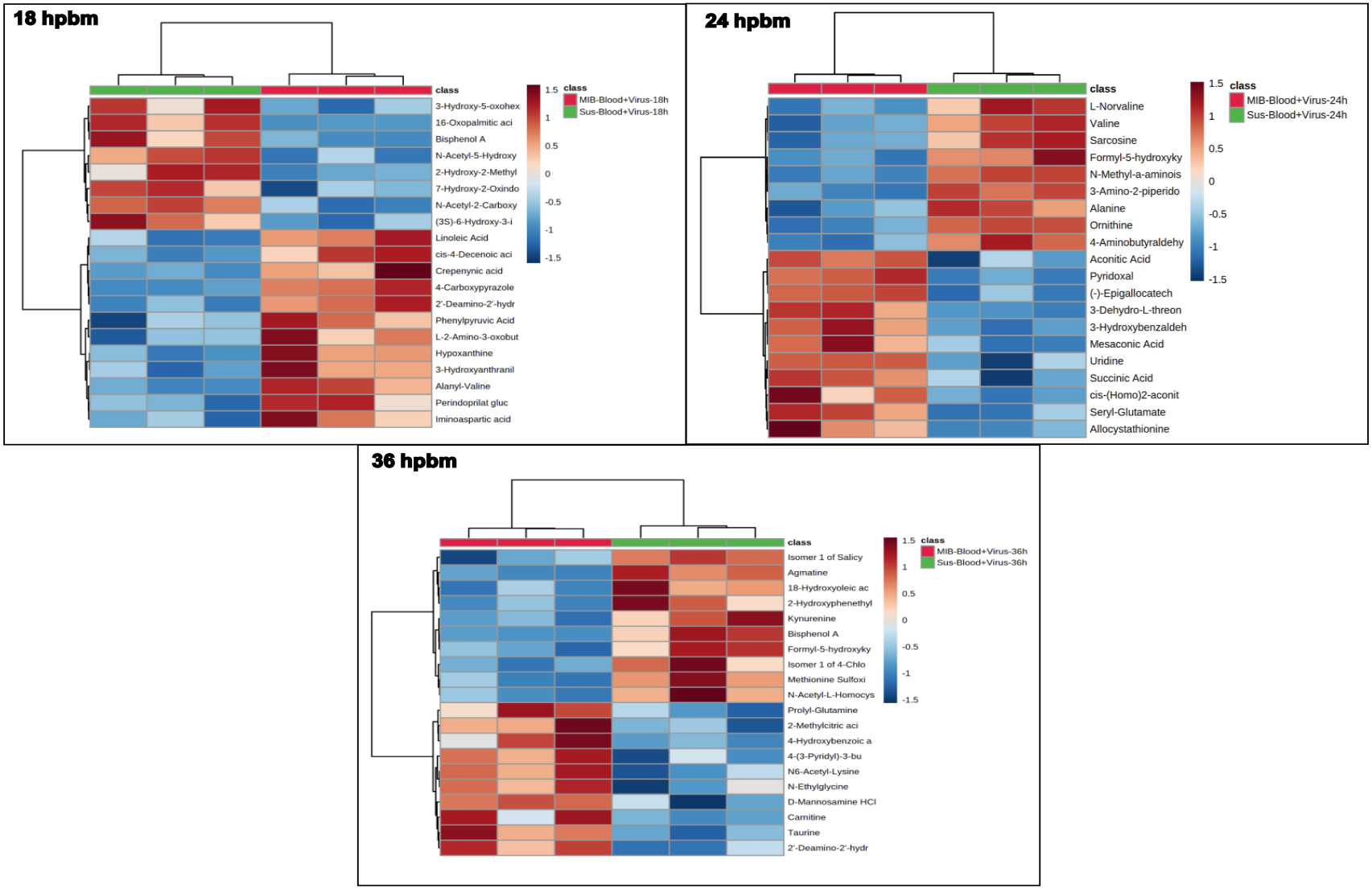
18 hpbm
class
3-Hydroxy-5-oxohex
16-Oxopalmitic aci
Bisphenol A
N-Acetyl-5-Hydroxy
2-Hydroxy-2-Methyl
7-Hydroxy-2-Oxindo
N-Acetyl-2-Carboxy
(3S)-6-Hydroxy-3-i
Linoleic Acid
cis-4-Decenoic aci
Crepenynic acid
4-Carboxypyrazole
2'-Deamino-2'-hydr
Phenylpyruvic Acid
L-2-Amino-3-oxobut
Hypoxanthine
3-Hydroxyanthranil
Alanyl-Valine
Perindoprilat gluc
Iminoaspartic acid
1.5
1
0.5
0
-0.5
-1
-1.5
class
MIB-Blood+Virus-18h
Sus-Blood+Virus-18h
24 hpbm
class
L-Norvaline
Valine
Sarcosine
Formyl-5-hydroxyky
N-Methyl-a-aminois
3-Amino-2-piperido
Alanine
Ornithine
4-Aminobutyraldehy
Aconitic Acid
Pyridoxal
(-)-Epigallocatech
3-Dehydro-L-threon
3-Hydroxybenzaldeh
Mesaconic Acid
Uridine
Succinic Acid
cis-(Homo)2-aconit
Seryl-Glutamate
Allocystathionine
1.5
1
0.5
0
-0.5
-1
-1.5
class
MIB-Blood+Virus-24h
Sus-Blood+Virus-24h
36 hpbm
class
Isomer 1 of Salicy
Agmatine
18-Hydroxyoleic ac
2-Hydroxyphenethyl
Kynurenine
Bisphenol A
Formyl-5-hydroxyky
Isomer 1 of 4-Chlo
Methionine Sulfoxi
N-Acetyl-L-Homocys
Prolyl-Glutamine
2-Methylcitric aci
4-Hydroxybenzoic a
4-(3-Pyridyl)-3-bu
N6-Acetyl-Lysine
N-Ethylglycine
D-Mannosamine HCl
Carnitine
Taurine
2'-Deamino-2'-hydr
1.5
1
0.5
0
-0.5
-1
-1.5
class
MIB-Blood+Virus-36h
Sus-Blood+Virus-36h

**Figure 2.7.** **Heatmaps of the top 20 changed metabolites, Tiers 1 & 2—between Cali-MIB and Cali-S strains of *Ae. aegypti*, at each time point. Results of hierarchical clustering are shown above the heatmap, with Cali-MIB samples displayed in red and Cali-S samples in green. The fold change concentration difference of the metabolite is displayed using the scale to the right of the heatmap.**

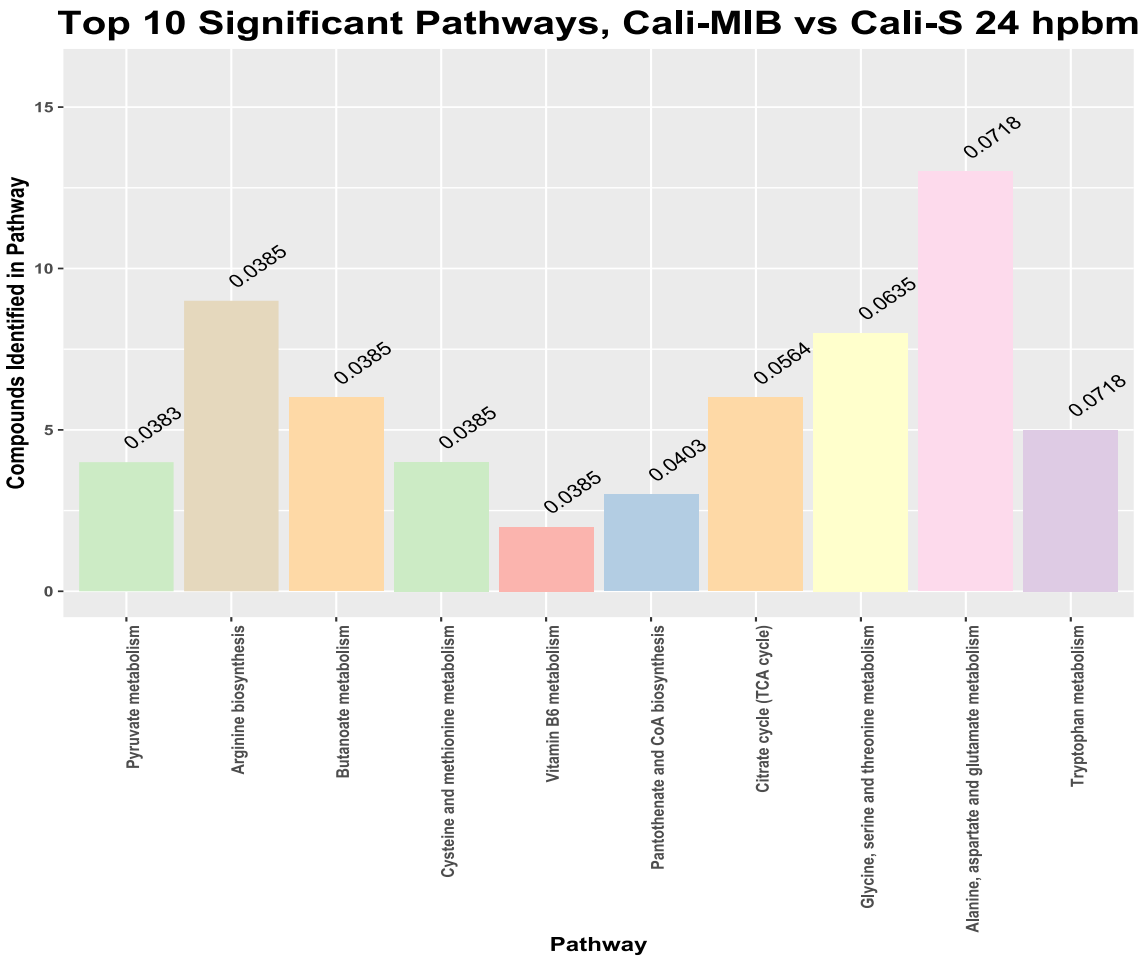


**Figure 2.8.** **Top Pathways altered by DENV infection, using Tier 1 & 2 metabolites—Cali-MIB vs Cali-S at 24 hpbm. The X-axis displays the pathway name, and the Y-axis shows the number of metabolites in that pathway identified in our dataset. The FDR-adjusted p-value of the pathway is shown above each bar.**

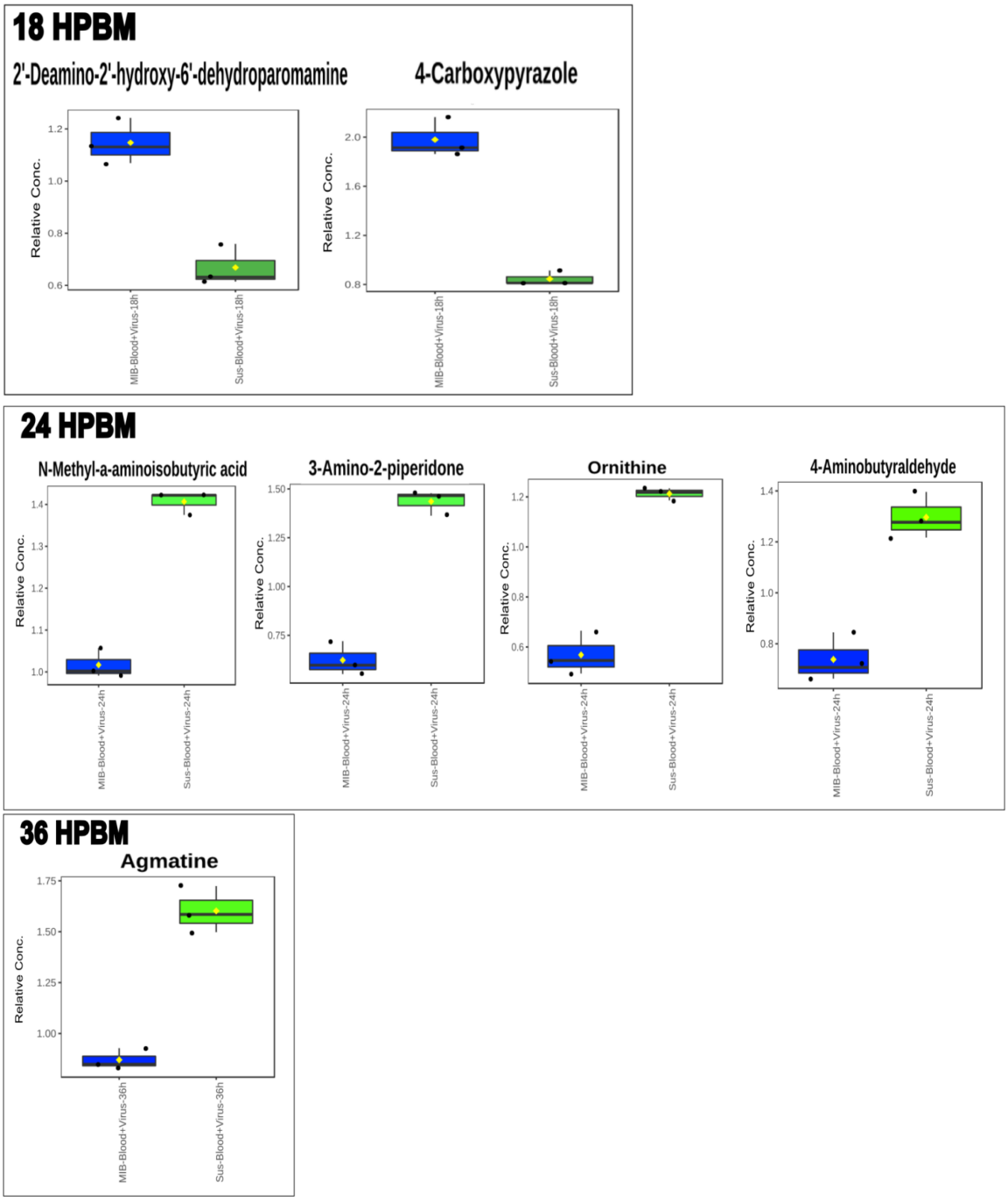


**Figure 2.9.** **Boxplots of discussed metabolites found in different concentrations in Cali-MIB and Cali-S strains of *Ae. aegypti* at all time points. Cali-MIB samples are shown in blue, and Cali-S samples in green. Relative concentration is calculated based on the amount of metabolite in a sample compared to a standard. Black points represent an individual sample's relative concentration of that metabolite. The three data points for each treatment represent the triplicate measurements of 10 pooled midguts**

**Table 2.1. Distribution of metabolite Identification results by confidence tier. The table displays the number of metabolites identified in each confidence tier and the total number of features detected in all samples.**

| | Total Metabolites Detected | High Confidence Metabolites | Putatively Identified Metabolites | Total Annotated Features (High Confidence + Putative) |
|---|---|---|---|---|
| # of features | 2192 | 450 | 1485 | 1935 |

**Table 2.2. Top 10 significantly identified features in Tiers 1 & 2. Significance was determined using SAM modelling, with an empirical FDR at 10%. If less than ten features were significant at the 10% threshold, then only those features are listed. Features appear in alphabetical order within each comparison. Features appearing in more than one comparison are listed in bold typeface.**

**18 HPBM**

| Cali-S-B+V vs Cali-S-B-18hpbm | Cali-MIB-B+V vs Cali-MIB-B-18hpbm | Cali-MIB-B+V vs Cali-s-B+V-18hpbm |
|---|---|---|
| Benzocaine-DR | **2'-Deamino-2'-hydroxy-6'-dehydroparomamine-UR** | **2'-Deamino-2'-hydroxy-6'-dehydroparomamine-UR** |
| **N-Acetyl-5-Hydroxy-L-tryptophan-UR** | 3,4-Dihydroxystyrene-UR | 4-Carboxypyrazole-UR |
| | **cis-(Homo)2-aconitic acid-UR** | **Alanyl-Valine-UR** |
| | Gamma-Aminobutyric acid-DR | |
| | **Kynurenine-DR** | |
| | Methionine Sulfoxide-DR | |
| | Methionine-DR | |
| | Methyloxaloacetic acid-UR | |
| | **N-Methyl-a-aminoisobutyric acid-DR** | |
| | **Sarcosine-DR** | |

**24 HPBM**

| Cali-S-B+V vs Cali-S-B-24hpbm | Cali-MIB-B+V vs Cali-MIB-B-24hpbm | Cali-MIB-B+V vs Cali-S-B+V-24hpbm |
|---|---|---|
| 3-Hydroxybenzaldehyde-DR | (-)-Epigallocatechin-UR | Valine-DR |
| 4-Hydroxybenzoic acid-DR | 5-Hydroxymethyl-2-furancarboxylic acid-UR | **Formyl-5-hydroxykynurenamine-DR** |
| **Alanine-UR** | **cis-(Homo)2-aconitic acid-UR** | **Ornithine-DR** |
| Aminoacetone-UR | L-2-Amino-3-oxobutanoic acid-UR | **Alanine-DR** |
| **Formyl-5-hydroxykynurenamine-UR** | Mesaconic Acid-UR | 4-Aminobutyraldehyde-DR |
| Isomer 1 of 5-Hydroxyindoleacetic acid-UR | **N-Acetyl-5-Hydroxy-L-tryptophan-UR** | **N-Methyl-a-aminoisobutyric acid-DR** |
| **Kynurenine-UR** | Succinic Acid-UR | 3-Amino-2-piperidone-DR |
| **N-Methyl-a-aminoisobutyric acid-UR** | | |
| **Ornithine-UR** | | **Sarcosine-DR** |
| **Sarcosine-UR** | | |

**36 HPBM**

| Cali-S-B+V vs Cali-S-B-36hpbm | Cali-MIB-B+V vs Cali-MIB-B-36hpbm | Cali-MIB-B+V vs Cali-S-B+V36hpbm |
|---|---|---|
| 18-Hydroxyoleic acid-DR | 16-Hydroxypalmitic acid-DR | Agmatine-DR |
| 4-Hydroxystyrene-DR | 2-Methylcitric acid-UR | |
| Alanyl-Alanine-DR | **Alanyl-Valine-DR** | |

| | |
|---|---|
| Glutamyl-Leucine-DR | Citrulline-UR |
| Glutamyl-Valine-DR | Glycine-DR |
| Glycyl-Threonine-DR | Isomer 1 of Salicylic Acid-DR |
| Leucyl-Aspartate-DR | **N-Acetyl-5-Hydroxy-L-tryptophan-UR** |
| Seryl-Threonine-DR | Prolyl-Valine-DR |
| **Valyl-Alanine-DR** | Tyramine-DR |
| Valyl-Glycine-DR | **Valyl-Alanine-DR** |

**Table 2.3. Significantly regulated pathways identified at 24 hours after blood feeding in Cali-MIB and Cali-S strains of *Ae. aegypti*. Significant pathways displayed an FDR-adjusted p-value<0.1. *Total cmpd* represents the number of compounds described in that pathway, and *hits* is the number of metabolites identified in our dataset that match that pathway. *Raw p-value* is an unadjusted p-value, and *FDR* displays the FDR-adjusted p-value. Pathways are based on the KEGG *Drosophila melanogaster* reference database.**

| Pathway | Total Cmpd | Hits | Raw P-value | FDR |
|---|---|---|---|---|
| Pyruvate metabolism | 22 | 4 | 9.58E-04 | 3.83E-02 |
| Cysteine and methionine metabolism | 32 | 4 | 2.71E-03 | 3.85E-02 |
| Vitamin B6 metabolism | 8 | 2 | 3.38E-03 | 3.85E-02 |
| Arginine biosynthesis | 12 | 9 | 4.61E-03 | 3.85E-02 |
| Butanoate metabolism | 14 | 6 | 4.82E-03 | 3.85E-02 |
| Pantothenate and CoA biosynthesis | 18 | 3 | 6.04E-03 | 4.03E-02 |
| Citrate cycle (TCA cycle) | 20 | 6 | 9.87E-03 | 5.64E-02 |
| Glycine, serine and threonine metabolism | 30 | 8 | 1.27E-02 | 6.35E-02 |
| Tryptophan metabolism | 30 | 5 | 1.67E-02 | 7.18E-02 |
| Alanine, aspartate and glutamate metabolism | 23 | 13 | 1.79E-02 | 7.18E-02 |
| Glutathione metabolism | 26 | 6 | 2.36E-02 | 7.88E-02 |
| Glycolysis / Gluconeogenesis | 26 | 3 | 2.62E-02 | 7.88E-02 |
| Ubiquinone and other terpenoid-quinone biosynthesis | 9 | 1 | 2.64E-02 | 7.88E-02 |
| D-Glutamine and D-glutamate metabolism | 5 | 3 | 2.86E-02 | 7.88E-02 |
| Synthesis and degradation of ketone bodies | 5 | 1 | 3.13E-02 | 7.88E-02 |
| Fatty acid biosynthesis | 43 | 1 | 3.25E-02 | 7.88E-02 |
| Pyrimidine metabolism | 40 | 3 | 3.40E-02 | 7.88E-02 |
| Glyoxylate and dicarboxylate metabolism | 24 | 6 | 3.55E-02 | 7.88E-02 |

## Connecting Statement 2

In Chapter two, we performed CIL LC-MS to identify metabolites that had different concentrations between Cali-MIB and Cali-S strains of *Ae. aegypti*. Numerous pathways and molecules were found to have significantly different concentrations between the two strains and may contribute to a refractory, anti-viral *milieu* in mosquito midguts. In addition to polar metabolites, lipids have demonstrated involvement during DENV replication in insect tissues. If this is true, then a similar evaluation of the lipidome of Cali-MIB and Cali-S insect midguts in response to DENV should identify differentially regulated lipid molecules that may determine the Cali-B or Cali-S phenotype. In the next chapter we describe our characterization of the lipidome in these two mosquito strains to identify lipids whose levels are differentially changed between the strains during DENV challenge.

# Chapter 3.

# Can Lipidomics analyses explain the difference in phenotype between two strains of Colombian *Aedes aegypti* that differ in their ability to transmit Dengue viruses?

## 3.1. Abstract

*Aedes aegypti* is the primary vector for all four serotypes of dengue viruses (DENV1-4), which infect millions across the globe each year. Traditional insecticide programs have been transiently effective at minimizing cases; however, insecticide resistance and habitat expansion has caused cases of DENV to skyrocket over the last decade. There is an urgent need to develop novel vector control measures, but these are contingent on a detailed understanding of host-parasite interactions. Here, we have utilized lipidomics to survey the profiles of naturally DENV-resistant (Cali-MIB) or susceptible (Cali-S) populations of *Aedes aegypti* when fed on DENV-containing blood meals; control insects were fed on a DENV-free blood meal. Midguts of Cali-MIB and Cali-S insects were dissected at three time points post-infectious blood meal, 18, 24 and 36h, to determine the lipidomic changes over time. We used PCA to visualize broad patterns in lipidomic profiles between the treatment groups and significance analysis of microarray to determine lipids that were altered in response to viral challenge. The results of this study can be used to systematically influence metabolic pathways to generate stable, DENV-resistant populations of *Ae. aegypti*.

## 3.2. Introduction

Approximately 1.7 billion people globally are currently at risk of contracting a neglected tropical disease (NTD) (WHO, 2021). NTDs are a group of infectious diseases that disproportionately affect marginalized individuals in developing nations (WHO, 2021). Among those diseases, dengue virus (DENV) has emerged as one of the most important viral NTDs.

DENV infection causes an acute febrile illness and has acquired the colloquial name *Break-bone fever* for the substantial symptoms associated with DENV infection (Clarke, 2002). Infection with one of four circulating DENV serotypes can have lethal consequences for an infected individual (World Health Organization, 2022). There are an estimated 390 million DENV infections per year, of which ~100 million present with clinical symptoms ranging from mild illness to severe dengue hemorrhagic fever (World Health Organization, 2022). Approximately half the world's population, 3.9 billion people, live in areas with circulating DENV throughout 129 countries. Alarmingly, cases reported to the WHO has seen an 8-fold increase in the past two decades (World Health Organization, 2022). Unfortunately, despite considerable effort, there are currently no effective vaccines or anti-viral treatments recommended by the World Health Organization. The drastic increase in infections and limited pharmaceutical interventions available for infected individuals has raised international concern among governments and researchers to uncover novel solutions to reduce viral transmission, infection, and disease.

DENV is a mosquito-transmitted virus primarily spread by female *Aedes aegypti* and, to a lesser extent *Aedes albopictus* (Moncayo et al., 2004). It is believed that a significant driver of increased case numbers is the expansion of suitable habitats for disease vectors (Kraemer et al., 2019). Historically, our most efficacious strategy for mitigating viral spread has been through vector control measures, such as insecticides (Maciel-de-Freitas & Valle, 2014), but these insecticides also may kill off-target and beneficial insect species such as honey bees. In addition, insecticide resistance has developed in many regions due to wide-spread insecticide application. Moreover, insecticide-based vector control measures require continual maintenance. Without proper coordination, insecticide control measures can fail and cause DENV infections to climb. This phenomenon was exemplified during the COVID-19 pandemic; some areas

of high-DENV prevalence saw explosions in reported cases due to the absence of vector control programs (Rahman et al., 2022).

More sophisticated molecular vector control measures are coming into use; one prominent example deploys genetically modified insects developed by Oxitec. In this system, large numbers of mosquitoes that are modified to contain a lethal gene are raised in specialized facilities. Each week males are released into an area with high DENV prevalence. These modified males mate with wild-type females, but their offspring never reach adulthood (Carvalho et al., 2015). The result is a significant depression in mosquito populations in the area where they were released, leading to a decrease in disease transmission.

Despite Oxitec insects' success, numerous problems are associated with their use. First, this method requires continual application of lab-reared males to reduce population numbers, driving up the cost of interventions. Second, for Oxitec's technology to work best, the immigration of neighbouring mosquito populations needs to be avoided. Therefore, it is most efficacious for small island settings. Finally, genetically modified organisms are often misunderstood and are considered controversial by the general public. Gaining public approval can be challenging, and Oxitec insect release has been stunted by government and public opinions in the past. Nevertheless, Oxitec remains a viable technology for mitigating viral infections under the correct circumstances.

An alternative vector control mechanism uses insect manipulations to reduce or eliminate vector competence (McGraw & O'Neill, 2013). Perhaps the most successful of these programs use the intracellular bacterium *Wolbachia*. Mosquitoes transinfected with *Wolbachia sp.* experience a considerable decrease in susceptibility to DENV infection and thus transmit DENV at a reduced or zero rate (Walker et al., 2011). *Wolbachia*-based vector control programs have been tested with success in the field. However, there is some concern over the circumstances with which *Wolbachia* sp. may block virus replication (King et al., 2018). More research is needed to determine the mechanisms and limitations of *Wolbachia*-based programs before wide-spread release.

Despite the role of *Ae. aegypti* as the principal vector for DENV and many other arboviruses, not all female *Ae. aegypti* will transmit DENV. Some females ingest the virus but through factors associated with their innate immune responses, they eliminate

rather than transmit DENV. In Cali Colombia, the proportion of refractory insects (those that do not transmit the virus) in field-collected insects is ~30% (Barón et al., 2010; Caicedo et al., 2013; Ocampo & Wesson, 2004). The susceptible females that transmit DENV and the refractory females are sympatric, and eggs from refractory and susceptible females can be collected within a single oviposition trap. Since their discovery, these susceptible and resistant populations have been reared in the laboratory to maximize the anti-DENV phenotype. One strain has been selected to have ~50% refractoriness while another is ~95% susceptible to DENV (Barón et al., 2010; Caicedo et al., 2013; Ocampo et al., 2013).

Populations with divergent susceptibilities to DENV are an extremely valuable research system. These populations identified in Colombia have natural barriers or bottlenecks that prevent the establishment, replication, and transmission of DENV. Some of these barriers have been described and are termed a midgut infection barrier (MIB) and a midgut escape barrier (MEB) (Ocampo et al., 2013). These barriers prevent DENV from entering and replicating within or egressing from midgut tissues, respectively. The populations described above have been identified to possess these barriers, and we have termed them Cali-MIB and Cali-MEB. Additionally, the susceptible population has been noted to possess neither barrier (Cali-S).

We have studied these populations extensively to understand their physiological differences from WT populations. Using suppressive subtractive hybridization assays (Baron et al., 2010), microarrays (Caicedo et al., 2019), RNA-seq (Coatsworth et al., 2021), RNA interference (RNAi) (Caicedo et al., 2019), and microbiome studies (Coatsworth et al., 2018) we have elucidated some of the mechanistic differences between the Cali-MIB and Cali-S strains. Several differences in immune activation have been observed, including changes in apoptosis regulation and initiation (Ocampo et al., 2013). However, despite considerable effort, we still have an incomplete understanding of the molecular details governing DENV immunity and which factors determine the MIB or S phenotype in these field-derived colonies.

Lipids are intricately involved in immune responses to viruses (Heaton & Randall, 2010; Lee et al., 2008; Schultz et al., 2018; Tree et al., 2019; Vial et al., 2020). Therefore, we hypothesized that the Cali-MIB refractory strain may have altered lipid regulation in response to DENV; specifically, we postulate that cholesterol and

phospholipid metabolism may contribute to the refractory phenotype. Cholesterol has been implicated in numerous studies with *Ae. aegypti* while infected with DENV (Chotiwan et al., 2018; Koh et al., 2020) and has been proposed as a mechanism for DENV resistance in *Wolbachia sp.* control programs (Caragata et al., 2013). Moreover, phospholipids and phospholipid remodelling have been shown to occur in response to DENV infection in *Ae. aegypti*. Altering the balance of lipid precursors to influence phospholipid concentrations impacts this relationship (Vial et al., 2019, 2020). The current literature indicates that these compounds are important to DENV replication, and we suspect that they may contribute to the resistance to DENV observed in Cali-MIB insects.

To test our hypothesis, we have utilized an untargeted Liquid Chromatography tandem mass spectrometry (LC-MS/MS) based lipidomics approach to observe changes in the metabolism of lipids in the midgut of refractory (Cali-MIB) and susceptible (Cali-S) insects in response to DENV challenge. The midgut lipidome was measured at three timepoints post DENV challenge, 18, 24, and 36 hours post blood meal (hpbm), to represent the time when DENV is entering, replicating within, and egressing from the midgut, respectively (Caicedo et al., 2013; Coatsworth et al., 2018, 2021; Serrato et al., 2017). Studies based on lipidomics have been utilized previously to ascertain host-virus interaction details (Chotiwan et al., 2018; Koh et al., 2020; Vial et al., 2019, 2020). Our study is unique in that it compares the role of lipids in two sympatric populations with a different vectorial capacity towards DENV after the ingestion of a normal blood meal or a bloodmeal containing DENV. This experimental framework is more likely to provide meaningful results for two reasons. First, the two populations are subject to the same metabolic stressor, DENV infection, and second, refractory insects can eliminate DENV before passaging to a new host. However, compounds found to be significantly different between the two populations must be validated experimentally for their roles in contributing to the DENV-induced phenotype. Our study found numerous compounds and pathways that were altered in the refractory strain after ingestion of DENV and generate novel hypotheses for DENV immunity in *Ae. aegypti*. If these molecules are found to be significant for viral resistance in controlled experiments, they may contribute to establishing stable DENV-resistant populations of *Ae. aegypti*.

## 3.3. Materials and Methods

### 3.3.1. Mosquito rearing

Mosquitoes were maintained under standard laboratory conditions (26 +/- 2°C, 12:12 light-dark cycle with 70% relative humidity). Adults were fed a 10% sugar solution ad libitum. Cali-S and Cali-MIB were selected as described in (Caicedo et al., 2013).

### 3.3.2. Virus Isolation

C6/36 HT cells (*Ae. albopictus)* were used to propagate DENV-2 New Guinea C strain. Cells were infected with DENV-2 and incubated for 14 days at 32°C in L15 media supplemented with 2% heat-inactivated fetal bovine serum, 1% penicillin/streptomycin, and 1% L-glutamine. Virally infected cells were collected in a 15mL centrifuge tube, and the infected cell suspension was mixed 1:1 with defibrinated rabbit blood to create an infectious blood meal. Infectious blood meal viral titers were quantified using the method described previously by (Bennett et al., 2002). Viral titers in the infectious blood meal ranged from 108 to 10 8.5 TCID50/mL for all oral challenges. Complete details on these procedures may be found in Ocampo et al. (2013) and Caicedo et al. (2013).

### 3.3.3. Mosquito Infections

Five-to-eight-day-old female adult Cali-S and Cali-MIB *Ae. aegypti* females were provided with an infectious blood meal containing DENV for 30 minutes via an artificial pig intestine membrane feeder described previously (Caicedo et al., 2013; Ocampo et al., 2013). Control mosquitoes of each phenotype were fed similarly on a blood meal that contained no DENV. After exposure to the blood meals containing, or not, DENV, fully-fed females were transferred to containers and given a 10% sucrose solution ad libitum. Containers had approx. 20 females/container and were maintained under the laboratory conditions described above.

### 3.3.4. Mosquito Dissections

Midguts from adult female mosquitoes fed on either an infectious DENV blood meal or blood control were dissected on a cold table and immediately transferred to a

microcentrifuge tube containing 100% ice-cold methanol at three timepoints; 18, 24, and 36 hours post blood meal (hpbm) (Fig. 3.1). Ten midguts were pooled at each timepoint for each treatment to obtain sufficient mass for lipid profiling. Each treatment and timepoint was performed in triplicate for a total of 36 samples. Samples were immediately frozen at -80°C and stored until transportation on dry ice from CIDEIM in Cali, Colombia, to Simon Fraser University in Burnaby, British Columbia. Upon arrival in Burnaby, BC, samples were stored at -80°C.

### 3.3.5. LC-MS/MS Analysis

Samples were processed and analyzed at The Metabolomics Innovation Centre (TMIC) in Edmonton, Alberta, using an LC-MS/MS global lipidomics approach. Lipids were extracted using a modified Folch liquid-liquid extraction protocol. Aliquots of samples were mixed with NovaMT LipidRep Internal Standard Basic Mix, dichloromethane, and methanol. LC-MS was performed in both positive and negative ionization (ESI) for each sample using a Thermo Vanquish UHPLC linked to a Bruker Impact II QTOF Mass Spectrometer. Flow rate was set at 250 µL/min with an m/z range of 150-1500 Da. MS/MS spectra were acquired for all samples with an MS/MS collision Energy of 10-60 eV. Injection volumes were 4 µL and 12 µL for positive and negative ionization, respectively.

### 3.3.6. Data Processing, Feature Identification, and Data Normalization

Data from positive and negative ionization injections were processed separately, and Lipid features were aligned using NovaMT LipidScreener. Aligned features from positive and negative injections were combined and merged into one intensity table for each sample. Missing values were substituted by one of three methods; 1) for features detected in at least 75% of injections within the group, the median intensity of the sample group was substituted; 2) for features detected in at least 50% of injections, the minimum intensity for features within the group was substituted; 3) for features detected in less than 50% of injections within the group, the global minimum for all samples and QC injections was substituted.

Lipid identification was performed using MS/MS spectral similarity, retention time (RT) and accurate mass. A three-tiered approach was used to determine identification

confidence; in tier one, MS/MS match score ≥500 and precursor m/s error ≤20.0 ppm and 5.0 mDa: in tier two, MS/MS match score <500 and precursor m/z error ≤20.0 ppm and 5.0 mDa; in tier three, Mass match with m/z error ≤20.0 ppm and 5.0 mDa.

Data Normalization was performed using a set of 15 internal standards of differing lipid classes (NovaMT LipidRep Internal Standard Basic Mix). Positive and putatively identified lipids (tiers 1-3) were matched to the internal standards based on similarity to the expected retention times for each lipid class. Intensity Ratios were calculated using the ratio of intensity of each lipid divided by the intensity of the matched internal standard. Unidentified features could not be normalized due to the inability to be matched to an internal standard.

Many duplicate features were identified in the dataset and were removed based on the following criteria. First, the highest tier identified feature was chosen from a set of duplicate features, and the others were discarded. In other words, the order of priority for keeping features was tier 1 > tier 2 > tier 3. If a tie occurred within tier 1 or tier 2 identifications, the feature with the higher MS/MS score was kept. If a tie occurred within tier 3 identifications, the feature with the lowest m/z error was kept.

### 3.3.7. Data Analysis and Visualization

Lipid intensity ratio tables were uploaded to Metaboanalyst 5.0 for analysis and statistical testing. Features with relative standard deviations >25% (SD/mean>25%) in quality control samples (QC) were removed. Samples were normalized by median, and data were scaled with auto-scaling (mean-centred and divided by the SD of each variable). Significance analysis of microarrays (SAM) was used to identify significantly changed features compared with the controls. The delta value for each test was adjusted to control the estimated false discovery rate (FDR) at 5%, and features with greater than expected variations after adjustment of the FDR were considered significant (Tusher et al., 2001). Principle Component analysis was performed to assess data quality and between-group differences. Hierarchical clustering was performed using the ward clustering algorithm with Euclidean distance measures. Data visualizations were constructed using a combination of Metaboanalyst 5.0 and R (v. 4.1.1).

## 3.4. Results

### 3.4.1. Feature Detection and Lipid Identification

Lipids have been implicated in the successful entry and replication of DENV in *Aedes aegypti* (Chotiwan et al., 2018; Heaton & Randall, 2010; Koh et al., 2020; Manokaran et al., 2020; Vial et al., 2019, 2020). Accordingly, we evaluated lipid modulations in response to DENV challenge in our system of refractory and susceptible field-derived *Ae. aegypti* strains at time points that are highly relevant to the entry, replication, and escape of DENV in midgut cells (Fig. 3.1).

Three replicates for each treatment and timepoint were extracted for a total of 36 samples. Across all samples, 18749 features were detected. A feature represents a distinct lipid molecule and herein, the terms feature and lipid will be used interchangeably. A three-tier approach was used for feature identification and provided accuracy estimates. If a feature was matched within a tier, it would not be matched again to a subsequent tier. Tiers one and two were matched using accurate mass and MS/MS spectral similarity to provide high-confidence identifications (see materials and methods). In tiers one and two, 863 (4.6%) and 169 (0.9%) features were identified, respectively (Fig. 3.2). Tier three uses mass-matching to provide putative lipid identifications. Within this tier, 6223 (33.2%) features were identified (Fig. 3.2). Two analyses were performed using these data, one containing all identified features (tiers 1, 2, and 3) and one using only high confidence metabolites (tiers 1 and 2).

### 3.4.2. Principal Component Analysis: Tiers 1, 2, and 3

Principal component analysis (PCA) was applied to the full dataset to assess data trends and data quality. PCA is a widely accepted form of data compression and aims to model high-dimensional data in a lower-dimensional space while preserving most of the variance within the data (Vidal et al., 2016). PCA is often used as an initial step for lipidomics data analysis to assess broad changes in lipid profiles and determine if the algorithm can resolve between-group differences. We performed three comparative PCAs at each timepoint: Cali-S blood and virus vs. Cali-S blood-fed, Cali-MIB blood and virus vs. Cali-MIB blood-fed, Cali-MIB blood and virus vs. Cali-S blood and virus. The third analysis compares the lipid profiles in each strain when they were both challenged

with DENV and is the focus of the present study. Because both strains are under the same metabolic stressor, DENV, this comparison has the highest potential to provide meaningful compounds contributing to their respective phenotypes.

PCA plots for all timepoints and treatments can be viewed in Fig. 3.3. Cali-S midgut samples show modest separation for all timepoints in the PCA plots (Fig. 3.3). At 18 hpbm, the Cali-S strain challenged with DENV overlaps with blood-fed controls, and some experimental replicates have low inter-group variation. The PCA plot of 24 hpbm shows increased separation, yet the 95% confidence intervals (coloured ellipses) overlap, and this trend holds at 36 hpbm. Interestingly, the plots of Cali-MIB samples show an inverse trend. At 18 hpbm, the greatest separation is observed with strong inter-group differences, which is reduced at 24 hpbm and 36 hpbm (Fig. 3.3). Moreover, at 18 hpbm, Cali-MIB samples challenged with virus cluster more closely together than any other sample or timepoint.

PCA plots from refractory and susceptible populations challenged with DENV show separation at all three timepoints (Fig. 3.3); 18 hpbm displays the largest distance that decreases with time. PCA profile differences between Cali-MIB and Cali-S strains challenged with DENV provide cause to compute significant feature differences between these populations.

### 3.4.3. Principal Component Analysis: Tiers 1 and 2

Our dataset was subdivided into high-confidence identifications and putative identifications. We evaluated the dataset's quality with PCA using only the high-confidence lipids. PCA plots for the susceptible strain challenged with DENV compared to susceptible blood control showed similar trends to the full feature set (tiers 1, 2, and 3). At 18 hpbm, there is modest separation between control and treatment (Fig. 3.4). However, by 24 and 36 hpbm, the two groups are distinguishable by PCA with little-to-no overlap, with 24 hpbm having the greatest separation (Fig. 3.4).

Observing PCA plots for the Cali-MIB strains challenged with DENV compared to their blood fed controls shows a strong separation at 18 and 24 hpbm, which is slightly ablated by 36 hpbm. PCA plots from Cali-S and Cali-MIB samples using the high-

confidence features trend similarly to plots using the full feature set. Interestingly, there is a greater resolution when using the reduced feature set.

PCA plots from Cali-MIB+DENV samples compared with Cali-S+DENV samples show strong separation at all three timepoints (Fig. 3.4). None of the plots have overlapping confidence bands. At 24 hpbm, the narrowest confidence band and the greatest separation can be observed. Our results indicate that there are likely differences in the Cali-MIB and Cali-S insects' lipid profiles after exposure to a challenge with DENV.

### 3.4.4. Identifying Significant Lipids and Lipid Categories- Tiers 1, 2, and 3

After observing trends across treatment groups using PCA, we determined the lipid categories and lipid features that were altered in each of the comparisons. Two statistical methods were considered to determine significant features, significance analysis of microarray (SAM) and partial least squares-discriminant analysis (PLS-DA). The features identified as significant for both models showed considerable overlap. Ultimately SAM was chosen to select significantly altered lipids due to the algorithm providing an estimated false discovery rate (FDR) (Tusher et al., 2001). For all tests, the delta value was adjusted to control the estimated FDR at 5%, and features that had greater than expected variation under the null hypothesis after adjustment were considered to be statistically significant.

The identities of the top lipids identified as significant for each time-point and treatment can be seen in Table 3.1. When comparing Cali-S challenged with DENV to non-infected controls, only one lipid was found to be significantly regulated at 18 hpbm (SAM FDR<0.05) (Fig. 3.5). This contrasts with the Cali-MIB strain that showed 538 differently regulated lipids at the same timepoint when compared to non-infected controls. Cali-MIB challenged with DENV had 328 significant lipids (SAM FDR<0.05) when compared to virally challenged Cali-S females (Fig. 3.5). Moreover, there is considerable overlap of the 538 lipids altered in Cali-MIB within-group comparisons and the 328 significant lipids in the Cali-MIB vs Cali- strains. The Venn diagram shows 248 lipids were identified as significant in both groups (Fig. 3.5). Additionally, there were noticeable patterns of lipid regulation among the various lipid profiles. The single lipid

deemed significant in the Cali-S strain was downregulated (decreased in concentration relative to the control), whereas in both other two strains, all lipids were upregulated (increased in concentration relative to controls) (Fig. 3.5).

Interestingly, with the full dataset, no lipid features were significantly different at 24 hpbm in susceptible and refractory insects challenged with DENV compared to their blood-fed controls (Table 3.1). However, Cali-MIB challenged with DENV compared to Cali-S challenged with DENV showed 38 significantly regulated lipids (SAM FDR<0.05), all downregulated in the Cali-MIB samples.

At 36 hpbm, more lipids were identified as significant (SAM FDR<0.05) than at the 24 hpbm time point; 32, 92 and 214 features were identified as significant in Cali-S+DENV vs control, Cali-MIB+DENV vs control, and Cali-MIB+DENV vs Cali-S+DENV comparisons (Fig. 3.5). Significant lipids in Cali-S+DENV samples were all downregulated, whereas, in Cali-MIB+DENV samples, all lipids were upregulated. Cali-MIB+DENV samples had a more balanced regulatory pattern, with 205 lipids upregulated and 59 downregulated. Cali-MIB samples also showed considerable overlap with 50 common lipids between the two comparisons (Fig. 3.5).

The lipidome is in constant flux with nearly infinite numbers of possible compounds. Therefore, it can be informative to observe changes in categories of lipids rather than observe alterations in individual lipid features. Lipids were placed into one of 72 different lipid subclasses based on their identification within the NovaMT LipidScreener platform. Significant features in the Cali-MIB+DENV vs Cali-S+DENV comparison were sorted by their lipid categorization and plotted to identify the most lipid categories with the most changed features at each timepoint (Fig. 3.6). At 18 hpbm, the top lipid categories among significant features are fatty acids (FA), diacylglycerols (DG), ceramides (Cer), and sterol lipids (ST) (Fig. 3.6). At 24 hpbm fewer features were significant (SAM FDR<0.05). Nonetheless, the lipid categories with the largest number of changed features were triacylglycerols and Phosphatidylcholines (Fig. 3.6). At 36 hpbm, the changes in lipid categories were broader, with ceramides having the greatest number of altered lipids (Fig. 3.6).

### 3.4.5. Identifying Significant Lipids and Lipid Categories- Tiers 1 and 2

Focusing on the high confidence identified metabolites can provide more accurate results for discussing individual lipid changes and broad lipid category differences. Using the lipids identified in tiers one and two, 14, 187, and 56 lipids were significant (SAM FDR<0.05) at 18 hpbm in Cali-S+DENV vs blood control, Cali-MIB+DENV vs blood control, and Cali-MIB+DENV vs Cali-S+DENV, respectively (Fig. 3.7). Many lipids with significantly different concentrations were shared among the Cali-MIB comparisons (39 lipid features). Cali-S+DENV midguts vs blood-fed controls had primarily downregulated features (93%). Whereas Cali-MIB+DENV vs Cali-S+DENV had primarily up-regulated features (89%) (Fig. 3.7). Cali-MIB+DENV vs blood-fed controls had an approximately even distribution of upregulated to down-regulated lipids (47% upregulated) (Fig. 3.7).

At 24 hpbm, Cali-S midguts challenged with DENV had 19 significant lipids compared to blood-fed controls (SAM FDR<0.05), and all lipids were upregulated (Fig. 3.7). Cali-MIB+DENV compared to Cali-S+DENV samples had eight features achieve statistical significance; all showed reduced concentrations in the Cali-MIB strain. The Cali-MIB challenged with DENV had no significant features at the 24 hpbm time point (Fig. 3.7). The 36 hpbm time point had 6, 32 and 3 significant features for the Cali-S strain, Cali-MIB strain, and the Cali-MIB vs Cali-S comparison (Fig. 3.7). Interestingly, none of the features were common among these groups. Both Cali-MIB+DENV vs control and Cali-MIB+DENV vs Cali-S+DENV had entirely upregulated significant features, whereas the Cali-S comparison had primarily decreased concentration lipids as significant (83%) (Fig. 3.7). The identities of the top 10 significant features for each comparison described above can be seen in Table 3.2.

Lipid classes for features identified as significant in the Cali-MIB+DENV vs Cali-S+DENV comparison can be seen in Figure 3.8. At 18 hpbm, phosphatidylethanolamines (PE), ceramides (Cer), and sphingomyelins (SM) are the most common lipid categories with altered concentrations (Fig. 3.8). At 24 hpbm, only fatty acids (FA), phosphatidylcholines (PC), and triglycerides (TG) are changed (Fig. 3.8). Similarly, at 36 hpbm, only ceramides and prenol Lipids (PR) have lipid features that are altered in concentration after DENV challenge.

### 3.4.6. Lipidomic Profiles of Cali-MIB and Cali-S Blood-fed Midguts

We have observed the metabolic changes associated with DENV in the refractory Cali-MIB strain, and we wanted to determine if the lipid profiles are different in response to blood meal alone. We performed PCA analysis on Cali-MIB+blood and Cali-S+blood samples at all three timepoints to test this. The PCA plots can be seen in Appendix C.

At 24 and 36 hpbm, PCA plots show separation between the Cali-MIB and Cali-S samples, which aligns with the PCA plots from DENV-challenged samples. However, at 24 hpbm, there is an overlap between the two profiles showing there may not be significant differences between the samples. Indeed, at 18 hpbm, SAM analysis shows only one significant feature (SAM FDR<0.05), whereas 24 and 36 hpbm have 35 and 190 significant features, respectively (Appendix C). Additionally, there was little overlap in significant features that were upregulated in the Cali-MIB strain with blood only and the Cali-MIB blood+DENV samples at 18 and 24 hpbm. However, by 36 hpbm, 38.8% of features upregulated by blood meal were shared with features upregulated by blood+DENV in the Cali-MIB strain. Moreover, the top lipid categories altered by blood meal were Ceramides, Diacylglycerols, Phosphatidylcholines, Sterol lipids, and Triacylglycerols.

### 3.4.7. Choosing Candidate Anti-DENV Lipid Features and Classes

The purpose of this work was foremost to identify the lipidome changes that occur in response to DENV challenge and identify lipids and pathways that may enhance or diminish DENV replication in *Ae. aegypti*. What makes our work unique is that we are measuring the lipidome of sympatric strains of *Ae. aegypti* that are refractory or susceptible to infection, and this provides stronger controls than other studies to date (Manokaran et al., 2020; Vial et al., 2019, 2020). Following this goal and our study design, we will focus our discussion on the Cali-MIB+DENV vs Cali-S+DENV comparison and the compounds significantly regulated between these two experimental groups (SAM FDR<0.05). Compounds that are higher in concentration in the Cali-MIB+DENV treatment will be considered *upregulated,* and inversely, those with lower concentrations in the Cali-MIB+DENV group will be considered *downregulated*. These compounds may exhibit anti-DENV character through one of a few mechanisms. First,

they may directly interfere with an aspect of viral entry into the cell, replication, or egress; second, they may act as precursors to anti-DENV immune responses and increase the concentration of immune mediators; or third, they may shift metabolism away from a pro-viral milieu and prevent viral components from being assembled.

## 3.5. Discussion

### 3.5.1. Altered Lipid Metabolism in DENV Infected MIB Populations

Lipid metabolism has been reported to influence DENV infection kinetics *in Ae. aegypti* (Chotiwan et al., 2018; Heaton & Randall, 2010; Vial et al., 2019, 2020) and has even been proposed as an explanation for *Wolbachia*-induced DENV resistance (Manokaran et al., 2020). Thus, we wanted to determine if modulations in lipid metabolism were present in our model system of field-derived refractory (Cali-MIB) and susceptible (Cali-S) strains of *Ae. aegypti*. We carried out LC-MS/MS profiling of pooled samples of midguts of Cali-MIB and Cali-S, with or without DENV challenge, at three timepoints post-infectious blood meal: 18, 24, and 36 hpbm. Using this method, 18,749 features were detected, of which 863, 169, and 6223 were identified in tiers 1, 2, and 3, respectively. In total, 7255 features, or 38.7%, were positively or putatively Identified.

Using PCA, we observed broad, whole lipidome changes for treatment groups at different time points. Unexpectedly, using all identified lipids (tiers 1, 2, and 3) and the reduced feature set (tiers 1 and 2), there was separation between the Cali-MIB and Cali-S samples at all timepoints. These data contrast with results from our metabolomics studies which showed low separation at 36 hpbm (Chapter 2). However, a stronger separation is seen at earlier timepoints (18 and 24 hpbm), indicating these times may have more significant lipid profile differences. We will discuss significantly altered lipid categories in the Cali-MIB strain compared with the Cali-S strain when both were challenged with DENV as this comparison provides the lipid metabolites most likely to influence DENV infection dynamics, given that both populations are under equivalent metabolic stress of DENV challenge.

We opted to use SAM modelling to determine significantly different lipids between treatment groups. Due to the increased number of features in the lipidomics data compared to the metabolomics data (Chapter 2), we applied a stricter criterion to

achieve statistical significance. A 5% FDR, as estimated by SAM, was chosen as the cut-off to achieve significance.

### 3.5.2. Regulatory Trends Among Treatment Groups

Although our main interest is to compare differences between the two strains when challenge with DENV, there were consistent trends in within-strain feature regulation that are worth noting. Generally, the Cali-S strain showed decreased concentrations of significant lipids in response to DENV compared with blood controls, whereas Cali-MIB samples had entirely upregulated significant features or a skewed balance towards upregulation. The only exception to this trend was the significant features in the tiers 1 and 2 data set at 24 hpbm. DENV has been demonstrated to reprogram its host lipid metabolism to reduce concentrations of various metabolites (Vial et al., 2019). Perhaps the stark contrast between regulation in Cali-MIB and Cali-S samples demonstrates some resistance to DENV-induced metabolic changes in the Cali-MIB midgut samples.

### 3.5.3. Lipid Categories Altered by DENV Infection

Lipids are a highly diverse macromolecule category with numerous categories, classes, and subclasses. Because of the incredible diversity of lipid structures, this classification system is often used to report lipidomics results within the literature. Here, we will discuss the significant features within the lipid categorization system described in Table 3.3.

#### *3.4.3.1 Sphingolipids (SLs)*

SLs are integral components of cellular membranes that are well conserved across eukaryotic organisms but also are found in a diverse range of species, including bacteria (Futerman, 2021; Quinville et al., 2021). Recent discoveries have shown that SLs are essential components of membrane-rafts and numerous signalling pathways (Futerman, 2021; Maceyka & Spiegel, 2014).

Unlike other membrane lipids, SLs are synthesized between the endoplasmic reticulum and the Golgi apparatus, displaying high compartmentalization during synthesis (Futerman, 2021; Quinville et al., 2021). SLs are amphipathic molecules made

of a sphinganine or sphingosine backbone with a fatty acid molecule attached; they comprise ~30% of cellular membranes (Futerman, 2021). Ceramide makes up the basic building block of SLs and is formed through the combination of serine and a fatty acid; often palmitoyl-CoA, but other CoA molecules can be utilized (Chotiwan et al., 2018; Futerman, 2021). Numerous complex SLs can be synthesized from ceramides, such as sphingomyelin and Glycosphingolipids, for various cellular functions.

The most common subclasses of SLs identified as changed in our analysis were Ceramides, Sphingomyelins (SM), and Ceramide Phosphoethanolamines (PE-Cer).

**Ceramides**

Ceramides are categorized as SLs but make up their own main classes and subcategories (Table 3.3). They are involved in numerous cellular processes and have gained interest in recent years due to their involvement in orchestrating cellular death and proliferation (Chotiwan et al., 2018; Futerman, 2021; Hannun et al., 2011; Maceyka & Spiegel, 2014; Quinville et al., 2021), and increased research has led to the expansion of known ceramide structures and their metabolism (Hannun et al., 2011).

Perhaps the most well-studied function of ceramides and SLs is their role in regulating apoptosis and autophagy. Ceramides and sphingosine-1-phosphate function to counter each other; the former induces a state of cell death (apoptosis), and the latter can induce cell survival pathways such as autophagy (Nganga et al., 2018; Young et al., 2013). These two compounds have been described as a molecular “switch” between these cellular states (Young et al., 2013). The mechanism of ceramide-induced cell death is not well resolved. However, a key step during the initiation of apoptosis involves the permeabilization of the mitochondrial membrane, and membrane permeability occurs with increased ceramide concentrations (Chang et al., 2015). Counter to ceramides, S1P has been shown to enhance pro-survival and growth pathways such as mTOR (Young et al., 2013).

Autophagy is crucial for DENV infection in *Ae. aegypti* (Brackney et al., 2020; Eng et al., 2016; Heaton & Randall, 2010; Lee et al., 2008; Sim et al., 2014). Moreover, we have shown previously that apoptosis can function to control DENV infection and that this mechanism is present in refractory insects (Ocampo et al., 2013). In our lipidomics analysis, ceramide compounds were overrepresented as a significantly altered lipid

class and were primarily upregulated (Fig. 3.6, Fig. 3.8). Significant increases in ceramide concentrations may act as a signalling mechanism, initiating an increased apoptosis response in the midguts of Cali-MIB mosquitoes. The mechanisms underlying viral sensing in Cali-MIB mosquitoes, or in other insects resulting in altered ceramide synthesis is unknown.

**Ceramide Phosphoethanolamine (PE-Cer) and Sphingomyelins (SM)**

SM is a ceramide derivative with an attached phosphorylcholine that can be converted back to ceramide through a degrative pathway (Futerman, 2021). SM is speculated to be important in lipid rafts, membrane fluidity, cell signalling, and other ordered membrane domains (Futerman, 2021; Mencarelli & Martinez-Martinez, 2013; Panevska et al., 2019). Moreover, PE-Cer is a SM derivative that has shown increased importance in invertebrates (Panevska et al., 2019). In mammals, SM interacts with cholesterol to increase membrane fluidity and membrane packing to facilitate various cellular processes (Panevska et al., 2019). Although the function of PE-Cer is not well understood, it does not interact favourably with cholesterol to facilitate membrane fluidity (Panevska et al., 2019).

Numerous SMs and PE-Cer compounds were significantly upregulated during DENV infection in Cali-MIB midguts at 18 and 36 hpbm (Fig. 3.6, Fig. 3.8). Interestingly, very few changes in SM species and no changes in PE-Cer were observed at 24 hpbm; those SM species that were significantly different showed decreased concentrations in Cali-MIB samples. Other studies on lipidomics results with SM and PE-Cer regulation have found contradictory results (Chotiwan et al., 2018; Perera et al., 2012). *Chotiwan et al.* (2018) reported decreased PE-Cer concentrations at early infection timepoints (3 days post blood meal) and no changes in SM (mosquito midguts); whereas *Perera et al.* (2012) reported ~2-fold increases in SM and reduced concentrations of PE-Cer (C6/36 cells). The reasons for the discrepancies between these data, including ours, may be related to differing tissues (midguts of refractory insects, midguts of WT insects, C6/36 cell culture) or differing time points. In our analysis, no PE-Ceramides species and only one SM species were identified as significant at any timepoint in the Cali-S strain challenged with DENV compared to their blood-fed controls. This may suggest that SM and PE-Cer species have either direct or indirect anti-viral action.

#### *3.4.3.2 Glycerolipids (GLs)*

Glycerolipid is a diverse category of structures with a glycerol backbone linked to at least one hydrophobic chain. GLs have diverse functions in animal, bacteria, and plant species (Veprintsev et al., 2013; Voelker, 2013). Broadly, glycerolipids have two important functional categories, neutral glycerolipids and polar glycerolipids (Veprintsev et al., 2013; Voelker, 2013). The former contains mono-, di, and triacylglycerols (MAGs, DAGs, TAGs), and the latter contains the glycerolphospholipids (alternatively: phospholipids, PLs), phosphatidic acid (PA), phosphatidylcholine (PC), phosphatidylethanolamine (PE), phosphatidylserine (PS), and phosphatidylinositol (PI), among others.

DAGs and TAGs can be utilized for energy metabolism in the insect. After a bloodmeal, fatty acids are absorbed and can be converted to TAGs and, to a lesser extent, DAGs for energy storage (Canavoso et al., 2004; Chotiwan et al., 2018; Veprintsev et al., 2013; Voelker, 2013). DAGs also serve as second messengers for cell signalling, regulating proliferation, mitochondrial function, and apoptosis (Chotiwan et al., 2018). TAGs are non-polar lipids and are often stored in lipid droplets (LD) within the cytosol (Veprintsev et al., 2013; Voelker, 2013). Alternatively, glycerolphospholipids are amphipathic lipid molecules that contain a polar headgroup with non-polar tails (Veprintsev et al., 2013; Voelker, 2013). Glycerolphospholipids make up most cell membranes, and the composition of glycerolphospholipids impacts membrane properties and functions (Veprintsev et al., 2013; Voelker, 2013).

In our study, the GLs that were most significantly dysregulated in Cali-MIB+DENV samples were DAGs, TAGs, PC, PE, and PG. These lipids are intricately related; DAG can be converted to PC or PE for membrane function, signalling, or the production of TAGs for energy storage (Gertruida O'neill et al., 2021; Takeuchi & Reue, 2009). Interestingly, TAGs are primarily stored within lipid droplets within the cytoplasm, often composed mainly of PC and PE (Gertruida O'neill et al., 2021). However, lipid droplets and the phospholipids PC and PE appear to have opposing roles in DENV infection (Ferreira Barletta et al., 2015; Vial et al., 2020) and DENV has been reported to halt the de novo synthesis of PL to aid its own replication (Vial et al., 2020).

Additionally, the induction of PL negatively influences viral particle assembly (Vial et al., 2020). There is an accumulation of LDs in the cytoplasm after DENV infection and

these may enhance the viral infection (Ferreira Barletta et al., 2015). With our current data, it is not possible to ascertain whether changes in PLs have a greater influence than LDs on DENV replication and whether increased TAG concentrations correlate with LD density in the cytoplasm.

An alternative mechanism explaining concentrations of DAG and PLs considers the PL remodelling cycle. PLs are produced through the remodelling of PCs via the lands cycle, and PCs are produced by the *de novo* synthesis pathway (Moessinger et al., 2014). In the *de novo* synthesis pathway, PC is produced through the reaction of DAG and phosphocholine (Moessinger et al., 2014; Vial et al., 2020). Counter to the *de novo* pathway, fatty acids are removed from PC in the Lands cycle to produce lysophophatidylcholine (lysoPC), which then can be modified to produce the other PLs to influence membrane properties (Moessinger et al., 2014). The *de novo* pathway and the lands cycle antagonize each other to regulate the amount and types of PLs produced. DENV has been shown to induce phospholipid remodelling in *Ae. aegypti* early in infection, as noted by increases in lysophospholipids (lysoPL) (Chotiwan et al., 2018; Vial et al., 2020) and activation of the remodelling pathway is speculated to increase PL diversity to positively influence virion formation. Our data revealed few changes in lysoPLS with significant increases in the concentrations of PC and PE. Taken together, significant changes in PC concentrations and minimal change to lysoPLs may indicate that the Cali-MIB strain is resisting DENV-induced PL remodelling.

#### *3.4.3.3 Fatty Acids (FAs)*

FAs are a lipid subclass under the broader category of fatty acyls (Table 3.3). FAs contribute to numerous fundamental metabolic constituents that are precursors to structural, energetic, and signalling molecules, including many of the molecules discussed above (TAGs, DAGs, Phospholipids) (Gaspar et al., 2011; Lehner & Quiroga, 2021). FAs are, however, a complex category of molecules ranging from a few carbons in length to long-chain FAs, and each of these compounds will possess a different proclivity for metabolic reactions (Watkins, 1997). Moreover, FAs require activation to function in many metabolic pathways (Lehner & Quiroga, 2021; Watkins, 1997). Activation involves the addition of a CoA molecule; this requirement was first noted as a requirement for β-oxidation in the mitochondria (Lehner & Quiroga, 2021; Watkins, 1997). Un-activated FA is alternatively called free FA (FFA).

There are numerous studies showing perturbed FA metabolism in DENV-infected tissues and that influencing the production of FAs through modulating fatty acid synthase affects DENV replication (Chotiwan et al., 2022; Heaton et al., 2010; Perera et al., 2012). However, it appears that the concentration of FA is not a determinant of a pro-DENV milieu but rather the ratio of activated FA to FFA (Chotiwan et al., 2018). While studying the anti-DENV effects of *Wolbachia* infection, it was noted that *Wolbachia* co-infection reduces concentrations of activated FA and increases FFA concentration. Interestingly, attempts to determine the effect of FFA on DENV replication through dsRNA knockdown failed to observe changes in DENV replication (Koh et al., 2020), possibly because FFAs can be obtained from numerous sources.

In our study, numerous FAs were altered in the Cali-MIB strain challenged with DENV compared to the Cali-S strain challenged with DENV (Fig. 3.6, Fig. 3.8). FAs were primarily upregulated, except for the 24 hpbm timepoint. FAs with significant concentration changes were primarily long-chain FAs (13-22 carbons in length) or very-long-chain FAs (22+ carbons) (Hidalgo et al., 2021; Watkins, 1997). Moreover, no activated FAs, or fatty Acyl CoAs, were significantly different in Cali-MIB midguts.

#### *3.4.3.4 Sterol Lipids (STs)*

Sterols are ringed lipid alcohols present in almost all living organisms, from bacteria to vertebrates (Myant, 1981; Weatherby & Carter, 2013). They are involved in eukaryotic membrane function, regulating metabolism, and developmental signalling (Jing et al., 2014; Wollam & Antebi, 2011). Although sterols perform very similar functions in vertebrates and invertebrates, insects lack the ability to synthesize sterols *de novo* and must obtain them from their diets (Jing et al., 2014). As in vertebrates, cholesterol is the dominant sterol found in invertebrates (Jing et al., 2014).

Our data show that sterols were significantly altered in response to DENV challenge in Cali-MIB insects when compared with Cali-S insects challenged with DENV (Fig. 3.6). Interestingly, there appeared to be temporal regulation of sterols. At 18 and 36 hpbm, sterols were primarily upregulated, whereas, at 24 hpbm, all significant sterols were down-regulated (Fig. 3.6). Many sterol lipids regulated early in infection (18 hpbm) were cholesterol and cholesterol derivatives. In contrast, those shown to be significant at later time points had diverse sterol categories. Cholesterol is the most researched sterol lipid, especially in viral infections.

Numerous articles have been published discussing the effects of cholesterol on flavivirus replication in mammals and *Ae. aegypti* (Carro & Damonte, 2013; Geoghegan et al., 2017; Lee et al., 2008; Mackenzie et al., 2007; Schultz et al., 2018; Tree et al., 2019). Cholesterol is essential for DENV entry, and selective depletion of cholesterol hinders viral success (Carro & Damonte, 2013; Lee et al., 2008). Moreover, to facilitate viral replication, flaviviruses have demonstrated the ability to influence cellular concentrations of cholesterol (Mackenzie et al., 2007; Tree et al., 2019). It is theorized that cholesterol competition is one of the mechanisms of viral resistance among *Wolbachia* transinfected insects (Caragata et al., 2013; Geoghegan et al., 2017; Koh et al., 2020; Schultz et al., 2018). However, the relationship between cholesterol and viral success may depend on cholesterol concentration and timing. Viral entry and uncoating early in infection may be negatively influenced by high cholesterol concentrations (Lee et al., 2008). Additionally, higher cholesterol levels are associated with DENV blocking, and importantly, esterified cholesterol and not free cholesterol are correlated with DENV blocking (Geoghegan et al., 2017).

### 3.5.4. Lipid Metabolism Changes in Response to Bloodmeal

We wanted to determine if the lipidomic changes in the Cali-MIB strain were a response to the virus or a conserved response to the blood meal. To answer this question, we observed the metabolic differences in Cali-MIB and Cali-S strains in response to blood meal at all three timepoints. The results showed at 24 and 36 hpbm, the lipidomic profiles of Cali-MIB and Cali-S strains differed in response to blood meal, but at 18 hpbm, the profiles were more similar. Moreover, in Cali-MIB samples at the 36 hpbm timepoint, many of the changed lipid features were similarly altered in Cali-MIB midguts after DENV challenge. These results were counter to our metabolomic results (Ch. 2), where Cali-MIB blood-only samples shared no features with Cali-MIB blood+DENV samples. Additionally, many of the significant lipid categories were similar to those found in the Cali-MIB blood+DENV screen.

Taken together, these results indicate the lipid metabolism in response to bloodmeal is altered in the Cali-MIB strain compared to Cali-S samples and that there are consistent features upregulated by blood meal and blood+DENV at 36 hpbm. Perhaps the features identified at 36 hpbm in the blood+virus screen are less involved in

maintaining DENV resistance and more indicative of metabolic demands associated with blood meal digestion.

## 3.6. Conclusions

We present the first Lipidomics profiling of a DENV-refractory population of *Ae. aegypti* challenged with DENV. Our study is unique in terms of being able to compare lipidomics differences in sympatric field-derived *Ae. aegypti* strains that are naturally resistant (Cali-MIB) or susceptible (Cali-S) to DENV. In lipidomics analyses done to date, only susceptible populations of *Ae. aegypti* have been studied, and thus, the data cannot explain metabolic changes and immune responses that can manage the infection. Therefore, our experimental design offers considerable advantages as the metabolic milieu present in refractory insects is more likely to represent one that negatively impacts viral infection, replication, and transmission.

We focused our discussion on the lipid categories that were altered in the Cali-MIB strain compared to the Cali-S strain when both were challenged with DENV. First, as described above, this comparison is the most likely to identify compounds or pathways possessing anti-DENV factors. Second, the lipidome is extremely diverse, understudied, and the literature available for individual lipid moieties is inadequate to determine their role in DENV replication. Lastly, the resolution of our data must be considered when connecting lipidomics data to a phenotypic difference. If we attempt to describe lipidomic changes with high granularity, we are more likely to make erroneous claims regarding the significance of our findings. This final point highlights the fact that our data are correlative, and none of the compounds identified here as significant have been validated to be causally important for DENV resistance in Cali-MIB insects. Further research is needed to provide a mechanistic understanding of anti-DENV lipidome changes in the refractory Cali-MIB strain of *Ae. aegypti.*

Notwithstanding these limitations, we have identified numerous lipid compounds and categories that may possess anti-DENV character, such as sphingolipids and ceramides, glycerolipids and phospholipids, fatty acids, and sterols. Perhaps the most intriguing of our results was the rapid increase in ceramide compounds within the Cali-MIB refractory population, as ceramides have demonstrated ability to initiate apoptosis (Nganga et al., 2018; Young et al., 2013). The stark increase in ceramide compounds

seen in our analysis, coupled with our previous work demonstrating a rapid onset of apoptosis in the refractory strain, provides a possible mechanism for apoptotic viral resistance in Cali-MIB females. This hypothesis should be evaluated using traditional molecular approaches to determine the magnitude of ceramides' effect on DENV replication. Moreover, there is an apparent resistance to phospholipid remodelling in Cali-MIB midguts, indicated by increased concentrations of PC and PE, with minimal perturbations in lysoPLs. To evaluate if lysoPL remodelling is stunted in refractory Cali-MIB insects, concentrations of lysoPLs and PLs could be modified, and the impacts on DENV replication observed, as has been done previously by (Vial et al., 2020). Overall, this research establishes numerous hypotheses to be systematically tested to validate novel anti-DENV lipid pathways and may contribute to the successful development of genetically modified, DENV-resistant populations of *Ae. aegypti*.

## 3.7. Figures and Tables

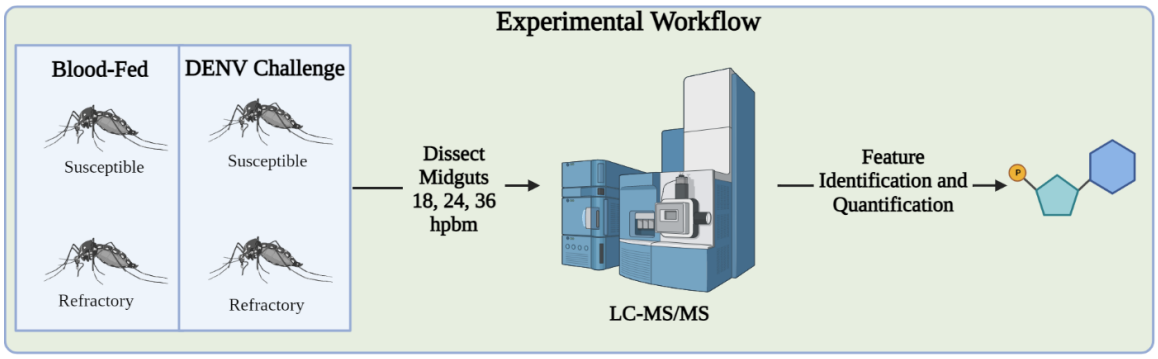


**Figure 3.1.** **Experimental workflow. Schematic showing the four treatment groups dissected in triplicate at three time points, 18, 24, and 36 hours post blood meal . Ten midguts were pooled for each treatment at each timepoint and subjected to LC-MS/MS.**

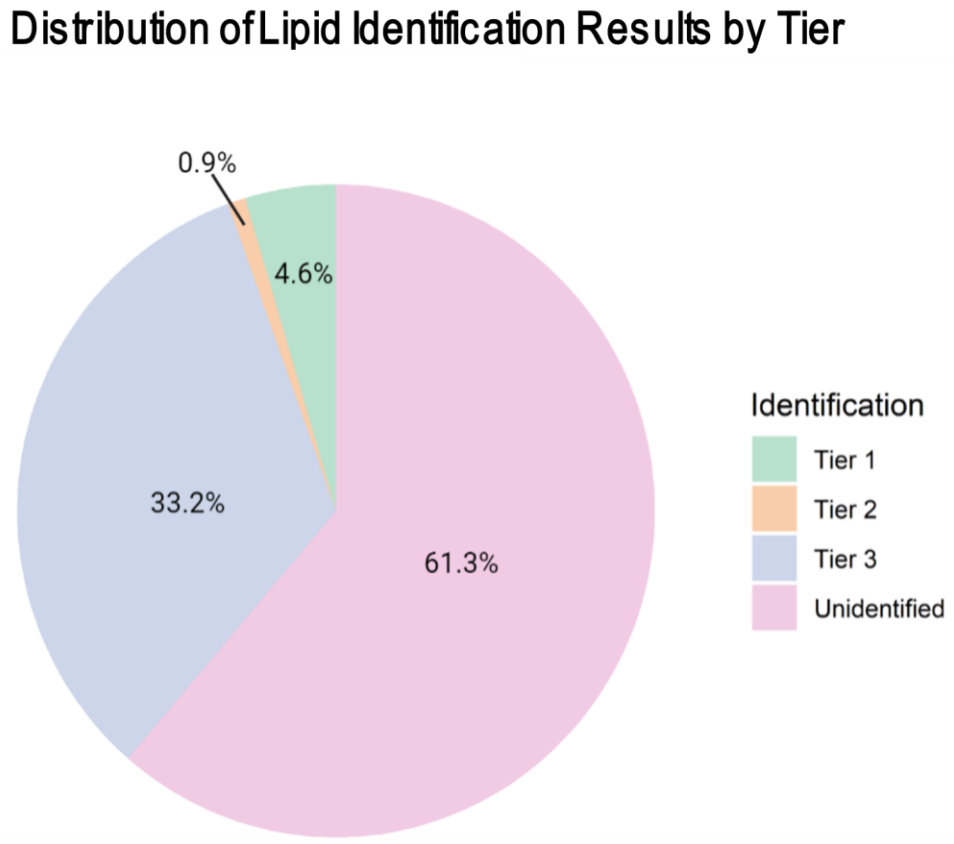


**Figure 3.2** **Distribution of lipid Identifications by identification tier. The pie chart shows the percentage of metabolites identified in each accuracy tier.**

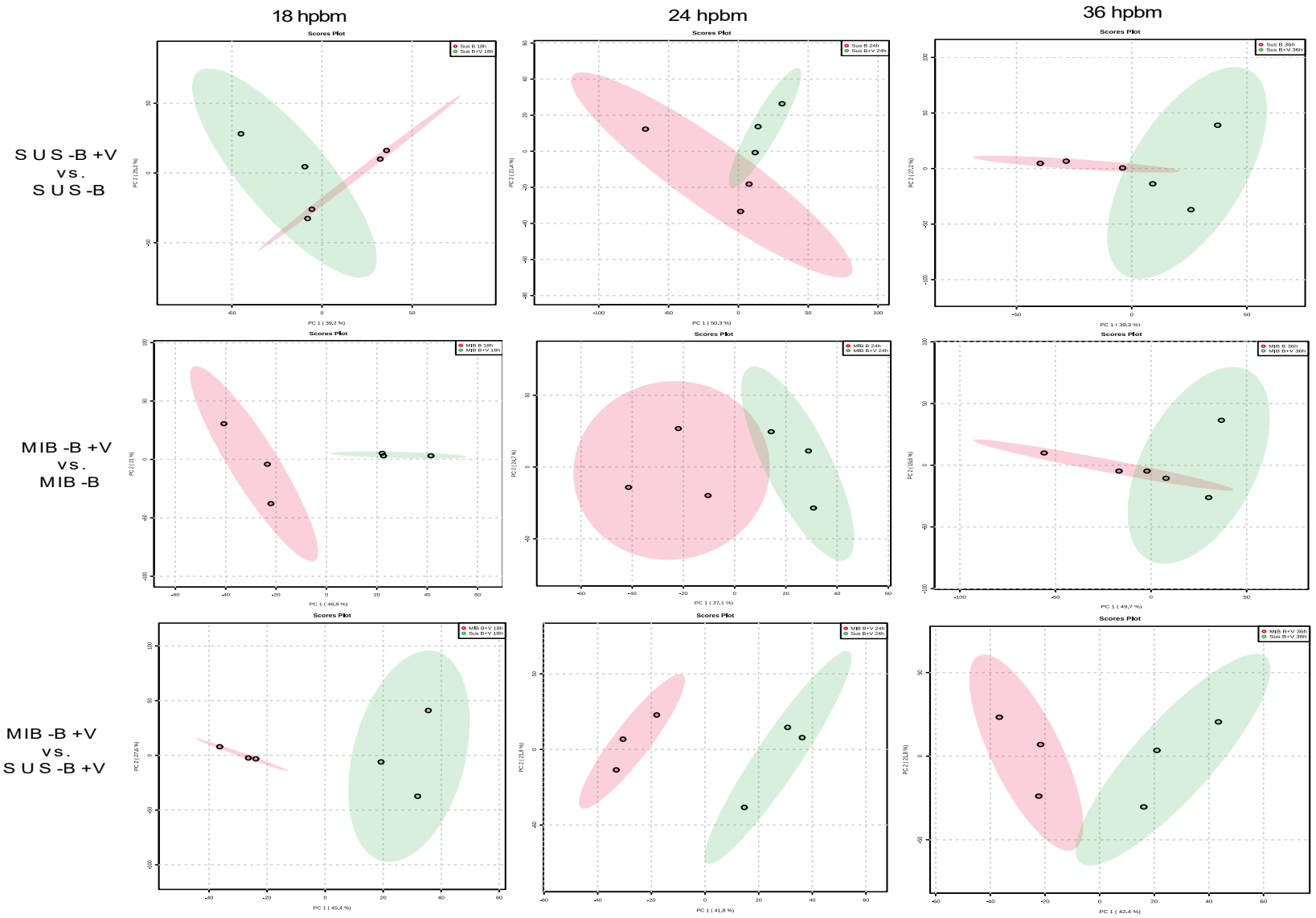
18 hpbm
24 hpbm
36 hpbm
S U S -B +V
vs.
S U S -B
MIB -B +V
vs.
MIB -B
MIB -B +V
vs.
S U S -B +V
Scores Plot
Sus B 18h
Sus B+V 18h
Sus B 24h
Sus B+V 24h
Sus B 36h
Sus B+V 36h
MIB B 18h
MIB B+V 18h
MIB B 24h
MIB B+V 24h
MIB B 36h
MIB B+V 36h
MIB B+V 18h
Sus B+V 18h
MIB B+V 24h
Sus B+V 24h
MIB B+V 36h
Sus B+V 36h

**Figure 3.3.** **PCA plots of all comparisons from Tier 1, 2, and 3 data. Principal component analysis (PCA) of a) Susceptible blood+virus fed (SUS-B+V) vs. Susceptible blood-fed (SUS-B), b) Refractory blood+virus fed (MIB-B+V) vs. Refractory blood-fed (MIB-B), and c) Refractory blood+virus fed vs. Susceptible blood+virus fed, at 18, 24, and 36 hpbm. The X-axis has the first principal component and the Y-axis the second. Each data point represents one sample of 10 pooled insect midguts with the 95% confidence interval displayed as the ellipsis. In a) and b) virus-challenged samples are shown in green, and blood-fed only samples are shown in red. In c) MIB samples are red, and SUS samples are green.**

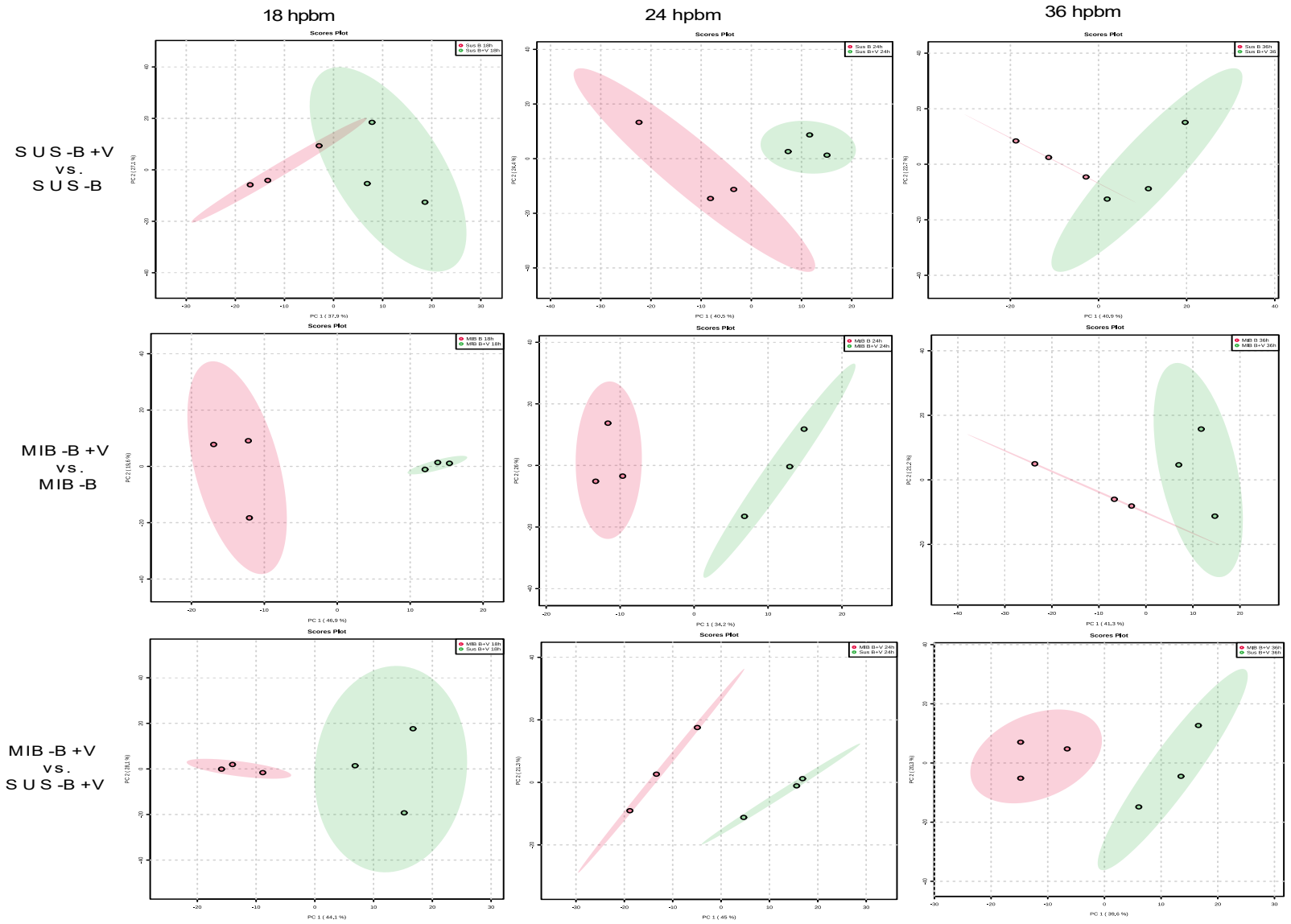
18 hpbm
24 hpbm
36 hpbm
S U S -B +V
vs.
S U S -B
MIB -B +V
vs.
MIB -B
MIB -B +V
vs.
S U S -B +V
Scores Plot
Sus B 18h
Sus B+V 18h
Sus B 24h
Sus B+V 24h
Sus B 36h
Sus B+V 36h
MIB B 18h
MIB B+V 18h
MIB B 24h
MIB B+V 24h
MIB B 36h
MIB B+V 36h
MIB B+V 18h
Sus B+V 18h
MIB B+V 24h
Sus B+V 24h
MIB B+V 36h
Sus B+V 36h

**Figure 3.4.** **PCA plots of all comparisons from Tier 1 and 2 data. Principal component analysis (PCA) of a) Susceptible blood+virus fed (SUS-B+V) vs. Susceptible blood-fed (SUS-B), b) Refractory blood+virus fed (MIB-B+V) vs. Refractory blood-fed (MIB-B), and c) Refractory blood+virus fed vs. Susceptible blood+virus fed, at 18, 24, and 36 hpbm. The X-axis has the first principal component, and the Y-axis the second. Each data point represents one sample of 10 pooled insect midguts with the 95% confidence interval displayed as the ellipsis. In a) and b) virus-challenged samples are shown in green, and blood-fed only samples are shown in red. In c) MIB samples are red, and SUS samples are green.**

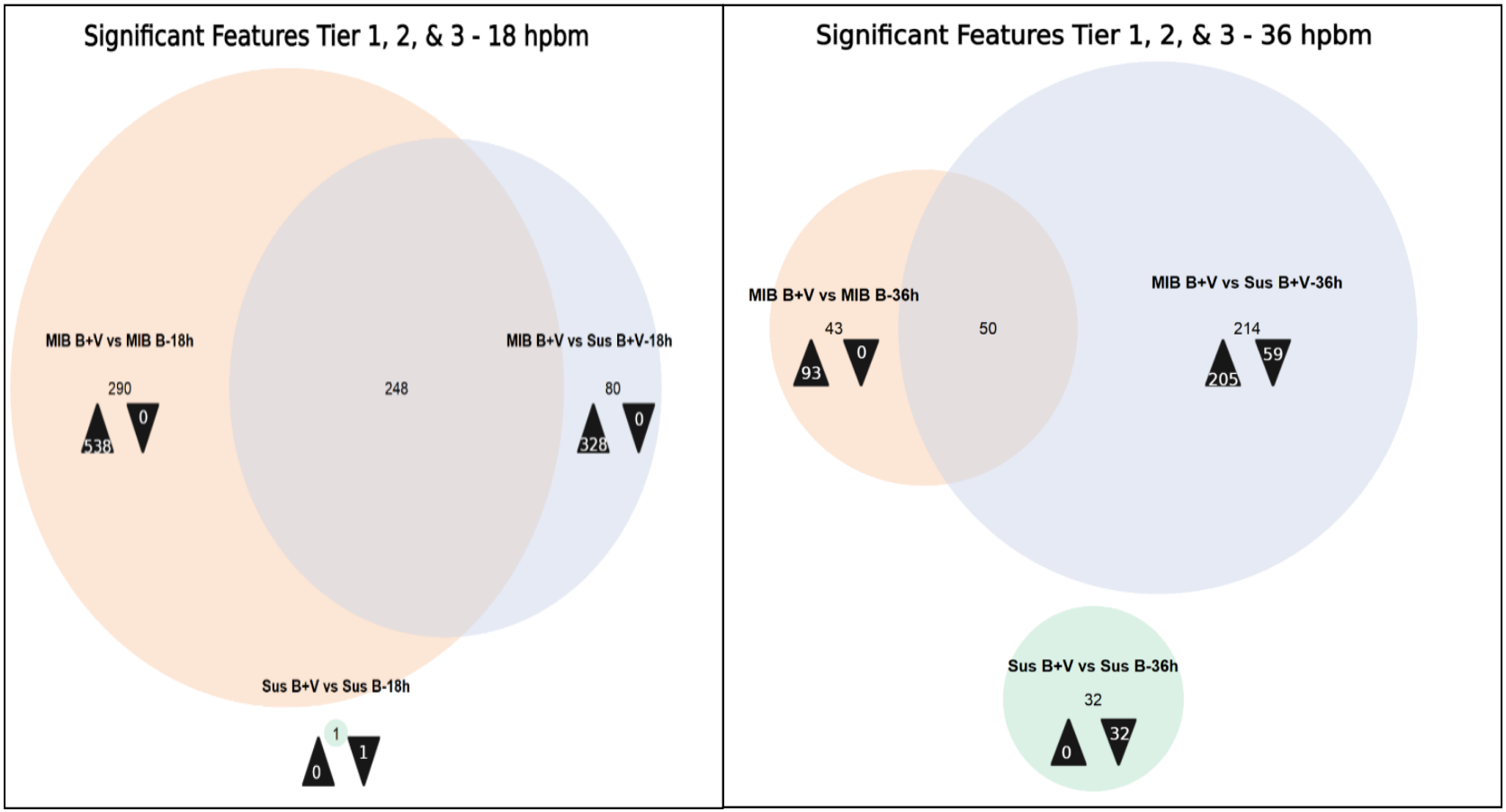


**Figure 3.5.** **Venn Diagram of significant features, Tier 1, 2, and 3- 18, 36 hpbm. Venn Diagrams showing the number of significantly differently regulated lipids selected using the SAM model at each time point, for each sample comparison (SUS-B+V vs. SUS-B, MIB-B+V vs. MIB-B, MIB-B+V vs. SUS-B+V). Black arrowheads pointing up depict the number of metabolites that were increased in concentration compared to the control group, and arrowheads pointing down show the number of metabolites that were decreased in concentration compared to the control. The control groups are listed second in each comparison.**

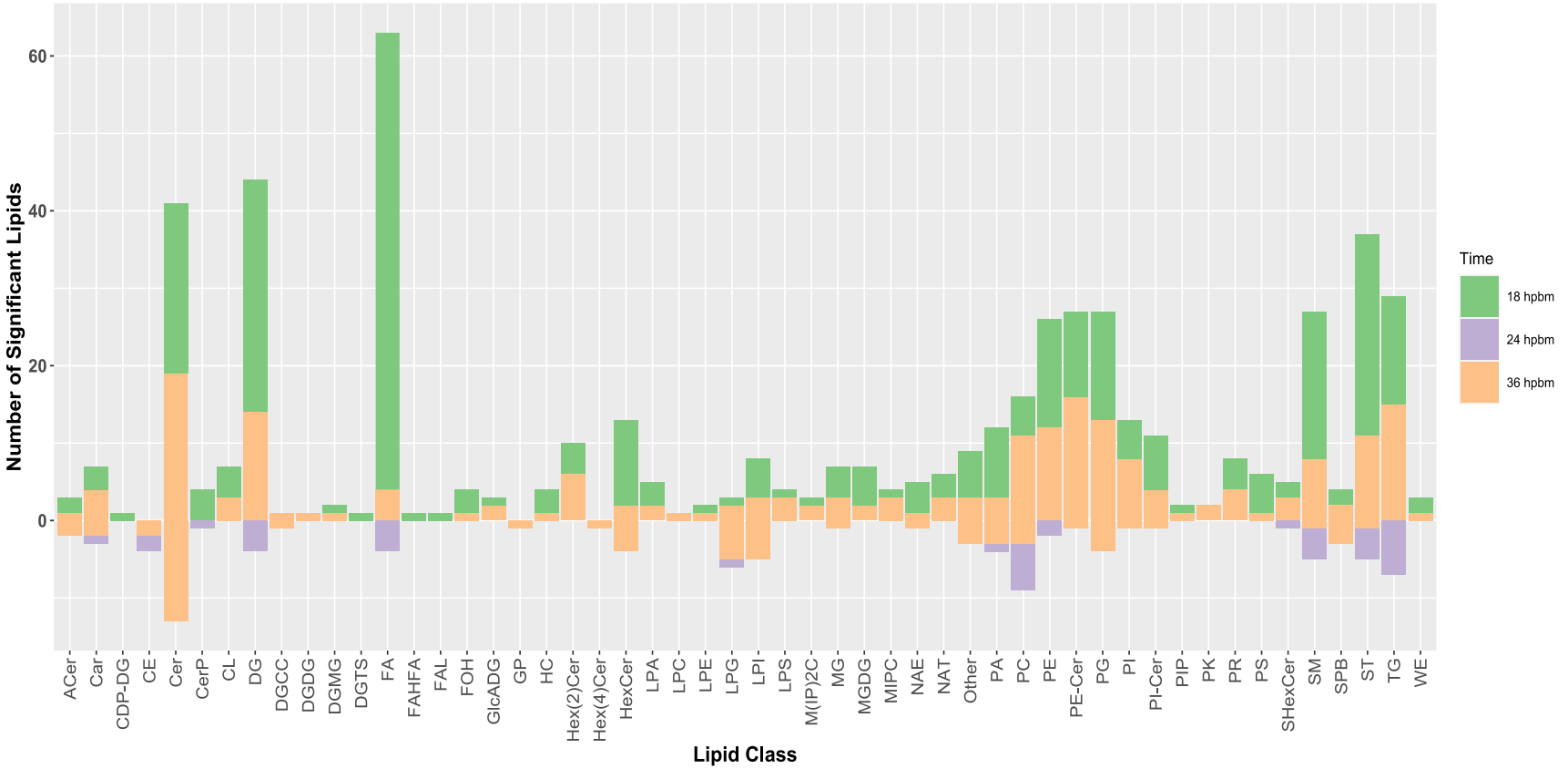


**Figure 3.6.** **Significant lipids by category-Tiers 1, 2, and 3. Number of significant lipids regulated in the Cali-MIB+DENV vs Cali-S+DENV comparison, by lipid category. Each lipid category is divided by timepoint, with 18 hpbm shown in green, 24 hpbm shown in purple, and 36 hpbm shown in orange. The number of significant lipids differently regulated is shown on the Y-axis, with positive values indicating an increase in concentration compared to Cali-S+DENV control, and negative values indicating a decrease in concentration. Abbreviations for lipid categories shown on the X-axis can be seen in Table 3.3.**

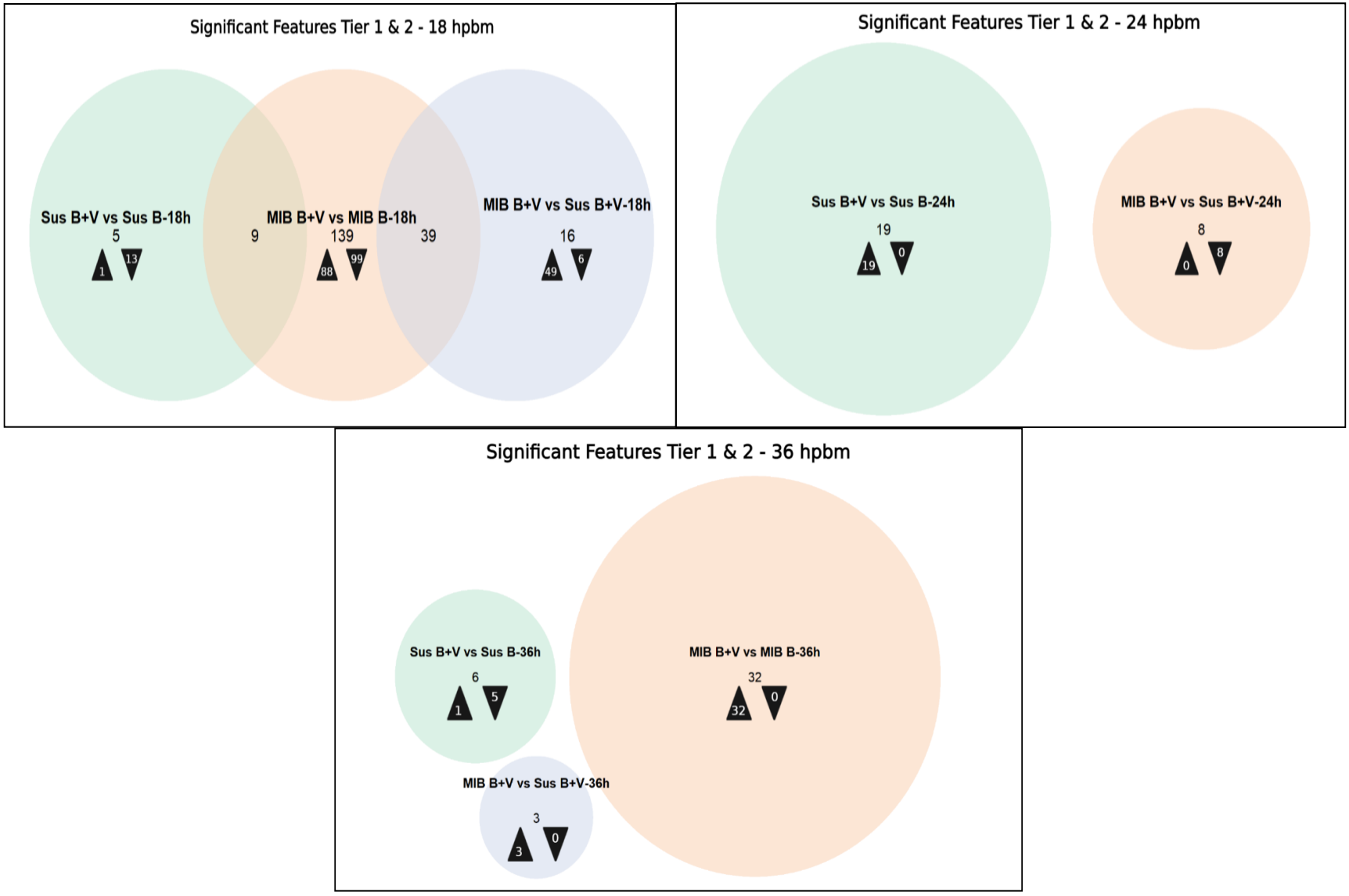
Significant Features Tier 1 & 2 - 18 hpbm
Sus B+V vs Sus B-18h
5
1
13
MIB B+V vs MIB B-18h
9
139
39
88
99
MIB B+V vs Sus B+V-18h
16
49
6
Significant Features Tier 1 & 2 - 24 hpbm
Sus B+V vs Sus B-24h
19
19
0
MIB B+V vs Sus B+V-24h
8
0
8
Significant Features Tier 1 & 2 - 36 hpbm
Sus B+V vs Sus B-36h
6
1
5
MIB B+V vs MIB B-36h
32
32
0
MIB B+V vs Sus B+V-36h
3
3
0

**Figure 3.7.** **Venn Diagram of significant features, Tier 1 and 2- 18, 24, 36 hpbm. Venn Diagrams showing the number of significantly differently regulated metabolites selected using the SAM model at each time point for each sample comparison (SUS-B+V vs. SUS-B, MIB-B+V vs. MIB-B, MIB-B+V vs. SUS-B+V). Black arrowheads pointing up show the number of metabolites that were increased in concentration compared to the control group, and arrowheads pointing down show the number of metabolites that were decreased in concentration compared to the control. The control groups are listed second in each comparison.**


**Figure 3.8.** **Significant Lipids by Category- Tiers 1 and 2. Number of significant lipids regulated in the Cali-MIB+DENV vs Cali-S+DENV comparison, by lipid category. Each lipid category is divided by timepoint, with 18 hpbm shown in green, 24 hpbm shown in purple, and 36 hpbm shown in orange. The number of significant lipids differently regulated is shown on the Y-axis, with positive values indicating an increase in concentration compared to Cali-S+virus control, and negative values indicating a decrease in concentration. Abbreviations for lipid categories shown on the X-axis can be seen in Table 3.3.**

**Table 3.1. Top 10 significantly identified features in tiers 1, 2, and 3. Significance was determined using SAM modelling, with an empirical FDR at 10%. If less than ten features were significant at the 10% threshold, then only those features are listed. Features are listed in alphabetical order, and those appearing in more than one comparison are listed in bold typeface. *3-hydroxy-3-methyl-5-oxo-5-[[(2R,3S,4S,5R,6S)-3,4,5-trihydroxy-6-(2-methyl-4-oxopyran-3-yl)oxyoxan-2-yl]methoxy]pentanoic acid.**

**18 HPBM**

| Cali-S-B+V vs Cali-S-B 18hpbm | Cali-MIB-B+V vs Cali-MIB-B 18hpbm | Cali-MIB-B+V vs Cali-S-B+V 18hpbm |
|---|---|---|
| PC O-20:2-DR | PA O-44:6-UR | ACer 62:0;O3-UR |
| | Cer 38:0;O3-UR | **Cer d16:0_12:0;O2-UR** |
| | **Cer d16:0_12:0;O2-UR** | **Cer d18:0_22:0;O2-UR** |
| | **Cer d18:0_22:0;O2-UR** | **Cer d18:0_22:1;O2-UR** |
| | **Cer d18:0_22:1;O2-UR** | **Cer d18:1_18:1;O3-UR** |
| | **Cer d18:1_18:1;O3-UR** | **Cer d22:0_16:0;O2-UR** |
| | **Cer d22:0_16:0;O2-UR** | **FA 14:0;O-UR** |
| | **FA 14:0;O-UR** | HexCer 36:0;O5-UR |
| | PG 30:8-UR | PR 32:0;O-UR |
| | **PR 40:15;O4-UR** | **PR 40:15;O4-UR** |

**24 HPBM**

| Cali-S-B+V vs Cali-S-B 24hpbm | Cali-MIB-B+V vs Cali-MIB-B 24hpbm | Cali-MIB-B+V vs Cali-S-B+V 24hpbm |
|---|---|---|
| | | FA 18:0-DR |
| | | FA 22:0;O4-DR |
| | | PA O-39:1-DR |
| | | PC 14:1_24:2-DR |
| | | PC 16:2_24:4-DR |
| | | PC 18:1_18:2-DR |
| | | SHexCer 44:0;O2-DR |
| | | ST 20:3;O4;GlcA-DR |
| | | TG 12:0_12:1_18:5-DR |
| | | TG 18:1_18:2_18:3-DR |

**36 HPBM**

| Cali-S-B+V vs Cali-S-B 36hpbm | Cali-MIB-B+V vs Cali-MIB-B 36hpbm | Cali-MIB-B+V vs Cali-S-B+V 36hpbm |
|---|---|---|
| ACer 92:4;O5-DR | Cer 35:2;O3-UR | 3-hydroxy-3-methyl-5-oxo-UR* |
| Cer 35:1;O4-DR | FA 38:6-UR | Car 24:0;O-UR |
| Hex2Cer 28:0;O6-DR | FA 43:0;O-UR | Car 25:0;O2-DR |
| Hex2Cer 32:5;O4-DR | Hex2Cer 30:0;O6-UR | Cer 34:0;O3-UR |
| Hex2Cer 43:3;O4-DR | PE-Cer 34:4;O2-UR | DGCC 36:5-UR |
| LPI O-32:6-DR | PE-Cer 36:4;O2-UR | Leupeptin-DR |
| PC 16:1_18:1-DR | PG O-37:0;O-UR | MIPC 30:2;O3-UR |
| PC 18:2_18:2-DR | PI O-40:0;O-UR | PC 26:3;O3-DR |
| PIP3 36:9-DR | SM d14:0_13:0-UR | PI-Cer 37:6;O6-UR |
| SHexCer 37:2;O2-DR | SM d14:0_15:0-UR | PR 20:0;O2 -UR |

**Table 3.2. Top 10 significantly identified features in tiers 1, and 2. Significance was determined using SAM modelling, with an empirical FDR at 10%. If less than ten features were significant at the 10% threshold, then only those features are listed. Features are listed in alphabetical order, with features appearing more than once included in bold typeface.**

**18 HPBM**

| Cali-S-B+V vs Cali-S-B 18hpbm | Cali-MIB-B+V vs Cali-MIB-B 18hpbm | Cali-MIB-B+V vs Cali-S-B+V 18hpbm |
|---|---|---|
| PE O-18:1_22:6-DR | Cer d15:0_20:0;O2-DR | Cer d16:0_16:0;O2-UR |
| FA 22:6-DR | Cer d17:0_20:0;O2-DR | **Cer d18:0_18:0-UR** |
| LDGTS 24:4-DR | **Cer d18:0_18:0-UR** | **Cer d18:0_22:0;O2-UR** |
| PC 16:0_20:3-DR | **Cer d18:0_22:0;O2-UR** | **Cer d18:0_22:1;O2-UR** |
| PC 16:4_24:4-DR | **Cer d18:0_22:1;O2-UR** | **Cer d18:1_18:1;O3-UR** |
| PE O-16:1_22:4-DR | **Cer d18:1_18:1;O3-UR** | **Cer d22:0_16:0;O2-UR** |
| PE O-18:1_22:4-DR | **Cer d22:0_16:0;O2-UR** | DG 6:0_27:0-UR |
| SM d14:0_22:0-DR | **MG 17:0-UR** | **MG 17:0-UR** |
| SM d14:2_17:0-UR | **TG 16:1_18:1_20:3-DR** | PE 16:4_24:4-UR |
| **TG 12:0_22:2_22:6-DR** | **TG 18:1_18:2_18:3-DR** | Stachybocin B (Fungi metabolite)-UR |

**24 HPBM**

| Cali-S-B+V vs Cali-S-B 24hpbm | Cali-MIB-B+V vs Cali-MIB-B 24hpbm | Cali-MIB-B+V vs Cali-S-B+V 24hpbm |
|---|---|---|
| **PC 14:1_24:2-UR** | | FA 18:0-DR |
| **PC 16:2_24:4-UR** | | FA 20:0-DR |
| **PC 18:1_18:2-UR** | | **PC 14:1_24:2-DR** |
| PC O-14:0_24:4-UR | | **PC 16:2_24:4-DR** |
| PC O-18:0_20:4-UR | | **PC 18:1_18:2-DR** |
| **TG 12:0_12:1_18:5-UR** | | **TG 12:0_12:1_18:5-DR** |
| **TG 12:0_22:2_22:6-UR** | | **TG 16:1_18:1_20:3-DR** |
| TG 16:0_20:4_22:5-UR | | **TG 18:1_18:2_18:3-DR** |
| **TG 16:1_18:1_20:3-UR** | | |
| **TG 18:1_18:2_18:3-UR** | | |

**36 HPBM**

| Cali-S-B+V vs Cali-S-B 36hpbm | Cali-MIB-B+V vs Cali-MIB-B 36hpbm | Cali-MIB-B+V vs Cali-S-B+V 36hpbm |
|---|---|---|
| Cer d14:2_20:0;O2-UR | PE O-18:0_16:1-UR | PR 20:0;O2-UR |
| DG 16:0_16:1-DR | Cer d14:2_20:1;O2-UR | Cer d16:0_22:1;O2-UR |
| PC 18:2_18:2-DR | Cer d18:1_24:2;O2-UR | **Cer d18:0_22:1;O2-UR** |
| PE 18:1_19:0-DR | CL 16:0_16:1_16:1_16:1-UR | |
| PEtOH 18:2_20:5-DR | HexCer d14:0_26:1;O2-UR | |
| SM d14:0_28:2-DR | HexCer d14:1_28:2;O2-UR | |
| | HexCer d18:1_24:1;O2-UR | |
| | PC 16:0_18:1-UR | |
| | PE 18:1_18:2;O-UR | |
| | SM d14:0_15:0-UR | |

**Table 3.3. List of lipid categories and abbreviations.**

| Classification (Category – Main Class – Subclass) | Abbreviation |
|---|---|
| Sphingolipids - Ceramides - Acylceramides | ACer |
| Glycerophospholipids - Glycerophosphoglycerols - Monoacylglycerophosphomonoradylglycerols | BMP |
| Fatty Acyls - Fatty esters - Fatty acyl carnitines | Car |
| Glycerophospholipids - Cytidine-5'-diphosphate (CDP)-Glycerols - CDP-diacylglycerols | CDP-DG |
| Sterol Lipids - Sterols - Steryl esters | CE |
| Sphingolipids - Ceramides - N-acylsphingosines (ceramides) | Cer |
| Sphingolipids - Ceramides - Ceramide 1-phosphates | CerP |
| Glycerophospholipids - Glycerophosphoglycerophosphoglycerols - Monoacylglycerophosphoglycerophosphomonoradylglycerols (Cardiolipins) | CL |
| Fatty Acyls - Fatty esters - Fatty acyl CoAs | CoA |
| Glycerolipids - Diradylglycerols - Diacylglycerols | DG |
| Glycerolipids - Other Glycerolipids (hydroxymethyl-choline) | DGCC |
| Glycerolipids - Glycosyldiradylglycerols – Glycosyldiacylglycerols (Digalactosyldiacylgylcerols) | DGDG |
| Glycerolipids - Glycosylmonoradylglycerols – Glycosylmonoacylglycerols (Digalactosylmonoacylgylcerols) | DGMG |
| Glycerolipids - Other Glycerolipids (trimethyl-alanine) | DGTA |
| Glycerolipids - Other Glycerolipids (trimethyl-homoserine) | DGTS |
| Fatty Acyls - Fatty Acids and Conjugates - Fatty acids | FA |
| Fatty Acyls - Fatty acyl glycosides - Fatty acyl glycosides of mono- and disaccharides | FAG |
| Fatty Acyls - Fatty esters - Fatty acid estolides | FAHFA |
| Fatty Acyls - Fatty aldehydes | FAL |
| Fatty Acyls - Fatty alcohols | FOH |
| Glycerolipids - Glycosyldiradylglycerols - Glycosyldiacylglycerols | GlcADG |
| Sphingolipids - Acidic glycosphingolipids - Glucuronosphingolipids | GlcCer |
| Glycerophospholipids - Glycosylglycerophospholipids - Diacylglycosylglycerophospholipids | Glc-GP |
| Glycerophospholipids - Other Glycerophospholipids | GP |
| Fatty Acyls - Hydrocarbons | HC |
| Sphingolipids - Glycosphingolipids - Hexosyl ceramides | HexCer |
| Sphingolipids - Glycosphingolipids - Hexosyl ceramides (2 hexosyl groups) | Hex(2)Cer |
| Sphingolipids - Glycosphingolipids - Hexosyl ceramides (3 hexosyl groups) | Hex(3)Cer |
| Sphingolipids - Glycosphingolipids - Hexosyl ceramides (4 hexosyl groups) | Hex(4)Cer |
| Sphingolipids - Glycosphingolipids - Hexosyl ceramides (5 hexosyl groups) | Hex(5)Cer |
| Sphingolipids - Glycosphingolipids - Hexosyl ceramides (6 hexosyl groups) | Hex(6)Cer |
| Sphingolipids - Glycosphingolipids - Hexosyl ceramides (7 hexosyl groups) | Hex(7)Cer |
| Sphingolipids - Glycosphingolipids - Hexosyl ceramides (8 hexosyl groups) | Hex(8)Cer |
| Sphingolipids - Glycosphingolipids - Hexosyl ceramides (9 hexosyl groups) | Hex(9)Cer |

| Classification (Category – Main Class – Subclass) | Abbreviation |
|---|---|
| Sphingolipids - Glycosphingolipids - Hexosyl ceramides (10 hexosyl groups) | Hex(10)Cer |
| Sphingolipids - Glycosphingolipids - Hexosyl ceramides (11 hexosyl groups) | Hex(11)Cer |
| Sphingolipids - Glycosphingolipids - Hexosyl ceramides (12 hexosyl groups) | Hex(12)Cer |
| Sphingolipids - Glycosphingolipids - Hexosyl ceramides (13 hexosyl groups) | Hex(13)Cer |
| Sphingolipids - Glycosphingolipids - Hexosyl ceramides (14 hexosyl groups) | Hex(14)Cer |
| Sphingolipids - Glycosphingolipids - Hexosyl ceramides (15 hexosyl groups) | Hex(15)Cer |
| Sphingolipids - Glycosphingolipids - Hexosyl ceramides (20 hexosyl groups) | Hex(20)Cer |
| Sphingolipids - Neutral glycosphingolipids - Hexosyl sphingoid bases | HexSPB |
| Glycerophospholipids - Glycerophosphates - Monoacylglycerophosphates (lysophosphatidic acids) | LPA |
| Glycerophospholipids - Glycerophosphocholines - Monoacylglycerophosphocholines (lysophosphatidylcholines) | LPC |
| Glycerophospholipids - Glycerophosphoethanolamines - Monoacylglycerophosphoethanolamines (lysophosphatidylethanolamines) | LPE |
| Glycerophospholipids - Glycerophosphoglycerols - Monoacylglycerophosphoglycerol (lysophosphatidylglycerol) | LPG |
| Glycerophospholipids - Glycerophosphoinositols - Monoacylglycerophosphoinositols (lysophosphatidylinositols) | LPI |
| Glycerophospholipids - Glycerophosphoinositolglycans - N-acylglycerophosphoinositolglycans | LPIM |
| Glycerophospholipids - Glycerophosphoserines - Monoacylglycerophosphoserines (lysophosphatidylserines) | LPS |
| Sphingolipids - Sphingoid bases - Lysosphingomyelins and lysoglycosphingolipids | LSM |
| Sphingolipids - Phosphosphingolipids - Ceramide phosphoinositols | M(IP)2C |
| Glycerolipids - Monoradylglycerols - Monoacylglycerols | MG |
| Glycerolipids - Glycosyldiradylglycerols – Glycosyldiacylglycerols (Monogalactosyldiacylgylcerols) | MGDG |
| Glycerolipids - Glycosylmonoradylglycerols - Glycosylmonoacylglycerols (Monogalactosylmonoacylgylcerols) | MGMG |
| Sphingolipids - Phosphosphingolipids - Ceramide phosphoinositols | MIPC |
| Fatty Acyls - Fatty Acids and Conjugates - Nitrogenated fatty acids (primary amides, N-acyl amides, fatty nitriles and others) | NA |
| Fatty Acyls - Fatty amides - N-acyl ethanolamines (endocannabinoids) | NAE |
| Glycerophospholipids - Glycerophosphoethanolamines - Diacylglycerophosphoethanolamines | NAPE |
| Fatty Acyls - Fatty amides - N-acyl amines (taurines) | NAT |
| Glycerophospholipids - Glycerophosphates – Diacylglycerophosphates (Phosphatidic Acids) | PA |
| Glycerophospholipids - Glycerophosphocholines – Diacylglycerophosphocholines (Phosphatidylcholines) | PC |
| Glycerophospholipids - Glycerophosphoethanolamines – Diacylglycerophosphoethanolamines (Phosphatidylethanolamines) | PE |
| Sphingolipids - Phosphosphingolipids - Ceramide phosphoethanolamines | PE-Cer |
| Glycerophospholipids - Other Glycerophospholipids | PE-isoK |

| Classification (Category – Main Class – Subclass) | Abbreviation |
|---|---|
| Glycerophospholipids - Glycerophosphoethanolamines – Diacylglycerophosphoethanolamines (N-methylethanolamine or N,N-dimethylethanolamine) | PE-NMe |
| Glycerophospholipids - Glycerophosphoglycerols - Monoacylglycerophosphoglycerols (Phosphatidylglycerols) | PG |
| Glycerophospholipids - Glycerophosphoglycerophosphates - Diacylglycerophosphoglycerophosphates | PGP |
| Glycerophospholipids - Other Glycerophospholipids (sulfate) | PGS |
| Glycerophospholipids - Glycerophosphoinositols – Diacylglycerophosphoinositols (Phosphatidylinositols) | PI |
| Sphingolipids - Phosphosphingolipids - Ceramide phosphoinositols | PI-Cer |
| Glycerophospholipids - Glycerophosphoinositolglycans - Diacylglycerophosphoinositolglycans | PIM |
| Glycerophospholipids - Glycerophosphoinositol monophosphates | PIP |
| Polyketides | PK |
| Glycerophospholipids - Glycerophosphonocholines - Diacylglycerophosphonocholines | PnC |
| Glycerophospholipids - Glycerophosphonoethanolamines - Diacylglycerophosphonoethanolamines | PnE |
| Glycerophospholipids - Glyceropyrophosphates - Diacylglyceropyrophosphates | PPA |
| Prenol Lipids | PR |
| Glycerophospholipids - Glycerophosphoserines – Diacylglycerophosphoserines (Phosphatidylserines) | PS |
| Glycerophospholipids - Glycerophosphoserines - Triacylglycerophosphoserines | PS-NAc |
| Glycerophospholipids - Other Glycerophospholipids | PT |
| Sphingolipids - Other Sphingolipids - Sulfoceramides | SCer |
| Sphingolipids - Acidic glycosphingolipids - Sulfoglycosphingolipids (sulfatides) | SHexCer |
| Saccharolipids | SL |
| Glycerophospholipids - Glycerophosphoglycerols - Diacylglycerophosphomonoradylglycerols | SLBPA |
| Sphingolipids - Phosphosphingolipids - Ceramide phosphocholines (sphingomyelins) | SM |
| Sphingolipids - Sphingoid bases | SPB |
| Sphingolipids - Sphingoid bases - Sphingoid base-1 phosphates | SPBP |
| Glycerolipids - Glycosyldiradylglycerols – Glycosyldiacylglycerols (Sulfoquinovosyldiacylglycerols) | SQDG |
| Glycerolipids - Glycosylmonoradylglycerols – Glycosylmonoacylglycerols (Sulfoquinovosylmonoacylglycerols) | SQMG |
| Sterol Lipids | ST |
| Sphingolipids - Amphoteric glycosphingolipids - Sulfohexosyl sphingoid bases | SulfateHexSPB |
| Glycerolipids - Triradylglycerols - Triacylglycerols | TG |
| Fatty Acyls - Fatty esters - Wax esters and diesters | WE |

# Chapter 4.

# Conclusions and Future Directions

## 4.1. Current DENV Control Measures

DENV is a mosquito-borne virus that causes significant morbidity and mortality when transmitted to humans. Currently, billions of individuals are living in areas with mosquito-to-human transmission of DENV, and these individuals are among the most marginalized people in the world (World Health Organization, 2022). As global temperature rises, and suitable habitats for *Ae. aegypti* increase, the number of serious cases of DENV will assuredly rise (Kraemer et al., 2019). Unfortunately, pharmaceutical interventions to help those who become infected with DENV and efforts to develop vaccines have been proved unsuccessful (World Health Organization, 2022). Consequently, eliminating or controlling the mosquito vector will be our greatest asset in reducing DENV infections.

Vector control strategies have traditionally employed insecticides to reduce vector populations. However, widespread insecticide application has developed resistance (Lindsay et al., 2021). A more modern approach has been developed by Oxitec, which requires the continual release of genetically modified insects containing a lethal gene (Carvalho et al., 2015). This approach is promising but has limited efficacy due to limitations in rearing GMO insects in the laboratory and difficulties in geographic suitability for release. As an alternative to population suppression, an encouraging solution involves manipulating *Ae. aegypti* populations to be less susceptible to DENV. The most notable of these strategies involves inoculating mosquitoes with the intracellular bacterium *Wolbachia* (Walker et al., 2011). To develop novel methods of DENV control, we must have a thorough understanding of host-virus molecular interactions.

## 4.2. Thesis Summary

The objectives of this thesis were to use metabolomics and lipidomics to characterize small molecule changes, in response to DENV, in a naturally refractory *Ae.*

*aegypti* strain. Refractory (Cali-MIB) insects provided a unique model system to investigate DENV-host interactions, given that the insect's response to DENV is capable of eliminating the pathogen (Caicedo et al., 2013). These insects were compared against a naturally occurring susceptible population (Cali-S), which provided a strong control group. We then used current literature to propose anti-DENV mechanisms that may arise from metabolic and lipidomic changes in Cali-MIB insects.

In chapter 2, we investigated the metabolic changes associated with DENV challenge in the midguts of susceptible and refractory insects using chemical isotope labelling LC-MS. First, we assessed data quality and determined broad patterns within our data using PCA. PCA was able to resolve differences between MIB and susceptible insects at 18 and 24 hpbm but could not separate the two phenotypes at 36 hpbm. This aligned well with our previous research indicating that by 36 hpbm, the virus has escaped from the midgut and disseminated systemically (Cooper et al., 2007) and indicated the metabolic profile was unlikely to be meaningfully different. Using the SAM model, we identified metabolites with significantly different concentrations between the two groups and established pathways that were altered upon DENV challenge. The most significant findings from this paper indicated two themes were consistently changed between the refractory and susceptible strains: energy metabolism and arginine biochemistry. Moreover, a unique compound, 4-carboxypyrazole, was upregulated in refractory midguts, and pyrazole derivatives have been previously investigated as anti-viral agents (Pancic et al., 1981; Shih et al., 2010).

In chapter 3, we measured the lipidome and how it responds to DENV in refractory and susceptible insects. Using PCA, we observed that the lipidome does not respond as the metabolome did; strong resolution was observed in the Cali-MIB vs Cali-S comparison at all three time points (Chapter 3). Using the features identified to be significantly different through SAM modelling, we identified the most prominent lipid classes that changed. Among these were, Ceramides, Fatty Acids, Sphingolipids, glycerolipids, and sterols. Through literature review, we discussed possible anti-viral mechanisms for these compounds.

It is important to note the limitations of the methods used in this study. The large quantity of data produced requires statistical modelling to identify compounds found to be different between the two groups. We have learned through our previous

transcriptomics studies that statistical significance does not determine biological relevance, and vice versa, a biologically relevant compound may not achieve statistical significance. Therefore, compounds found to be significant in Cali-MIB samples are correlative, and the mechanisms proposed are unsubstantiated and tenuous.

## 4.3. Future Directions

This thesis identified numerous pathways and molecules that were perturbed in refractory insects in response to DENV compared to the susceptible strain challenged with DENV. These compounds may be alternatively regulated in DENV infections for one of two reasons. First, they may positively or negatively influence viral replication or entry; these would be termed pro-viral or anti-viral compounds, respectively. A second alternative is that molecules that differ between refractory and susceptible midguts may be artifacts of a process unrelated to viral replication. These compounds and pathways should be systematically tested to determine their influence on DENV replication. To accomplish this, we propose using a combination of RNAi experiments and small molecule pathway inhibitors when available. These two experimental designs would function with a similar mechanism, which is to transiently alter the concentration of a specific molecule or pathway and observe the effect this has on DENV replication. These experiments could be tested *in vitro* before moving to an *in vivo* system.

Additionally, if we are to utilize these findings to develop DENV-resistant insects in the future, we must understand how refractory insects respond differently to DENV challenge. We have attempted to answer this question with other methods, including RNAi and qPCR studies, manipulating apoptosis, suppressive subtraction hybridization, transcriptomics, and microbiome analysis (Barón et al., 2010; Caicedo et al., 2019; Coatsworth et al., 2018, 2021; Ocampo et al., 2013) but have been unable to identify a single factor or combination of factors that determined the phenotype. However, new methods are emerging that will allow the integration of multiple omics methods for a more comprehensive understanding of biological processes (Reel et al., 2021). Perhaps combining our transcriptomics and metabolomics data may reveal previously undiscovered pathways to provide a cogent interpretation of the biology of DENV infection.

As mentioned previously, Cali-MIB and Cali-S populations are sympatric and exist in equilibrium, with ~30% of insects refractory to DENV and ~70% susceptible, and these characteristics persist in years with low or no DENV transmission. Moreover, susceptible insects do not appear to have diminished fitness through any of our measures when infected with DENV. This brings into question the selection pressure for evolving resistance to DENV, to which we have no sufficient answer. Given the apparent lack of pressure towards being refractory to DENV, possessing refractory character may be a by-product of another biological process within the insect. Two possible biological processes may be 1) an immunological advantage that has not been measured with our testing or 2) a metabolic advantage unrelated to immune activation, although many other possibilities exist. Considering option one, humans measure and observe DENV because it is relevant to our health; however, a different virus, irrelevant to human disease, may infect *Ae. aegypti* and have negative fitness consequences. Selection for resistance to another virus may spill over and impact DENV's ability to replicate. Considering option two, perhaps the refractory strain has different basal metabolic reactivity and responds differently to a bloodmeal, irrespective of the presence of DENV.

To test the last hypothesis, we performed an analysis on the Cali-MIB and Cali-S samples in response to blood meal alone. If there were little-to-no metabolic differences in the Cali-MIB strain responding to bloodmeal, this would indicate that the metabolic shift seen in Cali-MIB tissues after DENV challenge is primarily a response to viral infection. Our analysis showed several significantly different features in the Cali-MIB strain fed on blood compared to the Cali-S strain. Interestingly, the metabolomics data shows that Cali-MIB samples have numerous features in response to blood meal that do not overlap with the significant features identified in DENV-challenged samples. However, the lipidomics data shows some features are consistently changed in both the blood meal only and the blood+DENV samples. It is difficult to discern what this entails for DENV replication in the midguts; however, it is clear that Cali-MIB insects respond differently to the metabolic demands of digestion of a blood meal and infection with a virus. This may indicate critical biological differences in the Cali-MIB strain that impact all aspects of metabolism, and resistance to DENV may be a product of one of these changes.

The results from both lipidomics and metabolomics analysis reveal consistent biological processes that are altered in the midguts of the refractory Cali-MIB strain,

which often relate to mitochondrial function. Coupling this finding with our analysis showing that the Cali-MIB strain has altered metabolism after a blood meal alone, it may be pertinent to study mitochondrial genetics and function in these two populations. Mitochondria are central to energetics, lipid metabolism, and apoptosis and could explain why two genetically similar populations have significantly different responses to DENV.

## 4.4. Concluding Remarks

We completed the first metabolomic and lipidomic analysis of a naturally occurring DENV-resistant population of *Ae. aegypti*. We observed numerous and diverse metabolic changes in response to dengue virus challenge. As expected, no one compound or pathway was identified to change in response to DENV. Viral infection is a highly complicated process with numerous effector molecules, pathways, and a significant stochastic contribution. Host-parasite interactions are incredibly complex, and there may never be a complete understanding of the mechanisms governing vectorial capacity. Nonetheless, this work has provided one more piece to an ever-growing puzzle of understanding DENV infection, and may aid in generating the first DENV-resistant populations to manage viral spread and severe DENV disease worldwide.

# References


*2-(Methylamino)isobutyric acid | C5H11NO2 - PubChem*. (n.d.). Retrieved May 30, 2022, from https://pubchem.ncbi.nlm.nih.gov/compound/2-_Methylamino_isobutyric-acid

*2'-Deamino-2'-hydroxy-6'-dehydroparomamine | C12H22N2O8 - PubChem*. (n.d.). Retrieved August 2, 2022, from https://pubchem.ncbi.nlm.nih.gov/compound/2_-Deamino-2_-hydroxy-6_-dehydroparomamine

*Aedes | Description, Life Cycle, & Disease Transmission | Britannica*. (n.d.). Retrieved May 2, 2022, from https://www.britannica.com/animal/Aedes

Aliaga-Samanez, A., Cobos-Mayo, M., Real, R., Segura, M., Romero, D., Fa, J. E., & Olivero, J. (2021). *Worldwide dynamic biogeography of zoonotic and anthroponotic dengue*. https://doi.org/10.1371/journal.pntd.0009496

Alonso, A., Marsal, S., & Julià, A. (2015). Analytical methods in untargeted metabolomics: State of the art in 2015. *Frontiers in Bioengineering and Biotechnology*, *3*(MAR), 23. https://doi.org/10.3389/FBIOE.2015.00023/BIBTEX

Angleró-Rodríguez, Y. I., MacLeod, H. J., Kang, S., Carlson, J. S., Jupatanakul, N., & Dimopoulos, G. (2017). Aedes aegypti Molecular Responses to Zika Virus: Modulation of Infection by the Toll and Jak/Stat Immune Pathways and Virus Host Factors. *Frontiers in Microbiology*, *8*(OCT). https://doi.org/10.3389/FMICB.2017.02050

Barletta, A. B. F., Nascimento-Silva, M. C. L., Talyuli, O. A. C., Oliveira, J. H. M., Pereira, L. O. R., Oliveira, P. L., & Sorgine, M. H. F. (2017). Microbiota activates IMD pathway and limits Sindbis infection in Aedes aegypti. *Parasites & Vectors*, *10*(1). https://doi.org/10.1186/S13071-017-2040-9

Barón, O. L., Ursic-Bedoya, R. J., Lowenberger, C. A., & Ocampo, C. B. (2010). Differential gene expression from midguts of refractory and susceptible lines of the mosquito, Aedes aegypti, infected with Dengue-2 virus. *Journal of Insect Science (Online)*, *10*(1). https://doi.org/10.1673/031.010.4101

Bayliak, M. M., Lylyk, M. P., Maniukh, O. V., Storey, J. M., Storey, K. B., & Lushchak, V. I. (2018). Dietary l-arginine accelerates pupation and promotes high protein levels but induces oxidative stress and reduces fecundity and life span in Drosophila melanogaster. *Journal of Comparative Physiology B: Biochemical, Systemic, and Environmental Physiology*, *188*(1), 37–55. https://doi.org/10.1007/S00360-017-1113-6/TABLES/3

Bennett, K. E., Olson, K. E., Muñoz, M. de L., Fernandez-Salas, I., Farfan-Ale, J. A., Higgs, S., Black IV, W. C., & Beaty, B. J. (2002). Variation in vector competence for dengue 2 virus among 24 collections of Aedes aegypti from Mexico and the United States. *The American Journal of Tropical Medicine and Hygiene*, *67*(1), 85–92. https://doi.org/10.4269/AJTMH.2002.67.85

Bing, X., Attardo, G. M., Vigneron, A., Aksoy, E., Scolari, F., Malacrida, A., Weiss, B. L., & Aksoy, S. (2017). Unravelling the relationship between the tsetse fly and its obligate symbiont Wigglesworthia: Transcriptomic and metabolomic landscapes reveal highly integrated physiological networks. *Proceedings of the Royal Society B: Biological Sciences*, *284*(1857). https://doi.org/10.1098/RSPB.2017.0360

Black IV, W. C., Bennett, K. E., Gorrochótegui-Escalante, N., Barillas-Mury, C. V., Fernández-Salas, I., Muñoz, M. D. L., Farfán-Alé, J. A., Olson, K. E., & Beaty, B. J. (2002). Flavivirus susceptibility in Aedes aegypti. *Archives of Medical Research*, *33*(4), 379–388. https://doi.org/10.1016/S0188-4409(02)00373-9

Blomstrand, R., Ostling-Wintzell, H., Lof, A., McMartin, K., Tolf, B. R., & Hedström, K. G. (1979). Pyrazoles as inhibitors of alcohol oxidation and as important tools in alcohol research: An approach to therapy against methanol poisoning. *Proceedings of the National Academy of Sciences of the United States of America*, *76*(7), 3499. https://doi.org/10.1073/PNAS.76.7.3499

Brackney, D. E. (2017). Implications of autophagy on arbovirus infection of mosquitoes. *Current Opinion in Insect Science*, *22*, 1–6. https://doi.org/10.1016/J.COIS.2017.05.001

Brackney, D. E., Correa, M. A., & Cozens, D. W. (2020). The impact of autophagy on arbovirus infection of mosquito cells. *PLoS Neglected Tropical Diseases*, *14*(5), 1–18. https://doi.org/10.1371/journal.pntd.0007754

Brady, O. J., Johansson, M. A., Guerra, C. A., Bhatt, S., Golding, N., Pigott, D. M., Delatte, H., Grech, M. G., Leisnham, P. T., Maciel-De-Freitas, R., Styer, L. M., Smith, D. L., Scott, T. W., Gething, P. W., & Hay, S. I. (2013). Modelling adult Aedes aegypti and Aedes albopictus survival at different temperatures in laboratory and field settings. *Parasites and Vectors*, *6*(1), 1–12. https://doi.org/10.1186/1756-3305-6-351/FIGURES/5

Caicedo, P. A., Barón, O. L., Pérez, M., Alexander, N., Lowenberger, C., & Ocampo, C. B. (2013). Selection of Aedes aegypti (Diptera: Culicidae) strains that are susceptible or refractory to Dengue-2 virus. *The Canadian Entomologist*, *145*(3), 273–282. https://doi.org/10.4039/TCE.2012.105

Caicedo, P. A., Serrato, I. M., Sim, S., Dimopoulos, G., Coatsworth, H., Lowenberger, C., & Ocampo, C. B. (2019). Immune response-related genes associated to blocking midgut dengue virus infection in Aedes aegypti strains that differ in susceptibility. *Insect Science*, *26*(4), 635–648. https://doi.org/10.1111/1744-7917.12573

Campbell, C. L., Harrison, T., Hess, A. M., & Ebel, G. D. (2014). MicroRNA levels are modulated in Aedes aegypti after exposure to Dengue-2. *Insect Molecular Biology*, *23*(1), 132–139. https://doi.org/10.1111/IMB.12070

Canavoso, L. E., Frede, S., & Rubiolo, E. R. (2004). Metabolic pathways for dietary lipids in the midgut of hematophagous Panstrongylus megistus (Hemiptera: Reduviidae). *Insect Biochemistry and Molecular Biology*, *34*(8), 845–854. https://doi.org/10.1016/J.IBMB.2004.05.008

Caragata, E. P., Rancès, E., Hedges, L. M., Gofton, A. W., Johnson, K. N., O'Neill, S. L., & McGraw, E. A. (2013). Dietary Cholesterol Modulates Pathogen Blocking by Wolbachia. *PLOS Pathogens*, *9*(6), e1003459. https://doi.org/10.1371/JOURNAL.PPAT.1003459

Carro, A. C., & Damonte, E. B. (2013). Requirement of cholesterol in the viral envelope for dengue virus infection. *Virus Research*, *174*(1–2), 78–87. https://doi.org/10.1016/J.VIRUSRES.2013.03.005

Carvalho, D. O., McKemey, A. R., Garziera, L., Lacroix, R., Donnelly, C. A., Alphey, L., Malavasi, A., & Capurro, M. L. (2015). Suppression of a Field Population of Aedes aegypti in Brazil by Sustained Release of Transgenic Male Mosquitoes. *PLOS Neglected Tropical Diseases*, *9*(7), e0003864. https://doi.org/10.1371/JOURNAL.PNTD.0003864

Castillo-Méndez, M., & Valverde-Garduño, V. (2020). Aedes aegypti Immune Response and Its Potential Impact on Dengue Virus Transmission. *Viral Immunology*, *33*(1), 38–47. https://doi.org/10.1089/VIM.2019.0051

Chang, K. T., Anishkin, A., Patwardhan, G. A., Beverly, L. J., Siskind, L. J., & Colombini, M. (2015). Ceramide channels: destabilization by Bcl-xL and role in apoptosis. *Biochimica et Biophysica Acta (BBA) - Biomembranes*, *1848*(10), 2374–2384. https://doi.org/10.1016/J.BBAMEM.2015.07.013

Chotiwan, N., Andre, B. G., Sanchez-Vargas, I., Islam, M. N., Grabowski, J. M., Hopf-Jannasch, A., Gough, E., Nakayasu, E., Blair, C. D., Belisle, J. T., Hill, C. A., Kuhn, R. J., & Perera, R. (2018). Dynamic remodeling of lipids coincides with dengue virus replication in the midgut of Aedes aegypti mosquitoes. *PLOS Pathogens*, *14*(2), e1006853. https://doi.org/10.1371/JOURNAL.PPAT.1006853

Chotiwan, N., Brito-Sierra, C. A., Ramirez, G., Lian, E., Grabowski, J. M., Graham, B., Hill, C. A., & Perera, R. (2022). *Expression of fatty acid synthase genes and their role in development and arboviral infection of Aedes aegypti*. *15*(223). https://doi.org/10.1186/s13071-022-05336-1

Clarke, T. (2002). Dengue virus: Break-bone fever. *Nature*. https://doi.org/10.1038/news020415-10

Coatsworth, H., Caicedo, P. A., van Rossum, T., Ocampo, C. B., & Lowenberger, C. (2018). The Composition of Midgut Bacteria in Aedes aegypti (Diptera: Culicidae) That Are Naturally Susceptible or Refractory to Dengue Viruses. *Journal of Insect Science*, *18*(6), 12–13. https://doi.org/10.1093/JISESA/IEY118

Coatsworth, H., Caicedo, P. A., Winsor, G., Brinkman, F., Ocampo, C. B., & Lowenberger, C. (2021). Transcriptome comparison of dengue-susceptible and -resistant field derived strains of Colombian *Aedes aegypti* using RNA-sequencing. *Memórias Do Instituto Oswaldo Cruz*, *116*(1). https://doi.org/10.1590/0074-02760200547

Cole, L. M., Roush, R. T., & Casida, J. E. (1995). Drosophila GABA-gated chloride channel: Modified [3H]EBOB binding site associated with Ala → Ser or Gly mutants of Rdl subunit. *Life Sciences*, *56*(10), 757–765. https://doi.org/10.1016/0024-3205(95)00006-R

Comber, R. N., Gray, R. J., & Secrist, J. A. (1992). Acyclic analogues of pyrazofurin: syntheses and antiviral evaluation. *Carbohydrate Research*, *216*(C), 441–452. https://doi.org/10.1016/0008-6215(92)84179-V

Coon, K. L., Vogel, K. J., Brown, M. R., & Strand, M. R. (2014). Mosquitoes rely on their gut microbiota for development. *Molecular Ecology*, *23*(11), 2727–2739. https://doi.org/10.1111/MEC.12771

Cooper, D. M., Thi, E. P., Chamberlain, C. M., Pio, F., & Lowenberger, C. (2007). Aedes Dronc: a novel ecdysone-inducible caspase in the yellow fever mosquito, Aedes aegypti. *Insect Molecular Biology*, *16*(5), 563–572. https://doi.org/10.1111/J.1365-2583.2007.00758.X

Cooper, Dawn M., Granville, D. J., & Lowenberger, C. (2009). The insect caspases. *Apoptosis*, *14*(3), 247–256. https://doi.org/10.1007/S10495-009-0322-1/TABLES/1

Cooper, Dawn M., Pio, F., Thi, E. P., Theilmann, D., & Lowenberger, C. (2007). Characterization of Aedes Dredd: A novel initiator caspase from the yellow fever mosquito, Aedes aegypti. *Insect Biochemistry and Molecular Biology*, *37*(6), 559–569. https://doi.org/10.1016/J.IBMB.2007.03.005

Davenport, M., Alvarenga, P. H., Shao, L., Fujioka, H., Bianconi, M. L., Oliveira, P. L., & Jacobs-Lorena, M. (2006). Identification of the Aedes aegypti peritrophic matrix protein AeIMUCI as a heme-binding protein. *Biochemistry*, *45*(31), 9540–9549. https://doi.org/10.1021/BI0605991

de Borba, L., Villordo, S. M., Marsico, F. L., Carballeda, J. M., Filomatori, C. V., Gebhard, L. G., Pallarés, H. M., Lequime, S., Lambrechts, L., Vargas, I. S., Blair, C. D., & Gamarnik, A. V. (2019). RNA structure duplication in the dengue virus 3´ UTR: Redundancy or host specificity? *MBio*, *10*(1). https://doi.org/10.1128/MBIO.02506-18/SUPPL_FILE/MBIO.02506-18-ST001.PDF

Dennison, N. J., Jupatanakul, N., & Dimopoulos, G. (2014). The mosquito microbiota influences vector competence for human pathogens. *Current Opinion in Insect Science*, *3*, 6–13. https://doi.org/10.1016/J.COIS.2014.07.004

Emwas, A. H., Roy, R., McKay, R. T., Tenori, L., Saccenti, E., Nagana Gowda, G. A., Raftery, D., Alahmari, F., Jaremko, L., Jaremko, M., & Wishart, D. S. (2019). NMR Spectroscopy for Metabolomics Research. *Metabolites*, *9*(7). https://doi.org/10.3390/METABO9070123

Eng, M. W., van Zuylen, M. N., & Severson, D. W. (2016). Apoptosis-related genes control autophagy and influence DENV-2 infection in the mosquito vector, Aedes aegypti. *Insect Biochemistry and Molecular Biology*, *76*, 70–83. https://doi.org/10.1016/j.ibmb.2016.07.004

Feng, X., Zhou, S., Wang, J., & Hu, W. (2018). microRNA profiles and functions in mosquitoes. *PLoS Neglected Tropical Diseases*, *12*(5). https://doi.org/10.1371/JOURNAL.PNTD.0006463

Feng, Y., Piletz, J. E., & Leblanc, M. H. (2002). Agmatine Suppresses Nitric Oxide Production and Attenuates Hypoxic-Ischemic Brain Injury in Neonatal Rats. *Pediatric Research 2002 52:4*, *52*(4), 606–611. https://doi.org/10.1203/00006450-200210000-00023

Ferreira Barletta, A. B., Alves, L. R., Clara, M., Nascimento Silva, L., Sim, S., Dimopoulos, G., Liechocki, S., Maya-Monteiro, C. M., & Ferreira Sorgine, M. H. (2015). Emerging role of lipid droplets in Aedes aegypti immune response against bacteria and Dengue virus OPEN. *Scientific RepoRts* |, *6*. https://doi.org/10.1038/srep19928

Fiehn, O. (2016). Metabolomics by Gas Chromatography-Mass Spectrometry: the combination of targeted and untargeted profiling. *Current Protocols in Molecular Biology / Edited by Frederick M. Ausubel ... [et Al.]*, *114*, 30.4.1. https://doi.org/10.1002/0471142727.MB3004S114

Fire, A., Xu, S., Montgomery, M. K., Kostas, S. A., Driver, S. E., & Mello, C. C. (1998). Potent and specific genetic interference by double-stranded RNA in Caenorhabditis elegans. *Nature 1998 391:6669*, *391*(6669), 806–811. https://doi.org/10.1038/35888

Fontaine, K. A., Sanchez, E. L., Camarda, R., & Lagunoff, M. (2015). Dengue Virus Induces and Requires Glycolysis for Optimal Replication. *Journal of Virology*, *89*(4), 2358–2366. https://doi.org/10.1128/JVI.02309-14/SUPPL_FILE/ZJV999090072SD1.XLS

Futerman, A. H. (2021). Sphingolipids. *Biochemistry of Lipids, Lipoproteins and Membranes*, 281–316. https://doi.org/10.1016/B978-0-12-824048-9.00009-2

GADOW, A., VATER, J., SCHLUMBOHM, W., PALACZ, Z., SALNIKOW, J., & KLEINKAUF, H. (1983). Gramicidin S Synthetase: Stability of Reactive Thioester Intermediates and Formation of 3-Amino-2-piperidone. *European Journal of Biochemistry*, *132*(2), 229–234. https://doi.org/10.1111/J.1432-1033.1983.TB07352.X

Garver, L. S., Bahia, A. C., Das, S., Souza-Neto, J. A., Shiao, J., Dong, Y., & Dimopoulos, G. (2012). Anopheles Imd Pathway Factors and Effectors in Infection Intensity-Dependent Anti-Plasmodium Action. *PLOS Pathogens*, *8*(6), e1002737. https://doi.org/10.1371/JOURNAL.PPAT.1002737

Gaspar, M. L., Hofbauer, H. F., Kohlwein, S. D., & Henry, S. A. (2011). Coordination of Storage Lipid Synthesis and Membrane Biogenesis. *Journal of Biological Chemistry*, *286*(3), 1696–1708. https://doi.org/10.1074/jbc.m110.172296

Geoghegan, V., Stainton, K., Rainey, S. M., Ant, T. H., Dowle, A. A., Larson, T., Hester, S., Charles, P. D., Thomas, B., & Sinkins, S. P. (2017). Perturbed cholesterol and vesicular trafficking associated with dengue blocking in Wolbachia-infected Aedes aegypti cells. *Nature Communications 2017 8:1*, *8*(1), 1–10. https://doi.org/10.1038/s41467-017-00610-8

Gertruida O'neill, H., Perera, R., Gondim, K. C., Vial, T., Pompon, J., Marti, G., & Missé, D. (2021). Lipid Interactions Between Flaviviruses and Mosquito Vectors MOSQUITO-TRANSMITTED FLAVIVIRUSES Global Pathogens. *Frontiers in Physiology | Www.Frontiersin.Org*, *12*, 763195. https://doi.org/10.3389/fphys.2021.763195

Gertsman, I., & Barshop, B. A. (2018). Promises and Pitfalls of Untargeted Metabolomics. *Journal of Inherited Metabolic Disease*, *41*(3), 355. https://doi.org/10.1007/S10545-017-0130-7

Gilmore, T. D., & Wolenski, F. S. (2012). NF-κB: where did it come from and why? *Immunological Reviews*, *246*(1), 14–35. https://doi.org/10.1111/J.1600-065X.2012.01096.X

Guan, H., Wang, M., Liao, C., Liang, J., Mehere, P., Tian, M., Liu, H., Robinson, H., Li, J., & Han, Q. (2018). Identification of aaNAT5b as a spermine N-acetyltransferase in the mosquito, Aedes aegypti. *PLoS ONE*, *13*(3). https://doi.org/10.1371/JOURNAL.PONE.0194499

Guzman, M. G., & Harris, E. (2015). Dengue. *The Lancet*, *385*(9966), 453–465. https://doi.org/10.1016/S0140-6736(14)60572-9

Hannun, Y. A., Obeid, L. M., & Johnson, R. H. (2011). Many Ceramides. *Journal of Biological Chemistry*, *286*, 27855–27862. https://doi.org/10.1074/jbc.R111.254359

Heaton, N. S., Perera, R., Berger, K. L., Khadka, S., LaCount, D. J., Kuhn, R. J., & Randall, G. (2010). Dengue virus nonstructural protein 3 redistributes fatty acid synthase to sites of viral replication and increases cellular fatty acid synthesis. *Proceedings of the National Academy of Sciences of the United States of America*, *107*(40), 17345–17350. https://doi.org/10.1073/PNAS.1010811107/-/DCSUPPLEMENTAL/PNAS.201010811SI.PDF

Heaton, N. S., & Randall, G. (2010). Dengue virus-induced autophagy regulates lipid metabolism. *Cell Host & Microbe*, *8*(5), 422–432. https://doi.org/10.1016/J.CHOM.2010.10.006

Hidalgo, M. A., Carretta, M. D., & Burgos, R. A. (2021). Long Chain Fatty Acids as Modulators of Immune Cells Function: Contribution of FFA1 and FFA4 Receptors. *Frontiers in Physiology*, *12*, 979. https://doi.org/10.3389/FPHYS.2021.668330/BIBTEX

Hidari, K. I. P. J., & Suzuki, T. (2011). Dengue virus receptor. *Tropical Medicine and Health*, *39*(4 Suppl), 37. https://doi.org/10.2149/TMH.2011-S03

Horvath, T. D., Dagan, S., & Scaraffia, P. Y. (2021). Unraveling mosquito metabolism with mass spectrometry-based metabolomics. *Trends in Parasitology*, *37*(8), 747–761. https://doi.org/10.1016/J.PT.2021.03.010

Hottz, E., Tolley, N. D., Zimmerman, G. A., Weyrich, A. S., & Bozza, F. A. (2011). Platelets in dengue infection. *Drug Discovery Today: Disease Mechanisms*, *8*(1–2). https://doi.org/10.1016/J.DDMEC.2011.09.001

Hoxmeier, J. C., Thompson, B. D., Broeckling, C. D., Small, P., Foy, B. D., Prenni, J., & Dobos, K. M. (2015). Analysis of the metabolome of Anopheles gambiae mosquito after exposure to Mycobacterium ulcerans. *Scientific Reports 2015 5:1*, *5*(1), 1–8. https://doi.org/10.1038/srep09242

Huang, M., Zhang, W., Chen, H., & Zeng, J. (2020). Targeting Polyamine Metabolism for Control of Human Viral Diseases. *Infection and Drug Resistance*, *13*, 4335. https://doi.org/10.2147/IDR.S262024

*Human Metabolome Database: (HMDB0001432)*. (n.d.). Retrieved August 4, 2022, from https://hmdb.ca/metabolites/HMDB0001432

*Human Metabolome Database: (HMDB0060760)*. (n.d.). Retrieved August 2, 2022, from https://hmdb.ca/metabolites/HMDB0060760

*Human Metabolome Database: N-Methyl-a-aminoisobutyric acid (HMDB0002141)*. (n.d.). Retrieved May 30, 2022, from https://hmdb.ca/metabolites/HMDB0002141

Jing, X., Grebenok, R. J., & Behmer, S. T. (2014). Diet micronutrient balance matters: How the ratio of dietary sterols/steroids affects development, growth and reproduction in two lepidopteran insects. *Journal of Insect Physiology*, *67*, 85–96. https://doi.org/10.1016/J.JINSPHYS.2014.06.004

Joosten, J., Overheul, G. J., Van Rij, R. P., & Miesen, P. (2021). Endogenous piRNA-guided slicing triggers responder and trailer piRNA production from viral RNA in Aedes aegypti mosquitoes. *Nucleic Acids Research*, *49*(15), 8886–8899. https://doi.org/10.1093/NAR/GKAB640

Jupatanakul, N., Sim, S., Angleró-Rodríguez, Y. I., Souza-Neto, J., Das, S., Poti, K. E., Rossi, S. L., Bergren, N., Vasilakis, N., & Dimopoulos, G. (2017). Engineered Aedes aegypti JAK/STAT Pathway-Mediated Immunity to Dengue Virus. *PLOS Neglected Tropical Diseases*, *11*(1), e0005187. https://doi.org/10.1371/JOURNAL.PNTD.0005187

Kageyama, D., Fukatsu, T., Nishide, Y., Yokoi, K., Jouraku, A., Tanaka, H., & Futahashi, R. (2019). Functional crosstalk across IMD and Toll pathways: insight into the evolution of incomplete immune cascades. Proceedings of the Royal Society B: Biological Sciences, 286. https://doi.org/10.1098/rspb.2018.2207

Katzelnick, L. C., Gresh, L., Halloran, M. E., Mercado, J. C., Kuan, G., Gordon, A., Balmaseda, A., & Harris, E. (2017). Antibody-dependent enhancement of severe dengue disease in humans. *Science (New York, N.Y.)*, *358*(6365), 929. https://doi.org/10.1126/SCIENCE.AAN6836

*KEGG PATHWAY: Neomycin, kanamycin and gentamicin biosynthesis - Reference pathway*. (n.d.). Retrieved August 2, 2022, from https://www.genome.jp/pathway/map00524+C20351

King, J. G., Souto-Maior, C., Sartori, L. M., Maciel-De-Freitas, R., & Gomes, M. G. M. (2018). Variation in Wolbachia effects on Aedes mosquitoes as a determinant of invasiveness and vectorial capacity. *Nature Communications 2018 9:1*, *9*(1), 1–8. https://doi.org/10.1038/s41467-018-03981-8

Kistler, K. E., Vosshall, L. B., & Matthews, B. J. (2015). Genome engineering with CRISPR-Cas9 in the mosquito Aedes aegypti. *Cell Reports*, *11*(1), 51–60. https://doi.org/10.1016/J.CELREP.2015.03.009

Kogan, P. H., & Hagedorn, H. H. (2000). Polyamines, and effects from reducing their synthesis during egg development in the yellow fever mosquito, Aedes aegypti. *Journal of Insect Physiology*, *46*(7), 1079–1095. https://doi.org/10.1016/S0022-1910(99)00084-0

Koh, C., Islam, M. N., Ye, Y. H., Chotiwan, N., Graham, B., Belisle, J. T., Kouremenos, K. A., Dayalan, S., Tull, D. L., Klatt, S., Perera, R., & McGraw, E. A. (2020). Dengue virus dominates lipid metabolism modulations in Wolbachia-coinfected Aedes aegypti. *Communications Biology 2020 3:1*, *3*(1), 1–14. https://doi.org/10.1038/s42003-020-01254-z

Kraaijeveld, A. R., Elrayes, N. P., Schuppe, H., & Newland, P. L. (2011). l-Arginine enhances immunity to parasitoids in Drosophila melanogaster and increases NO production in lamellocytes. *Developmental & Comparative Immunology*, *35*(8), 857–864. https://doi.org/10.1016/J.DCI.2011.03.019

Kraemer, M. U. G., Reiner, R. C., Brady, O. J., Messina, J. P., Gilbert, M., Pigott, D. M., Yi, D., Johnson, K., Earl, L., Marczak, L. B., Shirude, S., Davis Weaver, N., Bisanzio, D., Perkins, T. A., Lai, S., Lu, X., Jones, P., Coelho, G. E., Carvalho, R. G., … Golding, N. (2019). Past and future spread of the arbovirus vectors Aedes aegypti and Aedes albopictus. *Nature Microbiology 2019 4:5*, *4*(5), 854–863. https://doi.org/10.1038/s41564-019-0376-y

Kraemer, M. U. G., Sinka, M. E., Duda, K. A., Mylne, A. Q. N., Shearer, F. M., Barker, C. M., Moore, C. G., Carvalho, R. G., Coelho, G. E., Van Bortel, W., Hendrickx, G., Schaffner, F., Elyazar, I. R., Teng, H. J., Brady, O. J., Messina, J. P., Pigott, D. M., Scott, T. W., Smith, D. L., … Hay, S. I. (2015). The global distribution of the arbovirus vectors Aedes aegypti and Ae. Albopictus. *ELife*, *4*(JUNE2015). https://doi.org/10.7554/ELIFE.08347

Kumar, Ankit, Srivastava, P., Sirisena, P. D. N. N., Dubey, S. K., Kumar, R., Shrinet, J., & Sunil, S. (2018). Mosquito Innate Immunity. *Insects*, *9*(3). https://doi.org/10.3390/INSECTS9030095

Kumar, Arun, Tauxe, G. M., Perry, S., Scott, C. A., Dahanukar, A., & Ray, A. (2020). Contributions of the Conserved Insect Carbon Dioxide Receptor Subunits to Odor Detection. *Cell Reports*, *31*(2), 107510. https://doi.org/10.1016/J.CELREP.2020.03.074

Kumar, V., Kaur, K., Gupta, G. K., & Sharma, A. K. (2013). Pyrazole containing natural products: Synthetic preview and biological significance. *European Journal of Medicinal Chemistry*, *69*, 735–753. https://doi.org/10.1016/J.EJMECH.2013.08.053

Kyrou, K., Hammond, A. M., Galizi, R., Kranjc, N., Burt, A., Beaghton, A. K., Nolan, T., & Crisanti, A. (2018). A CRISPR–Cas9 gene drive targeting doublesex causes complete population suppression in caged Anopheles gambiae mosquitoes. *Nature Biotechnology 2018 36:11*, *36*(11), 1062–1066. https://doi.org/10.1038/nbt.4245

Lamichhane, S., Sen, P., Dickens, A. M., Hyötyläinen, T., & Orešič, M. (2018). An Overview of Metabolomics Data Analysis: Current Tools and Future Perspectives. *Comprehensive Analytical Chemistry*, *82*, 387–413. https://doi.org/10.1016/BS.COAC.2018.07.001

Lee, C. J., Lin, H.-R., Liao, C.-L., & Lin, Y.-L. (2008). Cholesterol effectively blocks entry of flavivirus. *Journal of Virology*, *82*(13), 6470–6480. https://doi.org/10.1128/JVI.00117-08

Lee, Y. R., Lei, H. Y., Liu, M. T., Wang, J. R., Chen, S. H., Jiang-Shieh, Y. F., Lin, Y. S., Yeh, T. M., Liu, C. C., & Liu, H. S. (2008). Autophagic machinery activated by dengue virus enhances virus replication. *Virology*, *374*(2), 240–248. https://doi.org/10.1016/J.VIROL.2008.02.016

Lehner, R., & Quiroga, A. D. (2021). Fatty acid handling in mammalian cells. *Biochemistry of Lipids, Lipoproteins and Membranes*, 161–200. https://doi.org/10.1016/B978-0-12-824048-9.00001-8

Li, M., Akbari, O. S., & White, B. J. (2018). Highly Efficient Site-Specific Mutagenesis in Malaria Mosquitoes Using CRISPR. *G3 (Bethesda, Md.)*, *8*(2), 653–658. https://doi.org/10.1534/G3.117.1134

Lindsay, S. W., Thomas, M. B., & Kleinschmidt, I. (2021). Threats to the effectiveness of insecticide-treated bednets for malaria control: thinking beyond insecticide resistance. *The Lancet Global Health*, *9*(9), e1325–e1331. https://doi.org/10.1016/S2214-109X(21)00216-3

Liu, T., Yang, W. Q., Xie, Y. G., Liu, P. W., Xie, L. H., Lin, F., Li, C. Y., Gu, J. B., Wu, K., Yan, G. Y., & Chen, X. G. (2019). Construction of an efficient genomic editing system with CRISPR/Cas9 in the vector mosquito Aedes albopictus. *Insect Science*, *26*(6), 1045–1054. https://doi.org/10.1111/1744-7917.12645

Ma, J., Shojaie, A., & Michailidis, G. (2019). A comparative study of topology-based pathway enrichment analysis methods. *BMC Bioinformatics*, *20*(1), 1–14. https://doi.org/10.1186/S12859-019-3146-1/TABLES/1

Maceyka, M., & Spiegel, S. (2014). *Sphingolipid metabolites in inflammatory disease*. https://doi.org/10.1038/nature13475

Maciel-de-Freitas, R., & Valle, D. (2014). Challenges encountered using standard vector control measures for dengue in Boa Vista, Brazil. *Bulletin of the World Health Organization*, *92*(9), 685. https://doi.org/10.2471/BLT.13.119081

Mackenzie, J. M., Khromykh, A. A., & Parton, R. G. (2007). Cholesterol manipulation by West Nile virus perturbs the cellular immune response. *Cell Host & Microbe*, *2*(4), 229–239. https://doi.org/10.1016/J.CHOM.2007.09.003

Mamai, W., Mouline, K., Blais, C., Larvor, V., Dabiré, K. R., Ouedraogo, G. A., Simard, F., & Renault, D. (2014). Metabolomic and ecdysteroid variations in Anopheles gambiae s.l. mosquitoes exposed to the stressful conditions of the dry season in Burkina Faso, West Africa. *Physiological and Biochemical Zoology : PBZ*, *87*(3), 486–497. https://doi.org/10.1086/675697

Manokaran, G., Flores, H. A., Dickson, C. T., Narayana, V. K., Kanojia, K., Dayalan, S., Tull, D., McConville, M. J., Mackenzie, J. M., & Simmons, C. P. (2020). Modulation of acyl-carnitines, the broad mechanism behind Wolbachia-mediated inhibition of medically important flaviviruses in Aedes aegypti. *Proceedings of the National Academy of Sciences of the United States of America*, *117*(39), 24475–24483. https://doi.org/10.1073/PNAS.1914814117/SUPPL_FILE/PNAS.1914814117.SD02.XLSX

McFarlane, M., Arias-Goeta, C., Martin, E., O'Hara, Z., Lulla, A., Mousson, L., Rainey, S. M., Misbah, S., Schnettler, E., Donald, C. L., Merits, A., Kohl, A., & Failloux, A. B. (2014). Characterization of Aedes aegypti Innate-Immune Pathways that Limit Chikungunya Virus Replication. *PLOS Neglected Tropical Diseases*, *8*(7), e2994. https://doi.org/10.1371/JOURNAL.PNTD.0002994

McGraw, E. A., & O'Neill, S. L. (2013). *Beyond insecticides: new thinking on an ancient problem*. https://doi.org/10.1038/nrmicro2968

Meister, S., Kanzok, S. M., Zheng, X. L., Luna, C., Li, T. R., Hoa, N. T., Clayton, J. R., White, K. P., Kafatos, F. C., Christophides, G. K., & Zheng, L. (2005). Immune signaling pathways regulating bacterial and malaria parasite infection of the mosquito Anopheles gambiae. *Proceedings of the National Academy of Sciences of the United States of America*, *102*(32), 11420–11425. https://doi.org/10.1073/PNAS.0504950102/SUPPL_FILE/04950FIG8.PDF

Melkonian, E. A., & Schury, M. P. (2021). Biochemistry, Anaerobic Glycolysis. *StatPearls*. https://www.ncbi.nlm.nih.gov/books/NBK546695/

Mencarelli, C., & Martinez-Martinez, P. (2013). Ceramide function in the brain: when a slight tilt is enough. *Cellular and Molecular Life Sciences*, *70*(2), 181. https://doi.org/10.1007/S00018-012-1038-X

Moessinger, C., Klizaite, K., Steinhagen, A., Philippou-Massier, J., Shevchenko, A., Hoch, M., Ejsing, C. S., & Thiele, C. (2014). Two different pathways of phosphatidylcholine synthesis, the Kennedy Pathway and the Lands Cycle, differentially regulate cellular triacylglycerol storage. *BMC Cell Biology*, *15*(1), 1–17. https://doi.org/10.1186/S12860-014-0043-3/FIGURES/6

Moncayo, A. C., Fernandez, Z., Ortiz, D., Diallo, M., Sall, A., Hartman, S., Davis, C. T., Coffey, L., Mathiot, C. C., Tesh, R. B., & Weaver, S. C. (2004). Dengue Emergence and Adaptation to Peridomestic Mosquitoes. *Emerging Infectious Diseases*, *10*(10), 1790. https://doi.org/10.3201/EID1010.030846

Mounce, B. C., Cesaro, T., Moratorio, G., Hooikaas, P. J., Yakovleva, A., Werneke, S. W., Smith, E. C., Poirier, E. Z., Simon-Loriere, E., Prot, M., Tamietti, C., Vitry, S., Volle, R., Khou, C., Frenkiel, M.-P., Sakuntabhai, A., Delpeyroux, F., Pardigon, N., Flamand, M., … Vignuzzi, M. (2016). *Inhibition of Polyamine Biosynthesis Is a Broad-Spectrum Strategy against RNA Viruses*. https://doi.org/10.1128/JVI.01347-16

Mustafa, M. S., Rasotgi, V., Jain, S., & Gupta, V. (2015). Discovery of fifth serotype of dengue virus (DENV-5): A new public health dilemma in dengue control. *Medical Journal, Armed Forces India*, *71*(1), 67. https://doi.org/10.1016/J.MJAFI.2014.09.011

Myant, N. B. (1981). The Distribution of Sterols and Related Steroids in Nature. *The Biology of Cholesterol and Related Steroids*, 123–159. https://doi.org/10.1016/B978-0-433-22880-6.50010-2

Nganga, R., Oleinik, N., & Ogretmen, B. (2018). Mechanisms of Ceramide-Dependent Cancer Cell Death. *Advances in Cancer Research*, *140*, 1–25. https://doi.org/10.1016/BS.ACR.2018.04.007

Nomaguchi, M., Fujita, M., Miyazaki, Y., & Adachi, A. (2012). Viral tropism. *Frontiers in Microbiology*, *3*(AUG), 281. https://doi.org/10.3389/FMICB.2012.00281/BIBTEX

Nunes, E. da C., & Canuto, G. A. B. (2020). Metabolomics applied in the study of emerging arboviruses caused by Aedes aegypti mosquitoes: A review. *Electrophoresis*, *41*(24), 2102–2113. https://doi.org/10.1002/ELPS.202000133

Oberholzer, V. G., & Briddon, A. (1978). 3-Amino-2-piperidone in the urine of patients with hyperornithinemia. *Clinica Chimica Acta; International Journal of Clinical Chemistry*, *87*(3), 411–415. https://doi.org/10.1016/0009-8981(78)90186-9

Ocampo, C. B., Caicedo, P. A., Jaramillo, G., Ursic Bedoya, R., Baron, O., Serrato, I. M., Cooper, D. M., & Lowenberger, C. (2013). Differential Expression of Apoptosis Related Genes in Selected Strains of Aedes aegypti with Different Susceptibilities to Dengue Virus. *PLoS ONE*, *8*(4). https://doi.org/10.1371/journal.pone.0061187

Ocampo, C. B., & Wesson, D. M. (2004). Population dynamics of Aedes aegypti from a dengue hyperendemic urban setting in Colombia. *The American Journal of Tropical Medicine and Hygiene*, *71*(4), 506–513.

Olson, K. E., & Blair, C. D. (2015). Arbovirus-mosquito Interactions: RNAi Pathway. *Current Opinion in Virology*, *15*, 119. https://doi.org/10.1016/J.COVIRO.2015.10.001

Pancic, F., Steinberg, B. A., Diana, G. D., Carabateas, P. M., Gorman, W. G., & Came, P. E. (1981). Antiviral activity of Win 41258-3, a pyrazole compound, against herpes simplex virus in mouse genital infection and in guinea pig skin infection. *Antimicrobial Agents and Chemotherapy*, *19*(3), 470–476. https://doi.org/10.1128/AAC.19.3.470

Panevska, A., Skočaj, M., Križaj, I., Maček, P., & Sepčić, K. (2019). Ceramide phosphoethanolamine, an enigmatic cellular membrane sphingolipid. *Biochimica et Biophysica Acta (BBA) - Biomembranes*, *1861*(7), 1284–1292. https://doi.org/10.1016/J.BBAMEM.2019.05.001

Pang, Z., Chong, J., Zhou, G., De Lima Morais, D. A., Chang, L., Barrette, M., Gauthier, C., Jacques, P. É., Li, S., & Xia, J. (2021). MetaboAnalyst 5.0: narrowing the gap between raw spectra and functional insights. *Nucleic Acids Research*, *49*(W1), W388–W396. https://doi.org/10.1093/NAR/GKAB382

Pegg, A. E. (2009). Mammalian Polyamine Metabolism and Function. *IUBMB Life*, *61*(9), 880. https://doi.org/10.1002/IUB.230

Pegg, A. E., & McCann, P. P. (1982). Polyamine metabolism and function. *The American Journal of Physiology*, *243*(5). https://doi.org/10.1152/AJPCELL.1982.243.5.C212

Perera, R., Riley, C., Isaac, G., Hopf-Jannasch, A. S., Moore, R. J., Weitz, K. W., Pasa-Tolic, L., Metz, T. O., Adamec, J., & Kuhn, R. J. (2012). Dengue Virus Infection Perturbs Lipid Homeostasis in Infected Mosquito Cells. *PLOS Pathogens*, *8*(3), e1002584. https://doi.org/10.1371/JOURNAL.PPAT.1002584

Petrie III, C. R., Revankar, G. R., Kent Dailey, N., George, R. D., McKernan, P. A., Hamill, R. L., Robins, R. K., & Intersci, th. (1986). Synthesis and Biological Activity of Certain Nucleoside and Nucleotide Derivatives of Pyrazofurin. *Antimicrob. Agents Chemother*, *29*(3), 17. https://pubs.acs.org/sharingguidelines

Quinville, B. M., Deschenes, N. M., Ryckman, A. E., Walia, J. S., Ryckman, N. M. ;, & Walia, A. E. ; (2021). *Molecular Sciences A Comprehensive Review: Sphingolipid Metabolism and Implications of Disruption in Sphingolipid Homeostasis*. https://doi.org/10.3390/ijms22115793

Raghupathi Reddy, S. R., & Campbell, J. W. (1969). Arginine metabolism in insects. Role of arginase in proline formation during silkmoth development. *Biochemical Journal*, *115*(3), 495–503. https://doi.org/10.1042/BJ1150495

Rahman, F. I., Ether, S. A., & Islam, M. R. (2022). Upsurge of Dengue Prevalence During the Third Wave ofCOVID-19 Pandemic in Bangladesh: Pouring Gasoline toFire. *Clinical Pathology*, *15*. https://doi.org/10.1177/2632010X221076068

Ramirez, J. L., Muturi, E. J., Barletta, A. B. F., & Rooney, A. P. (2019). The Aedes aegypti IMD pathway is a critical component of the mosquito antifungal immune response. *Developmental and Comparative Immunology*, *95*, 1–9. https://doi.org/10.1016/J.DCI.2018.12.010

Rancès, E., Ye, Y. H., Woolfit, M., McGraw, E. A., & O'Neill, S. L. (2012). The Relative Importance of Innate Immune Priming in Wolbachia-Mediated Dengue Interference. *PLOS Pathogens*, *8*(2), e1002548. https://doi.org/10.1371/JOURNAL.PPAT.1002548

Rashmi, D., Zanan, R., John, S., Khandagale, K., & Nadaf, A. (2018). γ-Aminobutyric Acid (GABA): Biosynthesis, Role, Commercial Production, and Applications. *Studies in Natural Products Chemistry*, *57*, 413–452. https://doi.org/10.1016/B978-0-444-64057-4.00013-2

Reel, P. S., Reel, S., Pearson, E., Trucco, E., & Jefferson, E. (2021). Using machine learning approaches for multi-omics data analysis: A review. *Biotechnology Advances*, *49*, 107739. https://doi.org/10.1016/J.BIOTECHADV.2021.107739

Reyes-del Valle, J., Salas-Benito, J., Soto-Acosta, R., & del Angel, R. M. (2014). Dengue Virus Cellular Receptors and Tropism. *Current Tropical Medicine Reports*, *1*(1), 36–43. https://doi.org/10.1007/S40475-013-0002-7/TABLES/1

Roberts, L. D., Souza, A. L., Gerszten, R. E., & Clish, C. B. (2012). Targeted Metabolomics. *Current Protocols in Molecular Biology*, *98*(1), 30.2.1-30.2.24. https://doi.org/10.1002/0471142727.MB3002S98

Romagnolo, A. G., & Carvalho, K. I. (2021). Dengue and metabolomics in humans. *Metabolomics : Official Journal of the Metabolomic Society*, *17*(3). https://doi.org/10.1007/S11306-021-01783-6

Sachs, J., & Malaney, P. (2002). The economic and social burden of malaria. *Nature 2002 415:6872*, *415*(6872), 680–685. https://doi.org/10.1038/415680a

Salazar, M. I., Richardson, J. H., Sánchez-Vargas, I., Olson, K. E., & Beaty, B. J. (2007). Dengue virus type 2: replication and tropisms in orally infected Aedes aegypti mosquitoes. *BMC Microbiology*, *7*. https://doi.org/10.1186/1471-2180-7-9

Saldaña, M. A., Etebari, K., Hart, C. E., Widen, S. G., Wood, T. G., Thangamani, S., Asgari, S., & Hughes, G. L. (2017). Zika virus alters the microRNA expression profile and elicits an RNAi response in Aedes aegypti mosquitoes. *PLoS Neglected Tropical Diseases*, *11*(7). https://doi.org/10.1371/JOURNAL.PNTD.0005760

Sánchez-Vargas, I., Scott, J. C., Poole-Smith, B. K., Franz, A. W. E., Barbosa-Solomieu, V., Wilusz, J., Olson, K. E., & Blair, C. D. (2009). Dengue Virus Type 2 Infections of Aedes aegypti Are Modulated by the Mosquito's RNA Interference Pathway. *PLOS Pathogens*, *5*(2), e1000299. https://doi.org/10.1371/JOURNAL.PPAT.1000299

Schnettler, E., Donald, C. L., Human, S., Watson, M., Siu, R. W. C., McFarlane, M., Fazakerley, J. K., Kohl, A., & Fragkoudis, R. (2013). Knockdown of piRNA pathway proteins results in enhanced Semliki Forest virus production in mosquito cells. *The Journal of General Virology*, *94*(Pt 7), 1680–1689. https://doi.org/10.1099/VIR.0.053850-0

Schultz, M. J., Tan, A. L., Gray, C. N., Isern, S., Michael, S. F., Frydman, H. M., & Connor, J. H. (2018). Wolbachia wStri blocks Zika virus growth at two independent stages of viral replication. *MBio*, *9*(3). https://doi.org/10.1128/MBIO.00738-18/ASSET/AD2B2D56-9096-47FC-BBA0-07DB364C1EF5/ASSETS/GRAPHIC/MBO0031839020005.JPEG

Scott, T. W., Amerasinghe, P. H., Morrison, A. C., Lorenz, L. H., Clark, G. G., Strickman, D., Kittayapong, P., & Edman, J. D. (2000). Longitudinal studies of Aedes aegypti (Diptera: Culicidae) in Thailand and Puerto Rico: blood feeding frequency. *Journal of Medical Entomology*, *37*(1), 89–101. https://doi.org/10.1603/0022-2585-37.1.89

Seif, F., Khoshmirsafa, M., Aazami, H., Mohsenzadegan, M., Sedighi, G., & Bahar, M. (2017). The role of JAK-STAT signaling pathway and its regulators in the fate of T helper cells. *Cell Communication and Signaling 2017 15:1*, *15*(1), 1–13. https://doi.org/10.1186/S12964-017-0177-Y

Serrato, I. M., Caicedo, P. A., Orobio, Y., Lowenberger, C., & Ocampo, C. B. (2017). Vector competence and innate immune responses to dengue virus infection in selected laboratory and field-collected Stegomyia aegypti (= Aedes aegypti). *Medical and Veterinary Entomology*, *31*(3), 312–319. https://doi.org/10.1111/MVE.12237

Shepard, D. S., Undurraga, E. A., Halasa, Y. A., & Stanaway, J. D. (2016). The global economic burden of dengue: a systematic analysis. *The Lancet. Infectious Diseases*, *16*(8), 935–941. https://doi.org/10.1016/S1473-3099(16)00146-8

Shih, S. R., Chu, T. Y., Reddy, G. R., Tseng, S. N., Chen, H. L., Tang, W. F., Wu, M. sian, Yeh, J. Y., Chao, Y. S., Hsu, J. T., Hsieh, H. P., & Horng, J. T. (2010). Pyrazole compound BPR1P0034 with potent and selective anti-influenza virus activity. *Journal of Biomedical Science*, *17*(1), 13. https://doi.org/10.1186/1423-0127-17-13

Shrinet, J., Bhavesh, N. S., & Sunil, S. (2018). Understanding Oxidative Stress in Aedes during Chikungunya and Dengue Virus Infections Using Integromics Analysis. *Viruses*, *10*(6). https://doi.org/10.3390/V10060314

Sim, S., Jupatanakul, N., & Dimopoulos, G. (2014). Mosquito immunity against arboviruses. *Viruses*, *6*(11), 4479–4504. https://doi.org/10.3390/V6114479

Singh, K. R. P., & Brown, A. W. A. (1957). Nutritional requirements of Aedes aegypti L. *Journal of Insect Physiology*, *1*(3), 199–220. https://doi.org/10.1016/0022-1910(57)90036-7

Suzuki, Y., Frangeul, L., Dickson, L. B., Blanc, H., Verdier, Y., Vinh, J., Lambrechts, L., & Saleh, M.-C. (2017). Uncovering the Repertoire of Endogenous Flaviviral Elements in Aedes Mosquito Genomes. *Journal of Virology*, *91*(15). https://doi.org/10.1128/JVI.00571-17

Tabachnick, W. (1982). Geographic and Temporal Patterns of Genetic Variation of Aedes Aegypti in New Orleans Population Genetics of Aedes aegypti and its Infectability with Yellow Fever Virus View project. *The American Journal of Tropical Medicine and Hygiene*. https://doi.org/10.4269/ajtmh.1982.31.849

Takeuchi, K., & Reue, K. (2009). Biochemistry, physiology, and genetics of GPAT, AGPAT, and lipin enzymes in triglyceride synthesis. *American Journal of Physiology - Endocrinology and Metabolism*, *296*(6), 1195–1209. https://doi.org/10.1152/AJPENDO.90958.2008/ASSET/IMAGES/LARGE/ZH10060956840002.JPEG

The Lancet Global Health. (2017). Vector control: time for a planetary health approach. *The Lancet Global Health*, *5*(6), e556. https://doi.org/10.1016/S2214-109X(17)30185-7

Tikhe, C. V., & Dimopoulos, G. (2021). Mosquito antiviral immune pathways. *Developmental & Comparative Immunology*, *116*, 103964. https://doi.org/10.1016/J.DCI.2020.103964

Tree, M. O., Londono-Renteria, B., Troupin, A., Clark, K. M., Colpitts, T. M., & Conway, M. J. (2019). Dengue virus reduces expression of low-density lipoprotein receptor-related protein 1 to facilitate replication in Aedes aegypti. *Scientific Reports 2019 9:1*, *9*(1), 1–14. https://doi.org/10.1038/s41598-019-42803-9

Tremblay, R., Lee, S., & Rudy, B. (2016). GABAergic Interneurons in the Neocortex: From Cellular Properties to Circuits. *Neuron*, *91*(2), 260–292. https://doi.org/10.1016/J.NEURON.2016.06.033

Turelli, M., & Hoffmann, A. A. (1991). Rapid spread of an inherited incompatibility factor in California Drosophila. *Nature 1991 353:6343*, *353*(6343), 440–442. https://doi.org/10.1038/353440a0

Tusher, V. G., Tibshirani, R., & Chu, G. (2001). Significance analysis of microarrays applied to the ionizing radiation response. *Proceedings of the National Academy of Sciences of the United States of America*, *98*(9), 5116. https://doi.org/10.1073/PNAS.091062498

Varjak, M., Leggewie, M., & Schnettler, E. (2018). The antiviral piRNA response in mosquitoes? *The Journal of General Virology*, *99*(12), 1551–1562. https://doi.org/10.1099/JGV.0.001157

Veprintsev, D., Deupi, X., Standfuss, J., & Schertler, G. F. X. (2013). Glycerolipids: Chemistry. *Encyclopedia of Biophysics*, 907–914. https://doi.org/10.1007/978-3-642-16712-6_527

Vial, T., Tan, W.-L., Deharo, E., Missé, D., Marti, G., & Pompon, J. (2020). Mosquito metabolomics reveal that dengue virus replication requires phospholipid reconfiguration via the remodeling cycle. *Proceedings of the National Academy of Sciences*, *117*(44), 27627 LP – 27636. https://doi.org/10.1073/pnas.2015095117

Vial, T., Tan, W. L., Xiang, B. W. W., Missé, D., Deharo, E., Marti, G., & Pompon, J. (2019). Dengue virus reduces AGPAT1 expression to alter phospholipids and enhance infection in Aedes aegypti. *PLOS Pathogens*, *15*(12), e1008199. https://doi.org/10.1371/JOURNAL.PPAT.1008199

Vidal, R., Ma, Y., & Sastry, S. S. (2016). Principal component analysis. *Interdisciplinary Applied Mathematics*, *40*, 25–62. https://doi.org/10.1007/978-0-387-87811-9_2/FIGURES/8

Voelker, D. R. (2013). Glycerolipid Structure, Function, and Synthesis in Eukaryotes. *Encyclopedia of Biological Chemistry: Second Edition*, 412–418. https://doi.org/10.1016/B978-0-12-378630-2.00510-7

Walker, T., Johnson, P. H., Moreira, L. A., Iturbe-Ormaetxe, I., Frentiu, F. D., McMeniman, C. J., Leong, Y. S., Dong, Y., Axford, J., Kriesner, P., Lloyd, A. L., Ritchie, S. A., O'Neill, S. L., & Hoffmann, A. A. (2011). The wMel Wolbachia strain blocks dengue and invades caged Aedes aegypti populations. *Nature 2011 476:7361*, *476*(7361), 450–453. https://doi.org/10.1038/nature10355

Wang, S., & Beerntsen, B. T. (2015). Functional implications of the peptidoglycan recognition proteins in the immunity of the yellow fever mosquito, Aedes aegypti. *Insect Molecular Biology*, *24*(3), 293–310. https://doi.org/10.1111/IMB.12159

Wassel, M. M. S., Gamal El-Din, W. M., Ragab, A., Gameel, ;, Ali, A. M. E., & Ammar, Y. A. (2020). Antiviral Activity Of Adamantane-Pyrazole Derivatives Against Foot And Mouth Disease Virus Infection In Vivo And In Vitro With Molecular Docking Study. *Journal of Applied Veterinary Sciences*, *5*(4), 37–46. https://doi.org/10.21608/JAVS.2020.118001

Watkins, P. A. (1997). Fatty acid activation. *Progress in Lipid Research*, *36*(1), 55–83. https://doi.org/10.1016/S0163-7827(97)00004-0

Weatherby, K., & Carter, D. (2013). Chromera velia. The missing link in the evolution of parasitism. *Advances in Applied Microbiology*, *85*, 119–144. https://doi.org/10.1016/B978-0-12-407672-3.00004-6

WHO. (2021). *Ending the neglect to attain the Sustainable Development Goals: A road map for neglected tropical diseases 2021–2030*. https://www.who.int/publications/i/item/9789240010352

*WO2007039146A1 - 4-carboxy pyrazole derivatives as anti-viral agents - Google Patents*. (n.d.). Retrieved May 26, 2022, from https://patents.google.com/patent/WO2007039146A1/en

Wollam, J., & Antebi, A. (2011). Sterol Regulation of Metabolism, Homeostasis and Development. *Annual Review of Biochemistry*, *80*, 885. https://doi.org/10.1146/ANNUREV-BIOCHEM-081308-165917

Won Park, J., Ryeol Park, S., Kumar Nepal, K., Reum Han, A., Hee Ban, Y., Ji Yoo, Y., Ji Kim, E., Min Kim, E., Kim, D., Kyung Sohng, J., & Joon Yoon, Y. (2011). *Discovery of parallel pathways of kanamycin biosynthesis allows antibiotic manipulation*. https://doi.org/10.1038/nCHeMBIO.671

World Health Organization. (2020). *Vector-borne diseases*. Vector-Borne Diseases. https://www.who.int/news-room/fact-sheets/detail/vector-borne-diseases

World Health Organization. (2022). *Dengue and severe dengue*. https://www.who.int/news-room/fact-sheets/detail/dengue-and-severe-dengue

Xi, Z., Ramirez, J. L., & Dimopoulos, G. (2008). The Aedes aegypti Toll Pathway Controls Dengue Virus Infection. *PLOS Pathogens*, *4*(7), e1000098. https://doi.org/10.1371/JOURNAL.PPAT.1000098

Xia, J., Psychogios, N., Young, N., & Wishart, D. S. (2009). MetaboAnalyst: a web server for metabolomic data analysis and interpretation. *Nucleic Acids Research*, *37*(suppl_2), W652–W660. https://doi.org/10.1093/NAR/GKP356

Xia, J., Wishart, D. S., & Valencia, A. (2010). MetPA: a web-based metabolomics tool for pathway analysis and visualization. *Bioinformatics*, *26*(18), 2342–2344. https://doi.org/10.1093/BIOINFORMATICS/BTQ418

Young, M. M., Kester, M., & Wang, H. G. (2013). Sphingolipids: regulators of crosstalk between apoptosis and autophagy. *Journal of Lipid Research*, *54*(1), 5. https://doi.org/10.1194/JLR.R031278

Zhang, X. G., Mason, P. W., Dubovi, E. J., Xu, X., Bourne, N., Renshaw, R. W., Block, T. M., & Birk, A. V. (2009). Antiviral activity of geneticin against dengue virus. *Antiviral Research*, *83*(1), 21–27. https://doi.org/10.1016/J.ANTIVIRAL.2009.02.204

Zhao, S., Li, H., Han, W., Chan, W., & Li, L. (2022). *Metabolomic Coverage of Chemical-Group-Submetabolome Analysis: Group Classification and Four-Channel Chemical Isotope Labeling LC-MS*. *14*, 7. https://doi.org/10.1021/acs.analchem.9b03431

Zhao, S., & Li, L. (2020). Chemical derivatization in LC-MS-based metabolomics study. *TrAC Trends in Analytical Chemistry*, *131*, 115988. https://doi.org/10.1016/J.TRAC.2020.115988

Zhao, T., Li, B., Gao, H., Xing, D., Li, M., Dang, Y., Zhang, H., Zhao, Y., Liu, Z., & Li, C. (2022). Metagenome Sequencing Reveals the Microbiome of Aedes albopictus and Its Possible Relationship With Dengue Virus Susceptibility. *Frontiers in Microbiology*, *13*. https://doi.org/10.3389/FMICB.2022.891151

Zhou, R., Tseng, C. L., Huan, T., & Li, L. (2014). IsoMS: automated processing of LC-MS data generated by a chemical isotope labeling metabolomics platform. *Analytical Chemistry*, *86*(10), 4675–4679. https://doi.org/10.1021/AC5009089

Zhu, Y., Zhang, R., Zhang, B., Zhao, T., Wang, P., Liang, G., & Cheng, G. (2017). Blood meal acquisition enhances arbovirus replication in mosquitoes through activation of the GABAergic system. *Nature Communications 2017 8:1*, *8*(1), 1–13. https://doi.org/10.1038/s41467-017-01244-6

# Appendix A. Heatmaps from Metabolomics Analysis (Ch. 2)

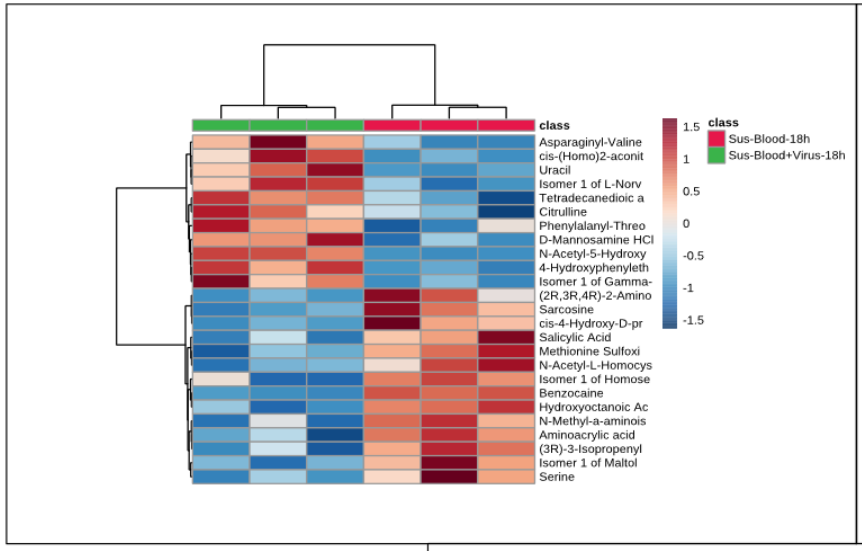
class
Asparaginyl-Valine
cis-(Homo)2-aconit
Uracil
Isomer 1 of L-Norv
Tetradecanedioic a
Citrulline
Phenylalanyl-Threo
D-Mannosamine HCl
N-Acetyl-5-Hydroxy
4-Hydroxyphenyleth
Isomer 1 of Gamma-
(2R,3R,4R)-2-Amino
Sarcosine
cis-4-Hydroxy-D-pr
Salicylic Acid
Methionine Sulfoxi
N-Acetyl-L-Homocys
Isomer 1 of Homose
Benzocaine
Hydroxyoctanoic Ac
N-Methyl-a-aminois
Aminoacrylic acid
(3R)-3-Isopropenyl
Isomer 1 of Maltol
Serine
1.5
1
0.5
0
-0.5
-1
-1.5
class
Sus-Blood-18h
Sus-Blood+Virus-18h

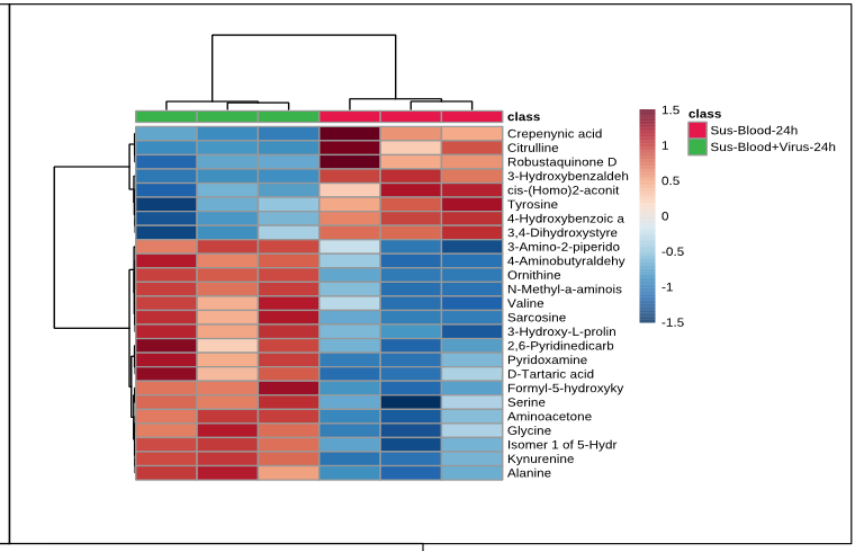
class
Crepenynic acid
Citrulline
Robustaquinone D
3-Hydroxybenzaldeh
cis-(Homo)2-aconit
Tyrosine
4-Hydroxybenzoic a
3,4-Dihydroxystyre
3-Amino-2-piperido
4-Aminobutyraldehy
Ornithine
N-Methyl-a-aminois
Valine
Sarcosine
3-Hydroxy-L-prolin
2,6-Pyridinedicarb
Pyridoxamine
D-Tartaric acid
Formyl-5-hydroxyky
Serine
Aminoacetone
Glycine
Isomer 1 of 5-Hydr
Kynurenine
Alanine
1.5
1
0.5
0
-0.5
-1
-1.5
class
Sus-Blood-24h
Sus-Blood+Virus-24h

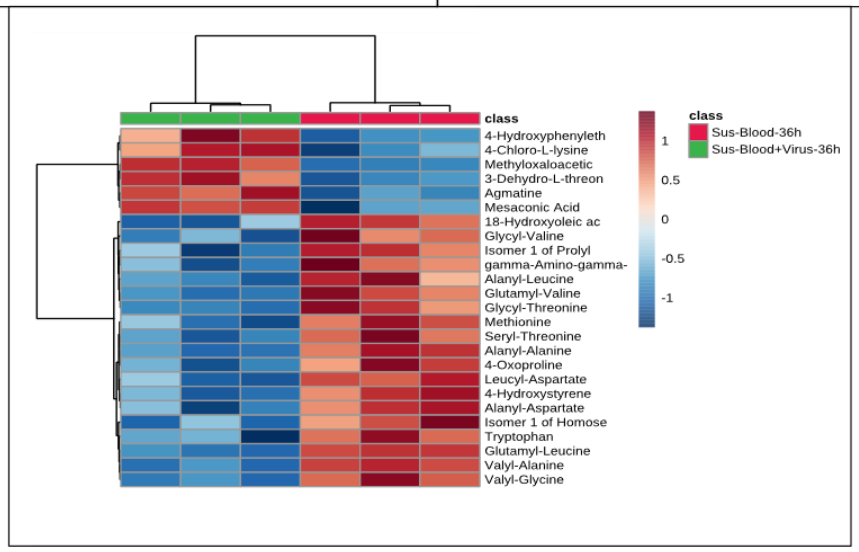
class
4-Hydroxyphenyleth
4-Chloro-L-lysine
Methyloxaloacetic
3-Dehydro-L-threon
Agmatine
Mesaconic Acid
18-Hydroxyoleic ac
Glycyl-Valine
Isomer 1 of Prolyl
gamma-Amino-gamma-
Alanyl-Leucine
Glutamyl-Valine
Glycyl-Threonine
Methionine
Seryl-Threonine
Alanyl-Alanine
4-Oxoproline
Leucyl-Aspartate
4-Hydroxystyrene
Alanyl-Aspartate
Isomer 1 of Homose
Tryptophan
Glutamyl-Leucine
Valyl-Alanine
Valyl-Glycine
1
0.5
0
-0.5
-1
class
Sus-Blood-36h
Sus-Blood+Virus-36h

**A. 1.** **Heatmaps of the top 20 changed metabolites, Tiers 1 & 2—between Cali-S Blood+Virus and Cali-S+Blood strains of *Ae. aegypti*, at each time point. Results of hierarchical clustering are shown above the heatmap, with Cali-S Blood samples displayed in red and Cali-S Blood+Virus samples in green. The fold change concentration difference of the metabolite is displayed using the scale to the right of the heatmap.**

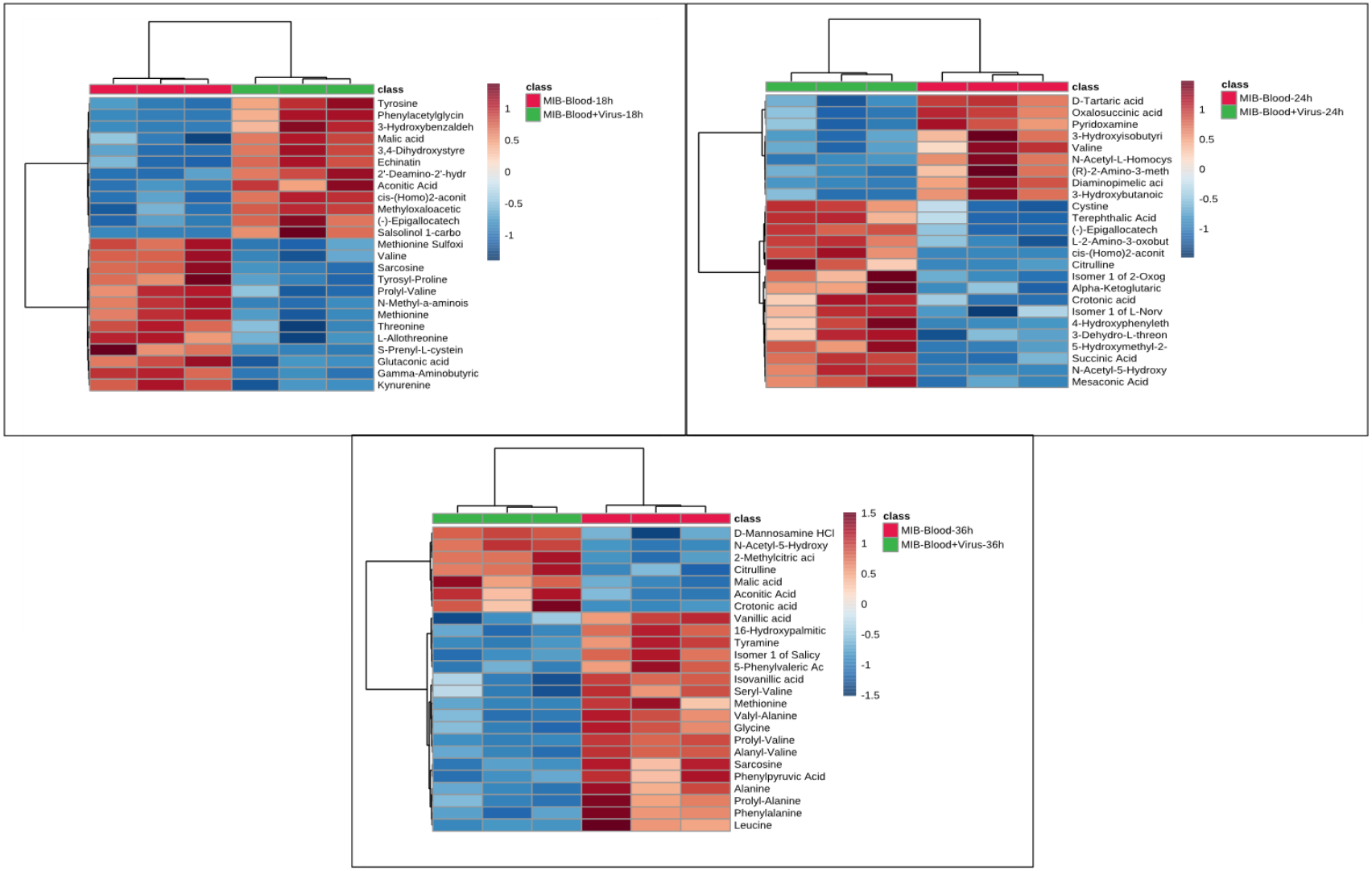
class
Tyrosine
Phenylacetylglycin
3-Hydroxybenzaldeh
Malic acid
3,4-Dihydroxystyre
Echinatin
2'-Deamino-2'-hydr
Aconitic Acid
cis-(Homo)2-aconit
Methyloxaloacetic
(-)-Epigallocatech
Salsolinol 1-carbo
Methionine Sulfoxi
Valine
Sarcosine
Tyrosyl-Proline
Prolyl-Valine
N-Methyl-a-aminois
Methionine
Threonine
L-Allothreonine
S-Prenyl-L-cystein
Glutaconic acid
Gamma-Aminobutyric
Kynurenine
1
0.5
0
-0.5
-1
class
MIB-Blood-18h
MIB-Blood+Virus-18h
class
D-Tartaric acid
Oxalosuccinic acid
Pyridoxamine
3-Hydroxyisobutyri
Valine
N-Acetyl-L-Homocys
(R)-2-Amino-3-meth
Diaminopimelic aci
3-Hydroxybutanoic
Cystine
Terephthalic Acid
(-)-Epigallocatech
L-2-Amino-3-oxobut
cis-(Homo)2-aconit
Citrulline
Isomer 1 of 2-Oxog
Alpha-Ketoglutaric
Crotonic acid
Isomer 1 of L-Norv
4-Hydroxyphenyleth
3-Dehydro-L-threon
5-Hydroxymethyl-2-
Succinic Acid
N-Acetyl-5-Hydroxy
Mesaconic Acid
1
0.5
0
-0.5
-1
class
MIB-Blood-24h
MIB-Blood+Virus-24h
class
D-Mannosamine HCl
N-Acetyl-5-Hydroxy
2-Methylcitric aci
Citrulline
Malic acid
Aconitic Acid
Crotonic acid
Vanillic acid
16-Hydroxypalmitic
Tyramine
Isomer 1 of Salicy
5-Phenylvaleric Ac
Isovanillic acid
Seryl-Valine
Methionine
Valyl-Alanine
Glycine
Prolyl-Valine
Alanyl-Valine
Sarcosine
Phenylpyruvic Acid
Alanine
Prolyl-Alanine
Phenylalanine
Leucine
1.5
1
0.5
0
-0.5
-1
-1.5
class
MIB-Blood-36h
MIB-Blood+Virus-36h

**A. 2.** **Heatmaps of the top 20 changed metabolites, Tiers 1 & 2—between Cali-MIB Blood+Virus and Cali-MIB+Blood strains of *Ae. aegypti*, at each time point. Results of hierarchical clustering are shown above the heatmap, with Cali-MIB+Blood samples displayed in red and Cali-MIB Blood+Virus samples in green. The fold change concentration difference of the metabolite is displayed using the scale to the right of the heatmap.**

# Appendix B. Metabolic Analysis of Blood-Fed Cali-MIB and Cali-S Midguts

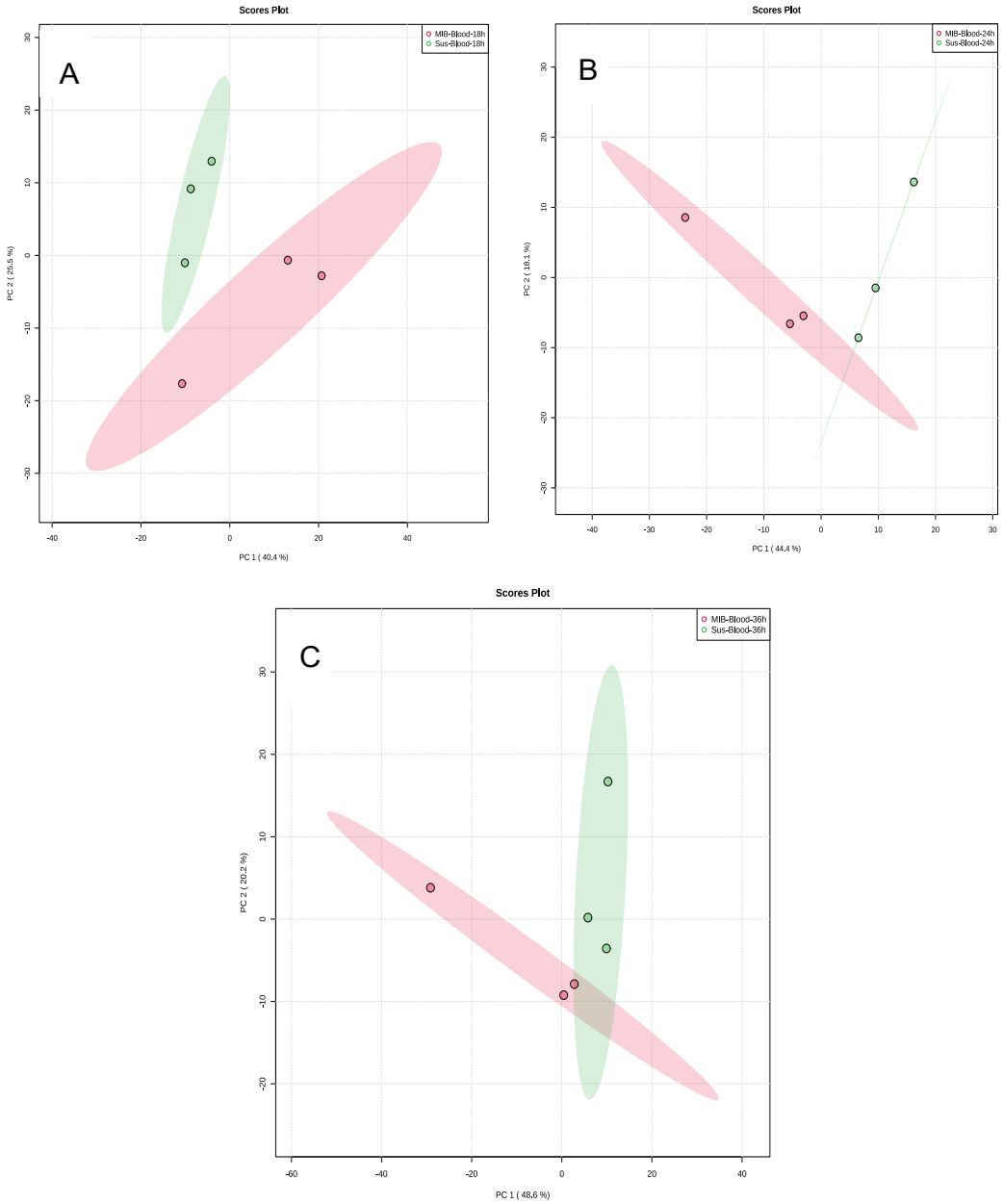


**B. 1.** **PCA plots of Cali-MIB+Blood and Cali-S+Blood Tier 1 and 2 data. Principal component analysis (PCA) of A) Cali-MIB+Blood vs Cali-S+Blood, 18 hpbm, B) Cali-MIB+Blood vs Cali-S+Blood, 24 hpbm, and C) Cali-MIB+Blood vs Cali-S+Blood, 36 hpbm. The X-axis has the first principal component and the Y-axis the second. Each data point represents one sample of 10 pooled insect midguts with the 95% confidence interval displayed as the ellipsis.**

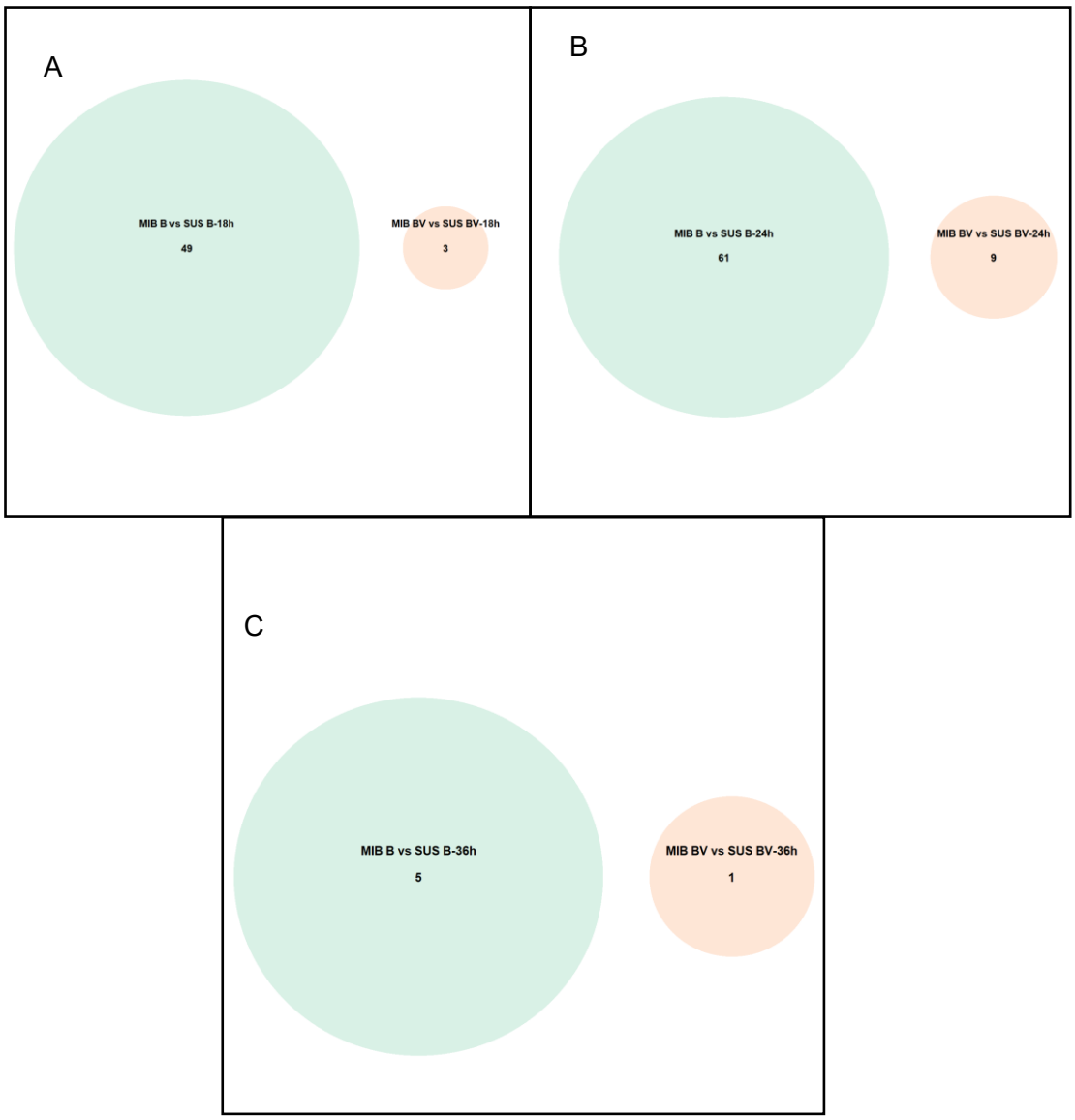


**B. 2** **Venn Diagram of significant features, Tier 1 and 2- 18, 24, and 36 hpbm. Venn Diagrams showing the number of significantly differently regulated metabolites selected using the SAM model at each time point, for each sample comparison (Cali-MIB+Blood vs Cali-S+Blood, Cali-MIB Blood+Virus vs Cali-S Blood+virus). The control groups are listed second in each comparison.**

# Appendix C. Lipidomics Analysis of Blood-Fed Cali-MIB and Cali-S Midguts

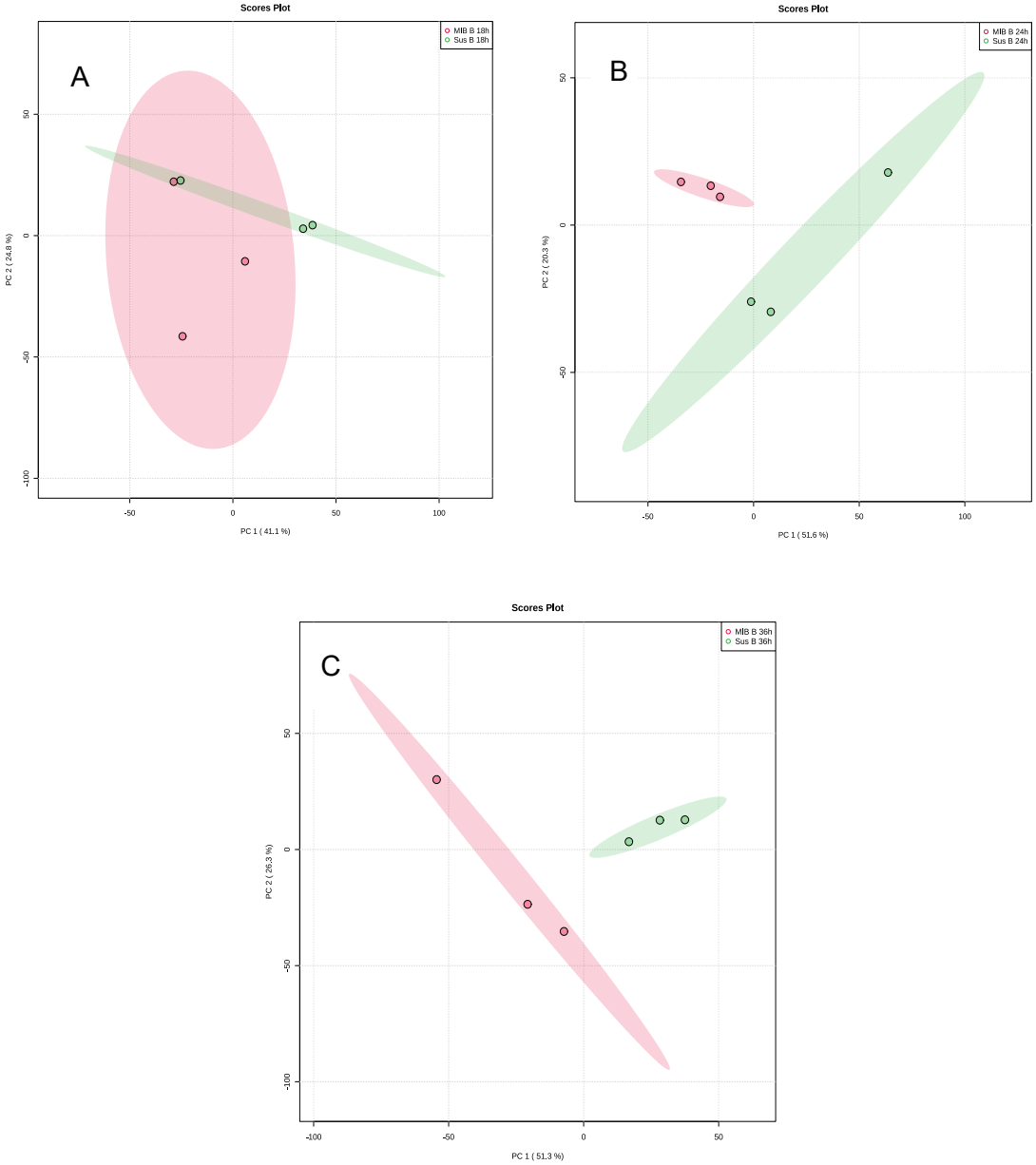


**C. 1.** **PCA plots of Cali-MIB+Blood and Cali-S+Blood lipidomics profiles. Principal component analysis (PCA) of A) Cali-MIB+Blood vs Cali-S+Blood, 18 hpbm, B) Cali-MIB+Blood vs Cali-S+Blood, 24 hpbm, and C) Cali-MIB+Blood vs Cali-S+Blood, 36 hpbm. The X-axis has the first principal component and the Y-axis the second. Each data point represents one sample of 10 pooled insect midguts with the 95% confidence interval displayed as the ellipsis.**


**C. 2.** **Venn Diagram of significant features, Tier 1 and 2- 18, 24, and 36 hpbm. Venn Diagrams showing the number of significantly differently regulated lipids selected using the SAM model at each time point, for each sample comparison (Cali-MIB+Blood vs Cali-S+Blood, Cali-MIB Blood+Virus vs Cali-S Blood+virus). The control groups are listed second in each comparison.**

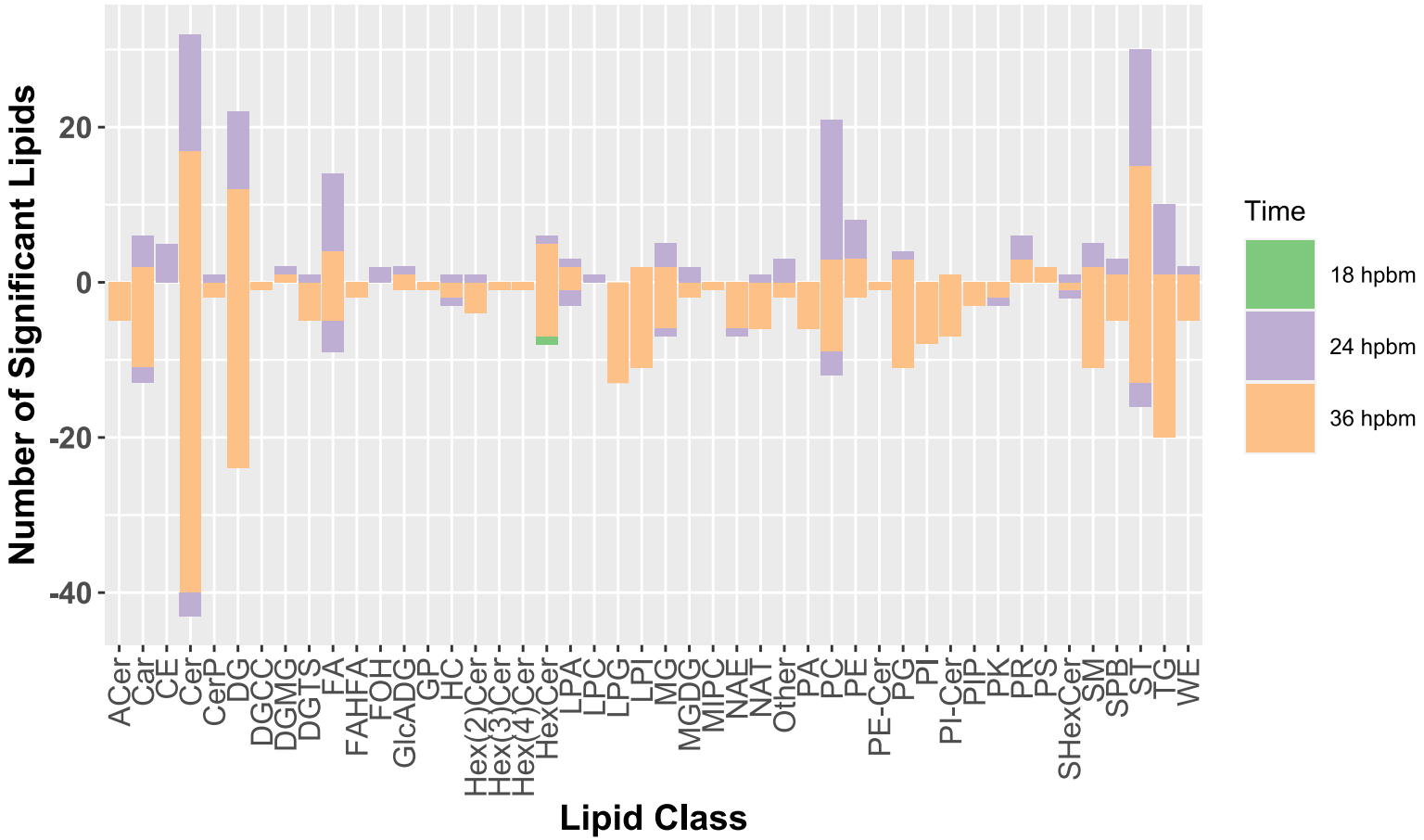


**C. 3.** **Significant lipids by category-Tiers 1, 2, and 3. Number of significant lipids regulated in the Cali-MIB+blood vs Cali-S+blood comparison, by lipid category. Each lipid category is divided by timepoint, with 18 hpbm shown in green, 24 hpbm shown in purple, and 36 hpbm shown in orange. The number of significant lipids differently regulated is shown on the Y-axis, with positive values indicating an increase in concentration compared to control, and negative values indicating a decrease in concentration. Abbreviations for lipid categories shown on the X-axis can be seen in Table 3.3**